

**Delivery of Mechanical And Chemical Stimuli to  
Advance Regeneration**

BY

GOLNAR DOROUDIAN  
B.S., University of New Mexico, 2009

THESIS

Submitted as partial fulfillment of the requirements  
for the degree of Doctor of Philosophy in Bioengineering  
in the Graduate College of the  
University of Illinois at Chicago, 2014

Chicago, Illinois

Defense Committee:

Brenda Russell, Chair and Advisor  
David Eddington  
Kathrin Banach, Physiology and Biophysics  
Ali Djalilian, Ophthalmology  
Ankit Desai, Cardiology

This thesis is dedicated to my beautiful and lovely mom, Soheila Darroudi, without her support and love none of the accomplishments I have made throughout my life would have been possible, so to her, I owe everything. I also thank other members of my family, my father, Massoud Doroudian, my sister, Bahareh Doroudian, my brother in law, Bijan Najafi, and my lovely nephew, Ryan Najafi. The influences from them were vital in determining my fate.

## **ACKNOWLEDGEMENTS**

I am grateful to my thesis committee: Dr. David Eddington, Dr. Kathrin Banach, Dr. Ali Djalilian, and Dr. Ankit Desai, for their guidance and support throughout these five past five years. I would especially like to thank my mentor and advisor, Dr. Brenda Russell who taught me the discipline required to attain a PhD. It was an honor to be her student. I will always be her student, and I will never forget her.

I thank current and former members of the Russell lab, including Shirley Li, Mike Mkrtshjan, Kathleen Broughton, Ying-Hsi Lin, Elina Sarmah, Tamara Los, Matthew Curtis, John Collins, and Anjulie Gang. This research would not have been possible without their friendship and support.

I also thank the members of the UIC Department of Physiology and Biophysics. I would especially like to thank Dr. John Solaro for funding me by his training grant which was an honor.

I would also like to thank Dr. Tejal Desai and her lab members, Perla Ayala, and especially James Pinney who contributed to the MGF elution project.

I am grateful to the members of the UIC Department of Bioengineering. I would like to thank Susan Lee for her kind help in administration.

GD

## TABLE OF CONTENTS

<u>CHAPTER</u>	<u>PAGE</u>
I. INTRODUCTION .....	1
A. Regenerative medicine.....	1
i. Cell sources for cardiac repair.....	1
ii. Bone marrow stem cells for the cardiac niche.....	3
iii. Stem cell niche.....	5
B. Physical cues.....	7
i. 3D vs 2D cell culture.....	7
ii. Microtopography.....	9
iii. Mechanical strain.....	10
iv. Stiffness.....	12
C. Chemical cues.....	14
i. Growth factors.....	14
ii. Oxygen tension in the developing heart.....	16
iii. Hypoxia effects on reactive oxygen species (ROS) and hypoxia inducible factor 1 alpha (HIF-1 $\alpha$ ).....	17
D. Biomaterials for stem cells.....	20
E. Cell engraftment for cardiac tissue engineering.....	21
F. Hypothesis and specific aims.....	24
II. CYCLIC STRAIN DOMINATES OVER MICROTOPOGRAPHY IN REGULATING CELLULAR FUNCTION OF HUMAN MESENCHYMAL STEM CELLS.....	26
A. Introduction.....	26
B. Materials and methods.....	27
i. Fabrication of microtopographic substrata.....	27
ii. Cell culture.....	30
iii. Cyclic strain.....	33
iv. Distribution of cells upon plating by time lapse movie.....	33
v. Proliferation.....	34
vi. F actin to G actin measurement.....	34
vii. Actin, focal adhesion, and nucleus staining.....	35
viii. Actin and nuclear distribution from post.....	36
ix. Imaging.....	36
x. DNA, RNA isolation and reverse transcription.....	36
xi. Microarray analysis.....	37
xii. Quantitative RT-PCR.....	37
xiii. Data analysis.....	38
C. Results.....	38
i. The time lapse images.....	41

ii.	The actin cytoskeleton.....	41
iii.	Nuclear shape, size, and distribution.....	46
iv.	Proliferation.....	46
v.	Focal adhesion.....	50
vi.	Gene expression.....	54
D.	Discussion.....	59
i.	Microtopography.....	64
ii.	Strain.....	64
iii.	Combination of microtopography and strain.....	65
iv.	Matrix remodeling.....	66
v.	Nuclear shape and location.....	66
vi.	Proliferation.....	67
vii.	Differentiation.....	68
E.	Conclusion and summary.....	69
III.	SUSTAINED DELIVERY OF MGF PEPTIDE FROM MICRORODS ATTRACTS STEM CELLS AND REDUCES APOPTOSIS OF MYOCYTES	70
A.	Introduction.....	70
B.	Materials and methods.....	72
i.	MGF peptide.....	72
ii.	Microfabrication and encapsulation of microrods with MGF.....	72
iii.	Microrod size and stiffness.....	75
iv.	Microrod degradation.....	76
v.	MGF elution from the microrods by ELISA.....	76
vi.	MGF elution from the microrods by HPLC.....	78
vii.	Cell culture for human mesenchymal stem cells and neonatal rat ventricular myocytes (NRVM).....	79
viii.	MGF bioactivity assessed by hMSC migration.....	80
ix.	Microrod and MGF effects on subcellular structure.....	81
x.	Microrod and MGF effects on proliferation.....	81
xi.	Chemical hypoxia.....	82
xii.	Caspase and HIF-1 $\alpha$ staining.....	82
xiii.	MGF bioactivity to reduce apoptosis of NRVM induced by hypoxia.....	82
xiv.	Statistical analysis.....	84
C.	Results.....	84
i.	Slow degradation of microrods.....	84
ii.	MGF elution time course detected by ELISA.....	84
iii.	MGF elution time course detected by HPLC.....	89
iv.	Subcellular structure and proliferation.....	89
v.	Migration.....	92
vi.	Hypoxia induction of apoptosis by chemicals.....	92
vii.	Hypoxic induction of apoptosis by hypoxia chamber.....	92
D.	Discussion.....	99
i.	PEGDMA microrods in drug elution applications.....	99
ii.	Microrods degradation.....	100

iii.	Physiological effect of the microrods alone.....	101
iv.	Microrods retain bioactivity of MGF.....	101
v.	Sustained delivery of MGF for two weeks.....	102
vi.	Migration of hMSCs as a bioactivity assay.....	103
vii.	Prevention of NRVM apoptosis as a bioactivity assay.....	104
E.	Conclusion and summary.....	105
IV.	MAJOR CONCLUSIONS.....	106
V.	FUTURE WORK.....	111
	CITED LITERATURE.....	113
	APPENDIX-animal approval forms.....	134
	APPENDIX-copy right clearance.....	136
	VITA.....	142

## LIST OF TABLES

<b><u>TABLE</u></b>		<b><u>PAGE</u></b>
I.	PRIMERS USED FOR qPCR CONFIRMATION OF MICROARRAY RESULTS.....	40
II.	MICROARRAY ANALYSIS OF DIFFERENTIATED GENES.....	56
III.	GLOBAL GENE EXPRESSION ONTOLOGY ANALYSIS.....	57
IV.	PRIMERS USED FOR qPCR .....	85

## LIST OF FIGURES

<b><u>FIGURE</u></b>	<b><u>PAGE</u></b>
1. Physical and chemical cues from the microenvironment affect stem cell niche	6
2. Effects of physical and chemical stimuli on other cells. ....	8
3. Schematic diagram of cyclic strain and microtopography.....	13
4. ROS and HIF-1 $\alpha$ effects on cells in hypoxia .....	19
5. Microfabrication of the micropost topography.....	28
6. Schematic of straining the microposts .....	31
7. Uniform laminin coating of microposts.....	32
8. Time lapse images of interaction of hMSCs with microposts.....	39
9. A phase image of hMSCs cultured on the microposts with less than 15 $\mu$ m height.....	42
10. Morphology of hMSCs change with microtopography and strain.....	43
11. Actin remodels with microtopography and strain.....	44
12. F actin to G actin ratio did not change with micropost and strain.....	45
13. Nuclear shape and size with strain and distance from microtopography.....	47
14. Proliferation of hMSCs is increased with strain.....	48
15. hMSC morphology with isotopic and anisotropic strain.....	49
16. Flow cytometry analysis for proliferation.....	51
17. Focal adhesions redistributed with microtopography and strain.....	52
18. Optical profilometry of the 3D reconstructions of focal adhesion of hMSC with post-relax and post strain.....	53



19.	"Heat map" with genes sorted to show matrix and focal adhesions, muscle proteins, proliferation, and differentiation.....	55
20.	Cell density and RNA/DNA/PROTEIN of hMSCs with post and strain.....	58
21.	Relative gene expression of the selected genes shown all together.....	60
22.	RT-PCR confirmed the dominant effect of strain over microtopography in regulating gene expression of the selected genes shown separately.....	61
23.	Schematic of micromechanics involved in the cell-substrata interactions for the post with or without strain.....	63
24.	Combination of physical and chemical stimuli enhances tissue regeneration..	73
25.	FITC-MGF encapsulation into PEGDMA microrods.....	74
26.	Microrod size and interaction with different cell types.....	77
27.	Degradation of microrods.....	86
28.	Testing MGF elution from the microrods by ELISA method.....	87
29.	Time course of elution of MGF from the microrods detected by HPLC method.....	88
30.	Microrods remodel hMSC morphology and adhesion.....	90
31.	Microrods blunt proliferation of hMSCs.....	91
32.	Eluted MGF is bioactive and regulates hMSCs migration.....	93
33.	Induction of chemical hypoxia was detected by caspase 3 and 7 assay.....	94
34.	Induction of chemical hypoxia was detected by HIF-1 $\alpha$ .....	95
35.	Induction of hypoxia by hypoxic chamber .....	96
36.	Cell death detection by TUNEL assay induced by hypoxia.....	97
37.	MGF protects NRVM from apoptosis induced by hypoxia.....	98

## LIST OF ABBREVIATIONS

2D	two-dimensional
3D	three-dimensional
BH	Benjamini-Hochberg procedure
CCM	complete culture media
DMEM	DMEM with 5% fetal bovine serum
DAPI	4',6-Diamidino-2-phenylindole
EdU	5-ethynyl-2'-deoxyuridine
EPC	endothelial progenitor cells
EPO	erythropoietin
bFGF	basic fibroblast growth factor
ECM	extracellular matrix
ESC	embryonic stem cell
FBS	fetal bovine serum
FGF	fibroblast growth factor
F	flat
FS	flat strain
GCSF	granulocyte-colony stimulating factor
hMSC	human mesenchymal stem cell
HCL	hydrochloric acid
IGF	insulin-like growth factor
iPS	induced pluripotent stem
LGM	low glucose media
LPE	local-pooled-error
BMSC	bone marrow mesenchymal stem cell

MGF	mechano growth factor
MGF-E	E-domain of MGF
MIP-1 $\alpha$	macrophage inflammatory protein-1 $\alpha$
MSC	mesenchymal stem cell
MMP13	matrix metalloproteinase 13
MCP-1	monocyte chemoattractant protein-1
MI	myocardial infarction
GF	growth factor
NRVM	neonatal rat ventricular myocyte
PBS	phosphate buffered saline
PEG	ethylene glycol
PVA	poly(vinyl alcohol)
PLA	poly(lactic acid)
PLGA	poly(lactic-co-glycolic acid)
PDMS	polydimethylsiloxane
PEGDMA	poly(ethylene glycol) dimethacrylate
qPCR	quantitative polymerase chain reaction
RGD	Arg-Gly-Asp
RT-PCR	real time polymerase chain reaction
SDF-1	stromal cell derived factor, type I
SEM	standard error of measurement
SPH	super porous hydrogel
TFA	trifluoroacetic acid
TUNEL labeling	terminal deoxynucleotidyltransferase (TdT)-mediated dUTP nick end-
VEGF	vascular endothelial growth factor

## SUMMARY

Innovations are needed to improve outcomes in the treatment of heart muscle disease worldwide, which world health organization (WHO) says will affect 23.6 million people by 2030 with 80% of deaths in low- and middle-income countries. In the U.S. 1,355,000 people suffer a new or recurrent heart attack every year according to American Heart Association (AHA) statistics (Roger, 2012, 2011). Regenerative medicine is rapidly showing promise for treating cardiac injuries and diseases with combinations of biomaterials and cells (e.g. stem cells) to restore the biological function that has been lost (Dai and Kloner, 2014). Stem cells have been popular in therapeutic applications due to their ability to self-renew and to differentiate into other cell lineages. One of the biomedical engineering approaches to mimic the physiological niche of stem cells is microfabrication of scaffolds with or without adding a chemical reagent. Biomaterials with various stiffness, geometry and dimension, and biochemical cues such as growth factors have been found to regulate stem cell function (Naderi, 2011).

This dissertation is divided into two main sections to analyze cell function in response to physical and chemical cues. In the first part, the effects of physical cues (cyclic strain and microtopography) are studied, and in the second part, the combination of chemical and physical cues (growth factor encapsulation into a microdevice) is addressed. The cells tested are neonatal rat ventricular myocytes (NRVMs) and human mesenchymal stem cells (hMSCs). Further, biological assays are used to determine functions such as stem cell morphology, proliferation, differentiation, migration, and apoptosis.

## SUMMARY (continued)

hMSC function depends not only on chemical factors but also on the physical cues of the microenvironmental niche for tissue regeneration. Here, this physical environment is recapitulated with controlled modes of mechanical strain applied to substrata containing three-dimensional features in order to analyze the effects on cell morphology, focal adhesion distribution, cell proliferation, and gene expression. 10% strain at 1 Hz is delivered for 48h to hMSCs cultured on flat surfaces, or on substrata with microtopographic posts 15  $\mu\text{m}$  high spaced 75  $\mu\text{m}$  apart. Introducing strain to microtopography produced stable semicircular focal adhesions, with anchored actin preferentially spanning post to post. Anisotropic strain caused a two-fold increase in the proliferation of hMSCs over equibiaxial strain with or without the posts. The nuclear position and flattened shape of hMSCs also changed with strain, adopting an ellipsoid shape in the middle of the cell on flat surfaces, or close to the post in textured substrata. Strain dominated microtopography for expression of genes coding proteins related to muscle function, cell adhesion, extracellular matrix remodeling, and cell differentiation ( $p < 0.05$ ). Overall, attention to external mechanical stimuli is necessary for optimizing the stem cell niche for regenerative medicine.

Additionally, local release of drugs may have many advantages for tissue repair but also presents major challenges. Bioengineering approaches allow microstructures to be fabricated that contain bioactive peptides for sustained local delivery. Heart tissue damage is associated with local increases in mechano growth factor (MGF), a member of the IGF-1 family. The E domain of MGF peptide is anti-apoptotic and a stem cell homing factor. The objectives of this study were to fabricate a microrod delivery device

## SUMMARY (continued)

of poly (ethylene glycol) dimethacrylate (PEGDMA) hydrogel loaded with MGF peptide and to determine the elution profile and bioactivity of MGF. The injectable microrods are 30 kPa stiffness and 15  $\mu\text{m}$  width by 100  $\mu\text{m}$  length, chosen to match heart stiffness and myocyte size. Successful encapsulation of native MGF peptide within microrods was achieved with delivery of MGF for two weeks, as measured by HPLC. Migration of human mesenchymal stem cells (hMSCs) increased with MGF microrod treatment ( $1.72 \pm 0.23$ ,  $p < 0.05$ ). Inhibition of the apoptotic pathway in neonatal rat ventricular myocytes was induced by 8 hours of hypoxia (1%  $\text{O}_2$ ). Protection from apoptosis by MGF microrod treatment was shown by the TUNEL assay and increased Bcl2 expression ( $2 \pm 0.19$ ,  $p < 0.05$ ). Microrods without MGF regulated the cytoskeleton, adhesion, and proliferation of hMSCs, and MGF had no effect on these properties. Therefore, the combination microdevice provided both the mechanical cues and two-week MGF bioactivity to reduce apoptosis and recruit stem cells, suggesting potential use of MGF microrods for cardiac regeneration therapy *in vivo*.

This thesis has yielded new information about how cells respond to local physical and chemical cues. Altogether, results suggest that it is possible to fabricate a stable and well-understood polymer system into microdevice platform to serve as both a mechanical stimulus as well as provide highly-localized, long-term delivery of bioactive peptides. Furthermore, this microdevice platform may be tuned in the future to permit the therapeutic profile of many existing biomolecules and expand delivery for regenerative therapy of other tissues. This understanding of the microenvironment is important to improve tissue regeneration.

## **I. INTRODUCTION**

### **A. Regenerative medicine**

Recovery of cardiac function after damage to the heart from ischemic stress could prove beneficial to the five million heart failure patients in the United States. Myocardial infarction (MI), a disease caused by a lack of blood flow supply in the heart, represents the most common cause of morbidity and mortality in the Western world. It has been estimated that hundreds of millions of cardiomyocytes are typically lost in large myocardial infarctions (MI) (Kehat and Gepstein, 2003). Therefore, to recover cardiac function, successful replacement of a sufficient number of cells is required in an infarcted heart. For the design of efficient therapeutic strategies, it is important to have a more detailed understanding of cell and tissue basic biological characteristics, as well as of the signals produced by damaged tissues and how the cells respond.

#### **i. Cell sources for cardiac repair**

Stem cell therapy arises as a promising alternative to conventional treatments, which are often ineffective in preventing loss of cardiomyocytes and fibrosis. Resident cardiac stem cells (Leri, 2006) may contribute to regeneration of the heart. Recent experimental data indicate that resident myocardial progenitor cells indeed exist in adult mammalian hearts, and are involved in physiological regeneration processes (Beltrami, 2003). Some, but not all of those cell types display the classic stem cell criteria, namely self-renewal, multi- or pluripotency. The existence of cells that express stem cell-typical markers in the heart cannot be doubted and the reproduction of emigrant cells from

myocardial tissue cultures that form spherical structures with progenitor cell properties ('cardiospheres') can easily be done (Stamm, 2009).

Stem cells for cardiomyogenesis for potential clinical use require two major steps: first improvement of the efficiency of differentiation into cardiomyocytes, and second the efficient proliferation for large numbers of the differentiated cells. Many attempts have been made to improve cardiogenic differentiation efficiencies (Wobus, 1997, Sauer, 1999, Pandur, 2002, Paquin, 2002, Kanno, 2004, Passier, 2005, E, 2006, Hosseinkhani, 2007a, 2007b). However, differentiation efficiency to improve cardiac regeneration has not yet been achieved (Hattori, 2010).

There are a variety of other sources of stem cells used in regenerative medicine and cell and tissue engineering applications. Embryonic stem cells (ESCs), induced pluripotent stem (iPS) cells, and adult stem cells from different tissues. ESCs and iPS cells have a relatively higher regenerative capacity than adult SCs and can be triggered to differentiate into other cell types (Boheler, 2011, Czyz 2003, Harun, 2006, Takahashi, 2007). However, ethical issues for the use of human embryos, and the potential for the embryonic stem cells to form teratomas, hinder therapeutic applications (Wakitani, 2003, Andrews, 2005). One way to overcome these issues is to induce pluripotent status in somatic cells by direct reprogramming (Yamanaka, 2008). Induced pluripotent stem cells can be generated from adult dermal fibroblasts and other somatic cells, which are comparable to ES cells in their differentiation potential in vitro and in teratomas (Takahashi and Yamanaka, 2006). Additionally, promising results have been reported using adult progenitor cells for tissue engineering (Polak, 2006). Adult stem cells can be isolated from many tissues such as bone marrow, blood, brain, liver,



muscle, and skin (Zwaginga , 2003, Sakai, 2002, Gronthos, 2003); they are capable to differentiate or trans-differentiate to other lineages due to their multipotency and high plasticity, and they have been used for treatment of various diseases including ischemia (Rezai, 2004). One of the examples of adult stem cells is bone-marrow-derived mesenchymal stem cells (MSCs) which are self-renewing cells that maintain their potential to differentiate into mesenchymal tissue including bone, cartilage, adipose tissue, skeletal muscle cells, liver cells, neural cells, smooth muscle cells, and fibroblasts (Nombela-Arrieta, 2011). These properties make MSCs an attractive cell source for regeneration of damaged tissue.

## ii. **Bone marrow stem cells for the cardiac niche**

Among these cells bone marrow stem cells (BMSC) are, at present, the most frequent source of cells used for human therapy. Bone marrow-derived progenitor cells can differentiate into vascular cell types, restoring blood flow (Segers, 2008). These cells are capable of secretion of growth factors or cytokines promoting angiogenesis and reducing apoptosis such as vascular endothelial factor (VEGF), monocyte chemoattractant protein-1 (MCP-1) and macrophage inflammatory protein-1 $\alpha$  (MIP-1 $\alpha$ ). Previous studies indicated muscle regeneration in mice after the BMSCs were injected into the infarcted area. Regeneration of heart tissue was observed in 40% of the treated mice, and new cells were found in 68% of the infarcted portion of the ventricle (Review, Collins, 2007). Postnatal bone marrow contains cells which express early cardiac markers and they are able to mobilize into the peripheral blood after myocardial infarction (Kucia, 2004).

The approach of mobilization, homing, and differentiation of bone marrow stem cells for cardiac application is first to harvest the BMSC, and then inject the purified stem cells into the infarcted recipient. Delivering bone marrow or blood derived progenitor cells have been done by different procedures such as intracoronary arterial route or other surgical approaches (Dimmeler, 2005). Another method to compensate the damage to the heart is to increase the number of stem cells from the bone marrow by enhancing their mobilization and delivering cytokines and growth factors to BMSC to improve their differentiation in the infarcted region (Vandervelde, 2005). In mobilization, homing, survival, proliferation and differentiation of the BMSCs, the knowledge of adequate cell signaling between the bone marrow, the peripheral circulation and the infarcted myocardium is valuable for myocardial regeneration.

Chemokines and other important signaling factors are known for their mobilizing and chemotactic abilities such as SDF-1, VEGF, GCSF, SCF, and IL-8. An approach to enhance cardiac repair is to enhance cytokine-induced mobilization, for example to increase endothelial progenitor cells (EPC)-one of the subpopulations from bone marrow-levels for neovascularization. After myocardial infarction some signaling factors are involved in the patho-physiological healing process (TNF- $\alpha$ , IL-8, IL-10, HIF-1 $\alpha$ , VEGF, GCSF) which may affect the stem cell engraftment, and signaling factors that are involved in cardiogenesis and neo-angiogenesis (VEGF, EPO, TGF- $\beta$ , HGF, HIF-1 $\alpha$ , IL-8) all have an important role in orchestrating the stem cell driven repair process (Vandervelde, 2005). The signaling factors including VEGF and GCSF were also found to increase EPC levels and improve neovascularization (Dimmeler, 2005).

After BMSC mobilization, the cells are attracted to the ischemic area by multiple signals. Homing of the stem cells is a multi-steps process: first adhesion to activated endothelium or exposed matrix, second transmigration through the endothelium, and, finally, migration and invasion of the target tissue (Dimmeler, 2005). SDF-1 and  $\beta$  integrins are the important factors in homing of stem and progenitor cells to the infarcted heart due to their ability to increase EPC level and neovascularization. Cell necrosis and mesoangioblasts are also essential for cell recruitment in the muscle regeneration process.

Angiogenic responses play a major role in the natural healing process after myocardial infarction. Cells engineered to over express angiogenic factors might enhance both their own survival and that of the recipient myocardium. Endothelial migration from pre-existing blood vessels and neo-angiogenesis by differentiation from migrated circulating EPCs, are the two sources of endothelialization. Formation of vessels is essential for transport and survival of transplanted or recruited stem cells, but stem cells themselves also appear to play a role in neo-angiogenesis (Vandervelde, 2005).

### **iii. Stem cell niche**

Stem cell function is dependent not only upon soluble stimuli, but also the physical microenvironmental niche. Stem cells either self-renew or differentiate depending upon various microenvironmental cues, including soluble growth factors, extracellular matrix, and mechanical forces (Figure 1). The microenvironment niche has been shown to regulate many aspects of stem cell function such as tissue generation, maintenance, and repair (Scadden, 2006). The niche provides physical and chemical signals that

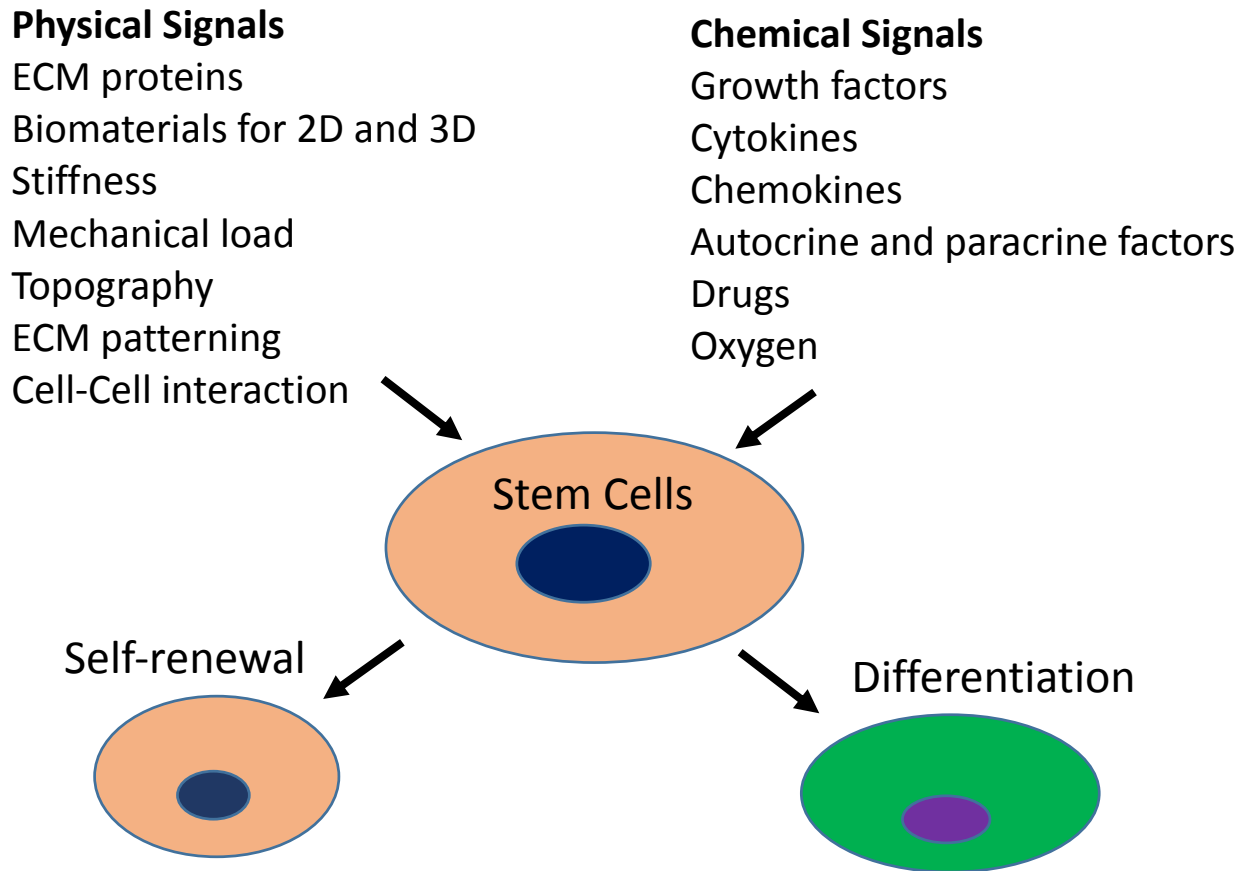


**Figure 1.** Physical and chemical cues from the microenvironment affect stem cell niche. Stem cell niche consists of chemical and physical signals which influence their self-renewal and differentiation.

allow stem cells to either maintain their primitive phenotype or differentiate along a specific lineage. In fact, combination of mechanical and chemical stimuli is critical to the function of other cell types (Figure 2) and tissues as well such as heart, being the most mechanical organ of the body. The physical niche can be considered as a combination of structural, cellular and physical components that vary from one tissue to another to control proliferation and differentiation (Spradling, 2001). The chemical niche can be considered as growth factors, genes, drugs, or cell signaling.

## **B. Physical cues**

Physical cues of the microenvironmental niche of stem cells can be considered as natural or synthetic biomaterials with topography (2D vs. 3D), and mechanical loads such as strain and stiffness which may regulate self-renewal and differentiation of the stem cells to cardiac lineage (e.g. cardiomyocytes, endothelial cells, or smooth muscle cells).

### **i. 3D vs 2D cell culture**

It is well known that cells cultured in 2D function differently than those cultured in 3D. These differences could be in morphology, adhesion, migration and differentiation (Pedersen, 2005). In addition, non-adherent cell types show otherwise absent migration capability inside a 3D matrix (Brown, 1982; Pedersen, 2005). The characteristics of cardiac cells in 3D culture have been investigated. Cardiac fibroblasts cultured in a 3D matrix have shown to convert to a myofibroblast phenotype with distinct differences with

**Physical Signals**

ECM proteins  
Biomaterials for 2D and 3D  
Stiffness  
Mechanical load  
Topography  
ECM patterning  
Cell-Cell interaction

**Chemical Signals**

Growth factors  
Cytokines  
Chemokines  
Autocrine and paracrine factors  
Drugs  
Oxygen

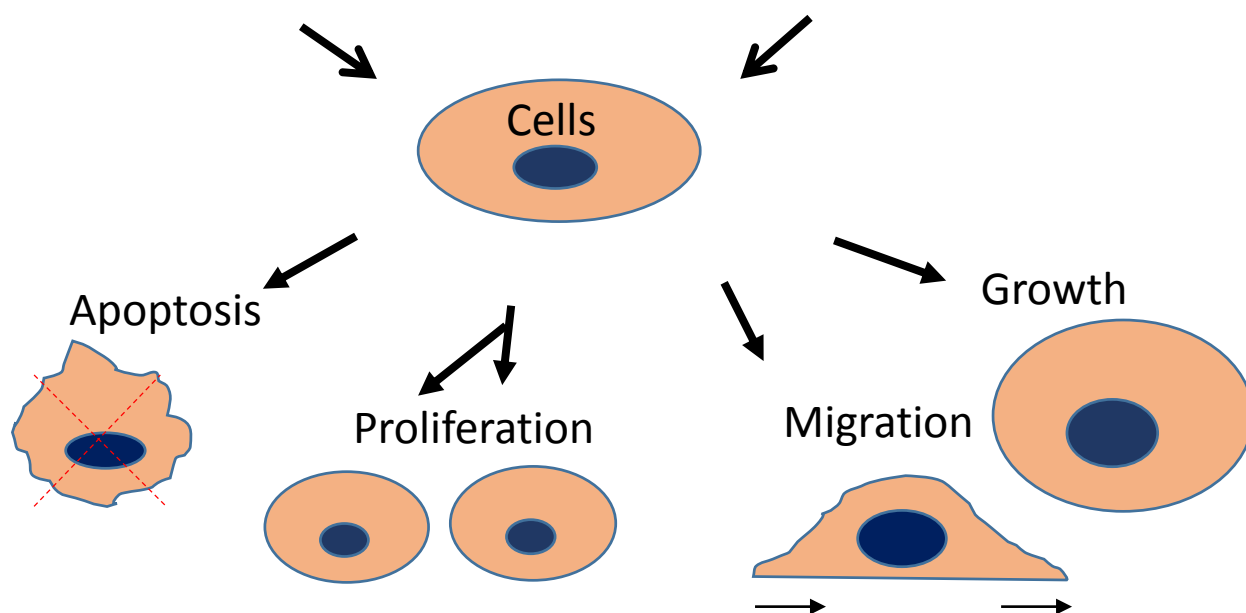


**Figure 2.** Effects of physical and chemical stimuli on other cells. Physical and chemical stimuli of the microenvironment also affect endogenous cells in terms of growth, migration, proliferation, and apoptosis.

ECM regulation (Poobalarahi, 2006). The embryonic ventricular myocytes transition from a highly proliferative phenotype to a quiescent phenotype after culture in a 3D scaffold, function similarly to those *in vivo* (Evans, 2003). MSCs in engineered 3D constructs increased cardiac markers such as smooth muscle alpha actin, h1-calponin, GATA4, Nkx2.5 and MEF2C (Nieponice, 2007, Guan, 2011). A 3D microenvironment was created through electrospinning to study the impact of geometry and different extracellular proteins on the development of cardiac progenitor cells from resident stem cells and their differentiation into functional cardiovascular cells (Heydarkhan, 2012). Organ development and tissue regeneration do not naturally occur in a uniform 3D environment, but occur where there is heterogeneity of topography. Therefore, it is possible that stem cells respond to more complex micro-mechanical and physical cues such as non-uniform topography.

## ii. **Microtopography**

3D topography has been shown by several studies to affect cellular organization (Motlagh, 2003a; 2003b, Norman, 2005, 2007). The micro-textured culture system prevented proliferation of fibroblasts in cardiac primary cultures and may ultimately be useful for *in vivo* tissue engineering applications (Boateng, 2003). Topography can align and/or guide a variety of cell types, including endothelial cells, epithelial cells, fibroblasts, oligodendrocytes, and astrocytes (Bettinger, 2006, Cheng, 2006). The surface micro-topography affects the behavior of neonatal and adult cardiac cells (Motlagh, 2003, Boateng, 2003, Thakar, 2008). The use of geometric boundaries forces

neonatal rat ventricular myocytes to spread into an elongated shape, similar to that of cardiomyocytes in vivo, which leads to more sarcomeric alignment and clear axes of contraction (Motlagh, 2003, Bray, 2008, Parker, 2008). Forces that act on function of the heart are three-dimensional. Therefore, exposing the cells to a 3D culture condition is crucial to mimic the environment in the living organ.

### iii. **Mechanical strain**

Cells remodel actin cytoskeletal organization and focal adhesions in response to changing loads. Physical forces encountered by cells within the cardiac microenvironment result from active force production, gain and loss of adhesion, and cytoskeletal stretch and compression due to changes in ventricular cavity pressure. The molecular systems through which cells convert mechanical cues from the extracellular matrix (ECM) into intracellular signals (mechanotransduction) have been extensively investigated (Wang, 1994, Ingber, 2003, Lele, 2006, Senyo, 2007). In the adult human heart, cells remodel in response to changing loads. The effect of cyclic strain as a physical force on either differentiation or proliferation of different types of stem cells has been well studied. The formation of the heart tube depends on local forces (Varner, 2010) and mechanical loads can influence gene expression patterns during development (Wozniak and Chen, 2009). Aortic stenosis in humans causes cardiac hypertrophy, and enhancement of the differentiation of cardiac stem cells, suggesting that these endogenous stem cells amplify and commit to the myocyte lineage in response to an increased workload (Urbanek, 2003).



Static and cyclic strain of cultured cells is often used to model mechanical influences on stem cells. The expression of cardiac differentiation markers increase including, sarcomeric  $\alpha$ -actinin, MEF2c and GATA-4 in mouse embryonic stem cells after static stretching at 10% strain for 2 hours (Schmelter, 2006). They further demonstrated that the mechanical strain stimulate the mRNA expression of transcriptional factors MEF2C and GATA-4 involved in cardiovascular differentiation in two-dimensional cultures of mouse ES cells and also that reactive oxygen species play a role in the process of mechanotransduction. The chronic stretch induced cardiomyocyte hypertrophy in vitro, was accompanied by marked improvement of contractile function (Fink, 2000). Exposure of human airway smooth muscle cells to cyclic strain caused a significant increase in their proliferation rate compared with HASM cells not exposed to strain, suggesting that cyclic mechanical strain regulates the development of engineered smooth muscle tissue. Cyclic strain of embryonic stem cells (ESC) or mesenchymal stem cells (MSC) on flat 2D membranes regulates cardiac differentiation markers (Gwak, 2008, Ge, 2009, Bhang, 2010, Heo, 2011, Wan, 2011). Strain amplitude has been varied from 1-20%, with the high end having the maximum effect on various stem cells (Fink, 2000, Weyts, 2003, Shimizu, 2008).

Markers considered to be specific for vessels (but also found in early cardiomyocytes), such as smooth muscle actin (SMA) increase in a strain-dependent manner for MSCs (Ghazanfari, 2009, Kearney, 2008). Uniaxial strain is the most effective in differentiation of MSC into smooth muscle cells (Park, 2004). Cell proliferation is enhanced and apoptosis decreased with cyclic strain of ESCs (Shimizu, 2008, Kearney, 2008). There is a great complexity of outcomes reported for the responses of different cell types to

various geometries and strains, which makes it difficult to evaluate stem cell differentiation. Embedded ESCs strained at 2 and 3 Hz increased cardiac markers (Guo, 2006, Shimko 2008), or low frequency of 0.2 Hz at 10% strain reduced differentiation of human embryonic stem cells, maintaining an undifferentiated state (Saha, 2006). Studies remain to be done on the importance of mechanical load and cyclic strain with 2D and 3D microprojections. Clearly more work is needed to understand how a cell type with potential clinical use responds to mechanical strain when the 3D geometry is tightly controlled (Figure 3). Condition that mimics the mechanical strain in 3D found in the developing heart tube is discussed further in chapter II.

#### **iv. Stiffness**

Substrate stiffness affects cellular phenotype. On more compliant substrates, cells are less spread, focal adhesions are irregular, and motility rates are higher than on stiffer substrata (Pelham, 1997). A softer substrate, by definition, allows for a greater length of contraction for the same generated force allowing for signaling mediated by contractile strain (Jacot, 2009). Matrices that mimic striated muscle elasticity of 8-12 kPa are ideal for MSCs growth and differentiation (Engler, 2006). Matrix stiffness modulates cellular tension, with force transmission occurring via focal adhesions. The change of the elastic modulus of the epicardium from an embryonic value of  $12 \pm 4$  kPa to a neonatal value of  $39 \pm 7$  kPa is in the range shown to significantly affect the development of neonatal

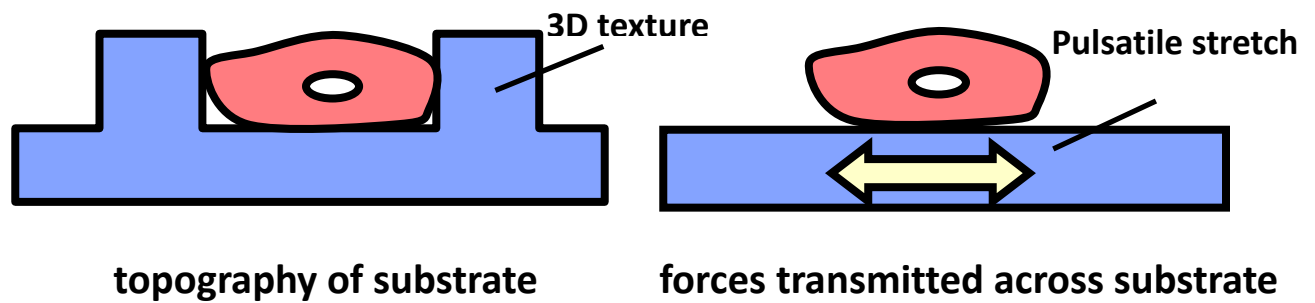


**Figure 3.** Schematic diagram of cyclic strain and microtopography. Physical cues can be considered as a combination of topography of substrate or the mechanical load induced by the substrate such as cyclic strain that affect shape, size, attachment, and function.

cardiomyocytes (Jacot, 2009). Understanding of how tissue cells including fibroblasts, myocytes, neurons, and other cell types sense matrix stiffness is emerging with quantitative studies of cells adhering to gels (or to other cells) with which elasticity can be tuned to approximate that of tissues. Note that factors such as gel porosity and film topography complicate identification of possible contributions of substrate stiffness.

### **C. Chemical cues**

#### **i. Growth factors**

Biological or chemical signals in the microenvironment of cells can directly regulate their function. These chemical cues can be a combination of specific growth factors, hormones, and cytokines. The paracrine/autocrine signals in the stem cell niche modulate stem cell biology and the tissue response in terms of cell survival, self-renewal, and cell growth (Gnecchi, 2008). One of the important roles of growth factors on improvement of regeneration is for the homing of stem cells to the injured tissue. There are various types of growth factors which induced regeneration. TGF- $\beta$  and TGF- $\alpha$  have shown beneficiary effects in cardiac repair by either boosting the adult cardiac progenitor cell formation or increasing the cardiomyogenic markers (Bujak, 2007, Bhang, 2010, Hermann, 2010). Fibroblast growth factor (FGF) has been demonstrated to improve cardiac function and reduce myocardial infarction size, and it also has the potential to increase proliferation of MSCs while maintaining their multi-lineage differentiation capability (Cuevas, 2000, Tsutsumi, 2001). Furthermore, bone morphogenetic proteins (BMPs) could increase the regeneration of specific cell types

including skeletal tissues (Reddi, 2000). Colony-stimulating factors such as granulocyte macrophage colony-stimulating factor (G-CSF) have been important in recruitment of stem cells such as bone marrow or resident progenitor cells to the infarcted heart (Orlic, 2001, Brunner, 2008, Steinhilber and Lee, 2009). A cardioprotective effect, is the cytokine receptor ligand (cardiotrophin), which has been implicated in increased neonatal rat cardiac myocyte cell survival (Stephanou, 1998, Hausenloy and Yellon, 2009).

Among all other growth factors, Insulin-like growth factor 1 (IGF-1) is a crucial systemic factor that regulates growth and has a wide variety of functions, such as promoting cells proliferation, migration, and inhibition of apoptosis (Muta 1993, Rodriguez 1992, Beurke 1995). Over-expression of the IGF-1 gene in the heart has proven beneficial in eliciting cardiac hyperplasia by inhibition of apoptosis and prevention of dilation (Reiss 1996, Li 1997, Welch 2002). Multiple isoforms of IGF-1 are expressed in different tissues that arise by alternative splicing and function as a paracrine/autocrine growth factor mediating regenerative processes (Russell 1985, Vetter 1986, Dai, 2010). Due to alternative splicing, IGF-1 pre-mRNA can generate three isoforms from the same mature IGF-1 but with different E domain with distinct function. There are three E domains in human: IGF-1Ea, IGF-1Eb and IGF-1Ec, but two isoforms in rodent: IGF-1Ea, IGF-1Eb (Chew, 1995, Lowe, 1988). IGF-1Ec in human (IGF-1Eb in rodents), which is also named mechano growth factor (MGF), was originally identified in skeletal muscle under conditions of increased growth after injury (Yang 2002, McKoy 1999). After muscle injury due to exercise or stress, there is an invasion of neutrophils into the site of injury within 1 hour, which causes muscle damage by

releasing free radicals or other oxidants that leads to a lysis of muscle cell membranes (Tidball, 2005). Expression of MGF has contributed to increasing the activity of superoxide dismutase, known to decrease the level of free radicals, and therefore limit muscle damage (Dobrowolny, 2005). Another property for the expression of MGF during muscle regeneration is its ability to enhance the chemoattractive effect of muscle satellite cells on bone marrow stem cells (Musaro, 2004). MGF increases the number of monocytes/macrophages into the injured muscle and favors muscle repair. Synthetic MGF has also been shown to promote survival in response to neurotoxins through a mechanism that may involve heme-oxygenase-1 (Quesada, 2009). The E-domain of MGF appears to have beneficiary effects in injured tissue either distinctly or synergistically to the mature peptide of IGF-1 (Carpenter, 2008, Dluzniewska 2005).

## ii. **Oxygen Tension in the Developing Heart**

During embryogenesis, and particularly the development of the cardiovascular system, the oxygen tension to which cells are exposed are substantially lower than atmospheric levels (Jauniaux, 2003, Lee, 2001), making O<sub>2</sub> content a potentially important parameter when designing new strategies for stem cell expansion and/or controlled differentiation. Hypoxia plays an important role in the proliferation, differentiation and maintenance of the cardiovascular system during development (Simon, 2008, Fisher, 2007, Ramirez-Bergeron, 2004, Xinping, 1999, Huang 1997). Low oxygen tension appears to direct the cultured ESCs to differentiate into cardiomyocytes (Niebruegge, 2009, Ezashi, 2005). The embryo in vivo develops under low oxygen tensions of 1.5-5.3% O<sub>2</sub> (Fischer, 1993).

The myocardium is broadly hypoxic (2% oxygen) at E9.5 in the mouse (Dunwoodi, 2009). The proliferation of ESC under hypoxia is not fully understood. ESC cells are reported to grow more efficiently under low O<sub>2</sub> conditions, as opposed to ambient air (Simon 2008, Ezashi, 2005, Harvey 2004). It has also been suggested that culture under low oxygen tension allows spontaneous ESC differentiation and hypoxia reduces the cell proliferation rate (Fernandes, 2010, Kurosawa, 2006). However, human ESC proliferate at a similar rate when cultured at 3–5% O<sub>2</sub> as they do at 21% O<sub>2</sub>. Therefore, hypoxic conditions may be required to maintain the full pluripotency of mammalian ESC (Ezashi, 2005).

iii. **Hypoxia effects on reactive oxygen species (ROS) and hypoxia inducible factor 1 alpha (HIF-1 $\alpha$ )**

Under hypoxia, ROS is also affected. It is an oxygen sensor, and is essential in the development and healthy existence of aerobic organisms and cardiovascular homeostasis. Hypoxia and robust endogenous ROS production have been previously shown to occur in differentiating ESC and may represent one key stimulus for induction of the cardiomyogenic cell lineage. ROS is generated by nicotinamide adenine dinucleotide phosphate (NADPH) oxidase (Sauer, 2000) and commonly during hypoxia (Blokhina, 2003, Hermes-Lima, 2002, Chandel, 2007, Guzy, 2006, Nanduri, 2007). ROS is thought to direct the cardiac differentiation of cultured ESCs via alteration of the redox status (Li, 2006, Buggisch, 2007), and, furthermore, it has been shown that change in redox status can lead to the activation of the HIF-1 $\alpha$  pathway (Goyal, 2004,

Martinez-Sanchez, 2007). An alteration of intracellular ROS levels may not only represent the stimulus to increase ES-cell-derived-cardiomyocyte (ESC-CM) numbers, but also enhance the expression of cardiac-specific genes and transcription factors such as MEF2C, DTEF, Nkx-2.5, GATA4 (Buggisch, 2007). The induction of ROS generation by mechanical stimuli and the involvement of redox signaling is seen in vascular remodeling responses to shear, stress, and stretch (Lehoux, 2006). Formation of ROS occurs when contraction frequency is increased in rat neonatal cardiomyocytes (Heinzel, 2006).

Hypoxia activates the expression of HIF-1 $\alpha$ , by the activation of a number of growth factors, including VEGF, erythropoietin (EPO), and basic fibroblast growth factor (bFGF). These all have a synergistic effect on mesoderm differentiation processes, which result in cardiogenesis (Ramirez-Bergeron and Simon, 2001, Semenza, 2001). Cultured ESCs without HIF-1 $\alpha$  expression fail to form beating embryoid bodies (Bauwens, 2005). Overall, HIF-1 $\alpha$  is essential in normal cardiac morphogenesis, myocardial and endocardial development, and development of vascular endothelial cells of the heart (Huang, 1997). By decreasing the concentration of oxygen from normoxia (20% O<sub>2</sub>) to hypoxia (less than 10%), the HIF-1 $\alpha$  level increases due to the suppressed degradation and it is maximized at lowest oxygen concentration (e.g. 0.5% O<sub>2</sub>) (Jiang, 1996, Semenza, 2006). In turn, exogenous expression of HIF-1 $\alpha$  promotes cardiac differentiation of embryonic stem cells (Ng, 2010). Therefore, hypoxic preconditioning of stem cells may optimize their potential for therapeutic approaches and have a direct clinical impact on the treatment of peripheral vascular disease and ischemic heart disease (Figure 4).



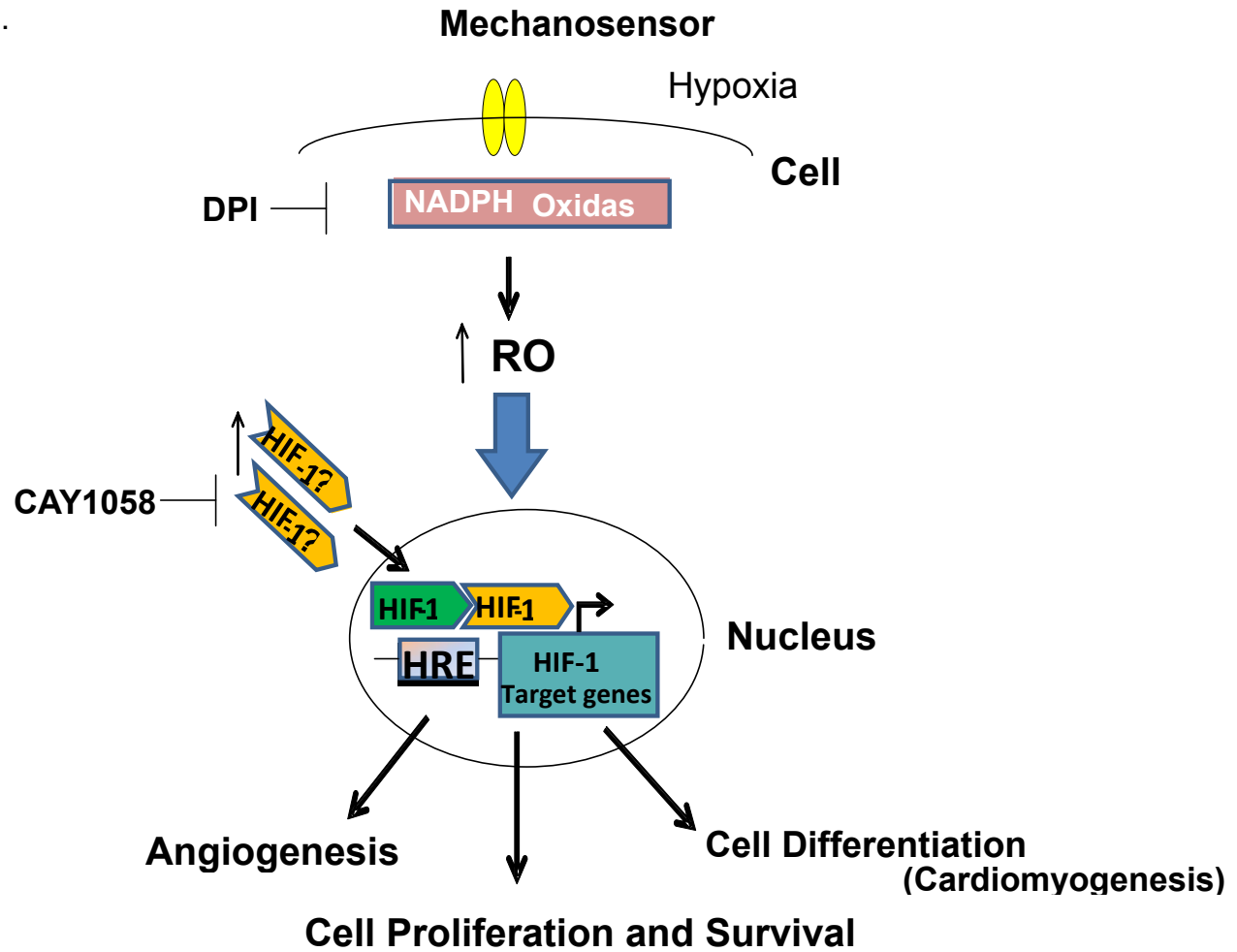


**Figure 4.** ROS and HIF-1 $\alpha$  effects on cells in hypoxia. Hypoxia is involved in increased ROS and accumulation of HIF-1 $\alpha$  in the nucleus which affect differentiation, proliferation, and angiogenesis.

#### **D. Biomaterials for stem cells**

Identification of appropriate biomaterials that support cellular attachment, proliferation, and specific differentiation are critical for tissue engineering and cellular therapy. In order to choose a specific biomaterial to mimic the physical microenvironment of cells and tissues through scaffolds, several factors need to be incorporated such as stiffness, biocompatibility, microenvironmental architecture, and degradation rate. While the typical tissue engineering approach involves a scaffold with cells, such biomaterials may also be used as cell free delivery vehicles for therapeutic chemical delivery, including proteins or peptides in order to stimulate tissue regeneration. Therefore, in addition to the physical factors, it is necessary to consider controlling the dose and duration of releasing chemical cues via polymeric (synthetic or natural) delivery systems (Review, Naderi, 2011).

Three dimensional biodegradable synthetic polymeric systems are of particular interest because their porosity, hydrophilicity and degradation time which all can be varied. Moreover, they can be manufactured with a high degree of reproducibility (Mooney, 2003). Hydrogels are 3D networks of hydrophilic polymers that imbibe a large quantity of water as well as biological fluids. Hydrogels have also been used as scaffold materials for drugs and growth factor delivery, engineering tissue replacements, and a variety of other applications. Most commonly used synthetic biomaterials are poly(ethylene glycol) (PEG), poly(vinyl alcohol) (PVA), poly(lactic acid) (PLA), or poly(lactic-co-glycolic acid) (PLGA), and poly(ethylene glycol) dimethacrylate (PEGDMA) (Review; Hoffman, 2002). There are a few drawbacks with some of these hydrogels. They are usually non-porous and non-adhesive because protein adsorption to the surface is weak. Therefore, some modifications of hydrogels are necessary. Conjugation of Arg-

Gly-Asp (RGD) which is a cell adhesive peptide to the hydrogels, promoted the differentiation of MSCs (Yang, 2005). Another approach to improve the properties of hydrogels is to synthesize them as super porous hydrogel (SPH). Seeding of cells is easier within macroporous scaffolds, and this results in rapid uptake cell seeding which makes the scaffolds more effective. Interconnected macroporous networks increase cellular ingrowth and communication influencing cell survival (Keskar, 2009, Dadsetan, 2008).

#### **E. Cell engraftment for cardiac tissue engineering**

A commonly used scaffolding approach for the treatment of myocardial infarction (MI) involves in vitro engineered cardiac tissue. Bundles of contractile rat myocytes are often made into patches for surgical implantation. Orientation is attained by peptide stamping (Reinecke, 1999), or by mechanical pacing (Zimmerman 2002, Feinberg, 2007).

However, the engraftment of patches is problematic because myocytes are covered with fibroblasts that prevent electrical connection with the healthy heart of the host (Zimmerman, 2006). Further, scale-up for use in human surgery is severely limited by poor diffusion of oxygen that causes death of myocytes 200  $\mu\text{m}$  within the surface of the patch.

The simplest *in situ* tissue engineering approach has been injection or mobilization of viable cells to replace necrotic cardiomyocytes. This is less invasive than patch surgery, therefore, considered more clinically realistic.

Clearly greater cardiac stem cell numbers would enhance repair of the heart. However, only small side-population of cells express stem cell markers with regenerative potential

(Beltrami 2003, Oh 2003, Martin 2004). Nonetheless, mobilized or exogenously administered adult stem cells have been shown to migrate into the heart following infarction (Wobus 1997, Glimm 2000, Orlic 2001, Uemura 2006), and embryonic stem cells have also been used (Laflamme 2007, Simpson 2007). Unfortunately, injection suffers from lack of cell retention and transplant survival (Hofmann 2005, Freyman 2006). Furthermore, recent findings in the field have demonstrated that the functional improvements associated with the direct delivery of hematopoietic stem cells to the heart is not due to their capacity to differentiate into myocytes, but rather their secretion of factors that appear to be beneficial (Fazel, 2006) or to increased angiogenesis (Kawamoto 2006) which is also advantageous.

Cell retention or death may be due to defects of the environment. Myocytes need cell-to-cell contacts for viability and when seeded in a hydrogel they are isolated from each other promoting programmed cell death, apoptosis, and the few surviving cells that are electrically connected function poorly (Langer, 1993).

Injectable gels such as fibrin glue (Christman 2004, Ryu 2005) have been used to deliver cells directly into the infarct wall to increase cell retention and survival. Other biomatrix vehicles used are collagen, matrigel, and alginate (Kofidis 2007, Leor 2007). However, long-term cardiac function was not maintained with cell/gel approaches due to lack of cell organization and the gel remaining at the injection site, but not widely disposed through the tissue. In the myocardium, basic fibroblast growth factor in gelatin microspheres (Iwakura 2003) and the angiogenic growth factor pleiotrophin in fibrin glue (Christman 2005) improved cardiac function by increasing neovascularization in ischemic myocardium. A novel injectable scaffold using peptides, which self-assemble

to form nanofibers recruited progenitor cells expressing endothelial and vascular smooth muscle cell markers to the infarct zone (Davis 2006). Similarly, self-assembling peptides with platelet-derived growth factor-BB (Hsieh 2006) sustained delivery for 14 days in infarcted myocardium, which decreased cardiomyocyte death and preserved cardiac function compared to the peptides or growth factor alone. In our case, the injectable polymeric structure provide both growth factor peptides and some architectural organization that may be more beneficial than either alone. Therefore, both cell source and engraftment remain unresolved challenges for cardiac tissue engineering despite progress with stem cell research.

## **F. Hypothesis and specific aims**

Cellular function depends not only on chemical factors but also on the physical cues that make up the microenvironmental niche. Therefore, it is necessary to introduce these parameters in vitro in order to mimic the complex cellular organization and function present in native tissue. Two hypotheses drive this research on regeneration of human mesenchymal stem cells (hMSCs): (1) Mechanical cues of the microenvironmental niche in 3D regulate cell function. Mechanical strain is combined in a 3D micropost system. (2) Combination of chemical and mechanical cues regulate hMSC function and neonatal rat ventricular myocyte (NRVM) apoptosis. The chemical cue is the mechano-growth factor (MGF); an isoform of the insulin-like growth factor (IGF) chosen because it is increased with hypoxic stress, is anti-apoptotic and acts as a chemokinetic agent for skeletal muscle myoblasts and stem cells.

**Hypothesis 1. Biaxial cyclic strain dominates over micropost topography in regulating cytoskeletal organization, focal adhesion formation, and matrix remodeling of hMSCs.**

**Specific Aim 1a.** Test the effects of the combination of biaxial strain and micropost topography on cytoskeletal reorganization and focal adhesions. hMSCs are anchored to microposts to mimic 3D and physiological mechanics are mimicked by 10% cyclic strain at 1 Hz for 48 hours. Assessment is made for the distribution of proteins by paxillin and actin immunostaining.

**Specific Aim 1b.** Test the effects of the combination of biaxial strain and micropost topography on hMSC proliferation. Cell number is determined by EdU assay.

**Specific Aim 1c.** Test the effects of the combination of biaxial strain and micropost topography on hMSC gene expression. Gene expression is assessed by microarray and RT-PCR for focal adhesions, cytoskeleton and matrix remodeling genes.

**Hypothesis 2.** Sustained delivery of MGF peptide from microrods attracts stem cells and reduces apoptosis of myocytes.

**Specific Aim 2a.** Test the delivery of MGF from the microrods. The MGF elution was assessed at day 1, 2, 4, 7, 14, and 21 by HPLC.

**Specific Aim 2b.** Test the effects of migration of hMSC towards MGF eluting from microrods for 20 hours. Migration is assessed by Boyden chamber with 8  $\mu$ m insert with cells cultured on top and the MGF-rods on the bottom. MGF added in media and empty rods are positive and negative controls.

**Specific Aim 2c.** Test the effects of interaction of hMSC and MGF-rods in terms of proliferation and morphology. Proliferation is tested by EdU and cytoskeleton and focal adhesion organization is assessed by actin and paxillin.

**Specific Aim 2d.** Test the effects of MGF elution from the microrods on NRVM apoptosis under hypoxia. NRVM are cultured under 1% O<sub>2</sub> for 8 hours. Cell viability and apoptosis are determined by TUNEL assay and RT-PCR to detect the level of anti-apoptotic gene Bcl-2 after stress.

## II. CYCLIC STRAIN DOMINATES OVER MICROTOPOGRAPHY IN REGULATING CELLULAR FUNCTION OF HUMAN MESENCHYMAL STEM CELLS

### A. Introduction

Stem cells have become a major focus for regenerative medicine. Among the different types of stem cells, human bone-marrow-derived mesenchymal stem cells (hMSCs) are an attractive cell source for regeneration of damaged tissue. They are known to differentiate into a variety of cell types, such as osteoblasts, adipocytes, chondrocytes, ligament cells, and smooth muscle cells. Their function depends not only on chemical factors but also physical cues of the microenvironmental niche. The niche can be considered as a combination of structural and cellular components that vary from one tissue to another to control proliferation and differentiation (Spradling, 2001). Nonetheless, precisely how mechanical parameters in the physical microenvironment affect cellular function is not yet well understood.

Cells remodel in response to changing mechanical loads that can influence gene expression patterns during development (Wozniak, 2009). Most cells are continuously subjected to physical stresses and mechanical forces from the external environment, which may regulate proliferation and gene expression (Gwak, 2008, Lee, 2007). In particular, the morphology, proliferation, and differentiation of mesenchymal stem cells are affected by mechanical stimuli (Jang, 2011, Nieponice, 2007). Cells in most tissues are in a three-dimensional (3D) environment. Therefore, in addition to cyclic mechanical stimuli to cells, it is desirable that the 3D microtopography begin to match the conditions *in vivo*. Cells are known to recognize topographical features and adapt by a



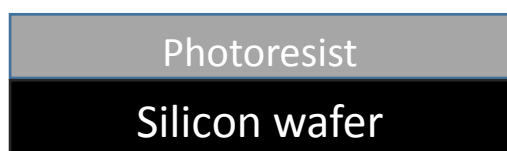
phenomenon called contact guidance (Rorth, 2011). Cellular processes affected by engineered microtopography in culture include cell adhesion, and proliferation (Boateng, 2003). Microtopography also affects the subcellular cytoskeleton and differentiation (Motlagh, 2003a; Motlagh, 2003b, Biehl, 2009).

Cells are sensitive to passive and active physical stimuli via external forces (eliciting outside-in signaling) and by forces generated in the cell (inside-out signaling) (Holle, 2011). External perturbation of force can occur *in vivo* with shear stress, extension, or compression (Chen, 1999, Ingber, 1997, Szafranski, 2004). Forces generated by motor proteins can reorganize the cytoskeleton in response to external stiffness, surface topography, or ligand density (Pelham, 1998, Xiao, 1996). In this study, we recapitulate the mechanical strain in 3D found *in vivo*. The effects of the combination of both external cyclic strain and the impact of 3D microtopography on cells are studied on cytoskeletal organization, focal adhesions, proliferation, and gene expression.

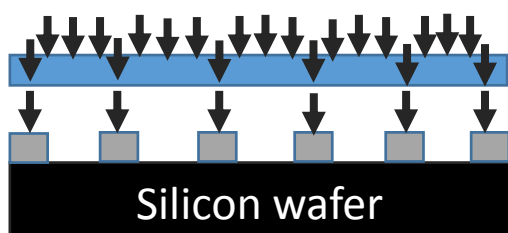
## **B. Materials and methods**

### **i. Fabrication of microtopographic substrata**

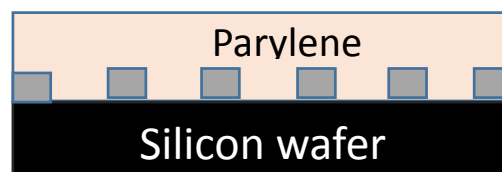
Microtextured surfaces with (15  $\mu\text{m}$  height, and 15  $\mu\text{m}$  diameter and 75  $\mu\text{m}$  spaced) projections were created using photolithography in the Nanocore facility Lab at UIC (Figure 5). This specific pattern was printed on the mask. To ensure that the photoresist does not delaminate from the silicon wafer, approximately 1 ml of hexamethyldisilazane was spun on a clean wafer at 6000 RPM for 50 seconds. Then a quarter sized droplet of negative photoresist (SU-8 2015, Microchem) was spun on the surface at 2700 RPM for 30 seconds to create a 15  $\mu\text{m}$  thick layer. The thickness of the SU-8 photoresist

**A**

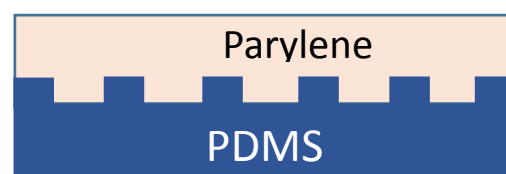
1) Spin photoresist on silicon



2) Pattern photoresist with UV



3) Deposit parylene



4) Cure the patterned PDMS with the parylene template

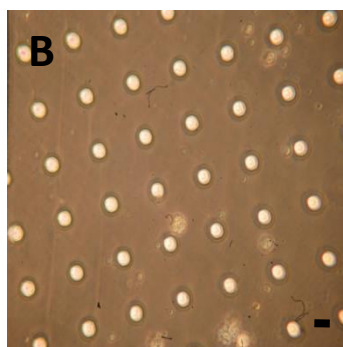


**Figure 5.** Microfabrication of the micropost topography. (A) Skematic of microfabrication of the PDMS posts (B) Phase image of the PDMS membrane with posts, scale bare, 20  $\mu\text{m}$

determines the height of the resulting posts. A soft bake followed in which the wafer was put on a 65°C hotplate for five minutes, transferred to 95°C hotplate for an additional five minutes before returning back to the 65°C for then seconds.

The SU-8 was then patterned by passing ultra violet (exposure energy of 140 mJ/cm<sup>2</sup> for 15 µm thick SU-8), light through the desired transparency kept flush against the wafer with a quartz glass weight for 24 seconds. The wafer was baked again at 65°C for five minutes and 95°C for seven minutes more. The wafer was placed in developer (Microchem) with continuous shaking motion for approximately 60 seconds and rinsed with isopropyl alcohol and blow dried with compressed air.

Before exposure to light, the height of the photoresist material can be controlled by the rate at which the material is spin-coated onto the silicon wafer. The incident light energy (J/cm<sup>2</sup>) which controls the extent to which the resist is cross-linked, is determined by multiplying the light intensity (W/cm<sup>2</sup>) by the exposure time (seconds). Areas of a negative photoresist that are exposed to UV light cross-link, and developer solution is used to rinse away undeveloped photoresist. Then, parylene is deposited on the patterned SU-8 wafer, and peeled off from the wafers ultimately, so the parylene mold could be used to make the patterns of the topography on the Liquid polydimethylsiloxane (PDMS).

The ratio of curing agent to silicon elastomer base was 1:10, which gives the Young's Modulus of about 1.7 MPa. PDMS was spread over the BioFlex plates, and the parylene mold was placed on top of the PDMS layer, which was about 1 mm thick, cured, and gently removed, resulting in flat or textured elastomeric membranes in the flex dishes. Flat two-dimensional sheets of PDMS were used as a control for the same surface

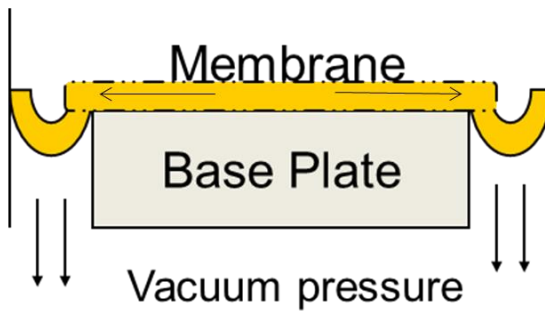
properties. As a result, PDMS post was created on top of the BioFlex plates in 15- $\mu$ m-high with tetragonal spacing 75- $\mu$ m center to center (Figure 6). PDMS membranes were treated with hydrochloric acid (11M, HCL) for one hour to remove contaminants and make the surface hydrophilic by hydrolysis of Si-O-Si bonds. The membranes were soaked in water for 5 minutes and placed in an oven for 2 hours at 45°C to dry. The membranes were then sterilized in ethanol and UV light for one hour

The posts were circular with a 15- $\mu$ m diameter. For cellular attachment to PDMS, all the flat and microtopography surfaces were treated with laminin (Invitrogen) at a concentration of 10  $\mu$ g/ml. In order to assess the uniformity of laminin distribution on the flat and microtopographic substrata, anti-laminin antibody produced in rabbit (Sigma) was incubated over night at a dilution of 1:25, and followed by the secondary antibody Alexa Fluor 568 conjugated goat-anti-rabbit antibody (Invitrogen) at a dilution of 1:200 for 30 min. All flat textured surfaces were uniformly coated with laminin as seen by confocal microscopy (Figure 7)

## **ii. Cell culture**

Institutional approval was received to obtain and use mesenchymal stem cells (hMSCs) isolated from human bone marrow aspirates from Texas A&M Health Science Center College of Medicine Temple, TX. Microarray analyses indicate that gene expression is consistent for hMSCs from different donors, isolated and expanded as described

A



B

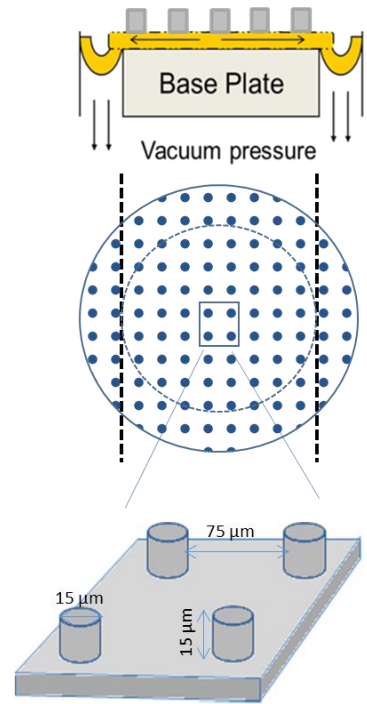


**Figure 6.** Schematic of straining the microposts. (A) Diagram of the FlexCell apparatus and vacuum system and (B) the BioFlex plates with the PDMS posts on the top layer. The equibiaxial stimulation was found to deliver a large central circular region of equal and constant tensile  $e_{rr}$  (radial), and  $e_{\theta\theta}$  (circumferential) on the base plate (isotropic strain), but the equibiaxial stimulation resulted in large  $e_{rr}$  and smaller  $e_{\theta\theta}$  on the circumferential region off the base plate (anisotropic strain). The radius of the flexible membrane of the Flexcell plates is 17.5 mm and the radius of the region on the base plate is 12.5 mm, leaving the peripheral 5 mm annulus subject to anisotropic strain.

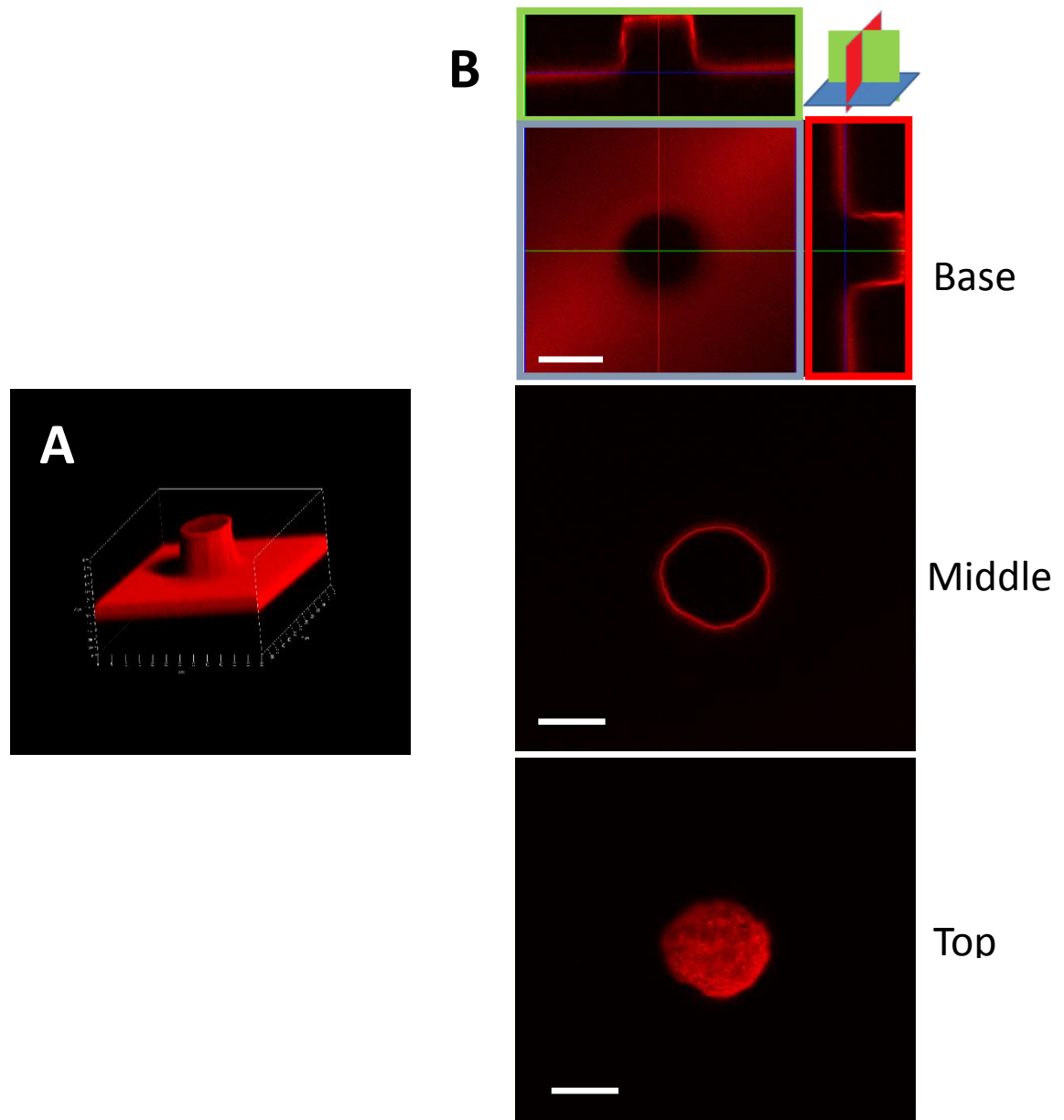


**Figure 7.** Uniform laminin coating of the microposts. (A) 3D image of a post 15  $\mu\text{m}$  high, and 15  $\mu\text{m}$  diameter with laminin coating (B) Uniform laminin staining on flat base, middle and top sides of a post seen by confocal microscopy, scale bar, 20  $\mu\text{m}$

previously (Collins, 2010). Experiments were performed on passage three or lower from hMSCs obtained from 3 separate donors. hMSCs were cultured in complete culture media (CCM) consisting of MEM- $\alpha$  supplemented with 16.5% fetal bovine serum (FBS), 2 mM L-glutamine, 100 units/mL penicillin and 100  $\mu$ g/mL streptomycin, and incubated at 37 °C.

### **iii. Cyclic strain**

After two days of cell culture, hMSCs were cyclically strained with 10% strain at 1 Hz for 48 hours in cell culture media using the Flexcell Strain Unit (Model FX-4000, Flexcell International, McKeesport, PA) (Figure 6A). The base plate with a diameter of 25 mm was used to produce equibiaxial strain for ~ 70% of the area (Fig. 6B). The computer system controlled the frequency of deformation and the negative pressure applied to the culture plates. There are four conditions in this study: Flat (control group), flat-strain, post, and post-strain. All the four conditions were cultured on the flexcell plates and kept in the same incubator.

### **iv. Distribution of cells upon plating by time lapse movie**

After plating the hMSCs on the flat and microtopography substrata, in order to determine the initial distribution of hMSCs on the flat or microtopographic substrata, time lapse movies were recorded using Olympus VivaView Incubator over 12 hours. However, due to the limitations, we could not record the time lapse movie of the cells

while they were strained. A frame is recorded every 5 min and played back 2300 times faster in the movies (Doroudian, 2013, movies are in the supplemental data).

#### **v. Proliferation**

To assess cell proliferation after 48 hours of strain: 1 hours incorporation of 5-ethynyl-2'-deoxyuridine was used (EdU, 10 mM, Invitrogen Corp.). EdU stains the new synthesis of DNA. Once incubation was complete, EdU incorporation was tested with EdU flow cytometry and EdU imaging kits. For imaging, the PDMS membranes which the cells were attached were cut from each dish before staining, and then mounted onto glass slides to stain the cells with 4', 6-Diamidino-2-phenylindole (DAPI) for nuclear staining. However, note that the equibiaxial stimulation was found to deliver a large central circular region of equal and constant tensile  $e_{rr}$  (radial), and  $e_{\theta\theta}$  (circumferential) on the base plate (isotropic strain), but the equibiaxial stimulation resulted in large  $e_{rr}$  and smaller  $e_{\theta\theta}$  on the circumferential region off the base plate (anisotropic strain) (VandeGeest, 2004). The radius of the flexible membrane of the Flexcell plates is 17.5 mm and the radius of the region on the base plate is 12.5 mm, leaving the peripheral 5 mm annulus subject to anisotropic strain.

#### **vi. F actin to G actin measurement**

Cells are harvested by lysis buffer and grouped in normal control, flat (F), positive control (Positive C), negative control (Negative C) and the experimental groups as post (P), flat-strain (FS), and post-strain (PS). 1  $\mu$ M of F-actin enhancing solution (100  $\mu$ M



phalloidin), and 10  $\mu$ M of F-actin depolymerization solution (1 mM Cytochalasin-D) was added to the positive control and the negative control respectively. The lysates were centrifuged at 2000 rpm for 5 min to pellet unbroken cells. The pellets were resuspended in to the same volume as the supernatant using ice cold Milli-Q water plus 10  $\mu$ M of Cytochalasin-D. In order to dissociate F-actin, every 15 min the pellets were sheared. Supernatant and pellet samples were diluted with 4  $\mu$ l of SDS buffer and heated to 95  $^{\circ}$ C for 2 min. The samples were loaded onto a 12% SDS-polyacrylamide gels and electrophoresed to separate the samples based on molecular mass followed by blotting the gel onto a nitrocellulose membrane. Ratio of F-actin to G-actin was determined by scanning densitometry from the X-ray film as shown in Figure 12.

#### **vii. Actin, focal adhesion, and nucleus staining**

In order to analyze subcellular features, cells were fixed with 4% paraformaldehyde in phosphate buffered saline (PBS) for 10 min at room temperature, rinsed three times with PBS and permeabilized by 0.1% Triton X-100 in PBS for 10 min, and washed 3 times with PBS. Cells were pre-incubated in blocking solution (PBS, 1% bovine serum albumin (BSA)) for 15 min and then incubated with rhodamine conjugated phalloidin (Molecular Probes) at a dilution of 1: 400 to stain actin, or paxillin anti-rabbit antibody (Abcam) at a dilution of 1:250 for 1.5 hours followed by another incubation with secondary antibody Alexa Fluor 488 conjugated goat-anti-rabbit antibody (Invitrogen) at a dilution of 1:1000 for 45 min to stain the focal adhesions of the cells. DAPI (Sigma) was used for nuclear staining.

### **viii. Actin and nuclear distribution from post**

The location of actin and nuclei as a function of distance from the post was determined morphometrically at intervals of 15  $\mu\text{m}$ , 22.5  $\mu\text{m}$ , 30  $\mu\text{m}$ , and 37.5  $\mu\text{m}$  on a line drawn from post to post. The presence of actin was tallied by detectable phalloidin staining at the given distances from the post. For nuclear distribution, the region less than 37.5  $\mu\text{m}$  from center of the post was considered as the “close” region, and beyond that was called the “far” region. In all, over 60 posts in 3 samples were pooled for frequency distribution and statistical analysis

### **ix. Imaging**

A Nikon TMS inverted phase-contrast microscope was used to observe hMSC cultured on post substrata with or without strain. Confocal images were obtained with Zeiss LSM 510 META and LSM 710 microscopes. The images were analyzed using the Cell Counter plug-in for the ImageJ software program (NIH). The nuclear surface area and the length/width were determined from Image J.

### **x. DNA, RNA isolation and reverse transcription**

Total DNA and RNA were isolated from hMSCs from the experimental conditions of flat, flat-strain, post, and post-strain. After two days of strain, the AllPrep DNA/RNA Mini Kit (QIAGEN) was used to isolate DNA and RNA per manufacturer’s protocols. DNA and RNA concentration was quantified using the Qubit Quantitation Platform (Invitrogen). RNA was reverse-transcribed for 50 min at 37  $^{\circ}\text{C}$  and 15 min at 65  $^{\circ}\text{C}$  (inactivation)

using M-MLV Reverse Transcriptase (Invitrogen) and a thermal cycler (BioRadCycler, Hercules, CA).

#### **xi. Microarray analysis**

For microarray analysis, total RNA was pooled from five independently prepared cultures of hMSCs with or without post and strain, and the control. RNA was labeled, hybridized onto 3 microarray chips per condition (Human Gene Chip ST. 1.0, Affymetrix, Santa Clara, CA) and scanned by the Genomics Core Facility at the University of Illinois at Chicago. All hybridizations passed standard quality criteria. Raw data and probe intensity levels were normalized within the DNA-Chip Analyzer (dChip) as based on the median baseline intensity of the whole array (Li, 2001). All subsequent pair wise analysis was also performed using dChip. For pair-wise comparisons, statistically significant, differentially expressed transcripts were identified by raw local-pooled-error (LPE) test p values. For global functional clustering analysis a list of the genes was imported into the DAVID Functional Annotation Clustering tool (<http://david.abcc.ncifcrf.gov>). Raw LPE test p-values were then corrected for False Discovery Rate by the Benjamini–Hochberg (BH) procedure (p-value <0.05). The "heat map" was obtained by the dChip Windows software.

#### **xii. Quantitative RT-PCR**

For RT-PCR experiments, total RNA was isolated and reverse transcribed, as described above, from independently prepared flat or strained hMSCs with or without posts but without pooling. Experiments were performed with the SYBR Green PCR Master Mix

and a 7500 Fast Real-Time PCR System (Applied Biosystems, Foster City, CA).

Amplification was achieved by the following protocol: 1 cycle of 50 °C for 2 min; 1 cycle of 95 °C for 10 min; 0 cycles of 95 °C for 15 s and 60 °C for 1 min. To ensure specificity of PCR, melt-curve analyses were performed at the end of all PCRs. The relative amount of target cDNA was determined from the appropriate standard curve and divided by the amount of  $\beta$ 2-microglobulin ( $\beta$ 2M) cDNA present in each sample for normalization. Each sample was analyzed in triplicate, and results were expressed relative to control condition. The primer sequence (Sigma Aldrich) is shown in table 1.

### **xiii. Data analysis**

Data were expressed as mean  $\pm$  SD (n= 3 or more experiments). Differences were analyzed by the Student's paired and unpaired t-test with significance at  $P < 0.05$ .

## **C. Results**

In this study, hMCSs were exposed to various mechanical forces to explore the effects of physical cues while retaining chemical conditions constant. Changes in cell and nuclei morphology, proliferation, focal adhesions, and gene expression of hMSCs were assessed for four conditions: flat (F), flat-strain (FS), post (P), and post-strain (PS).

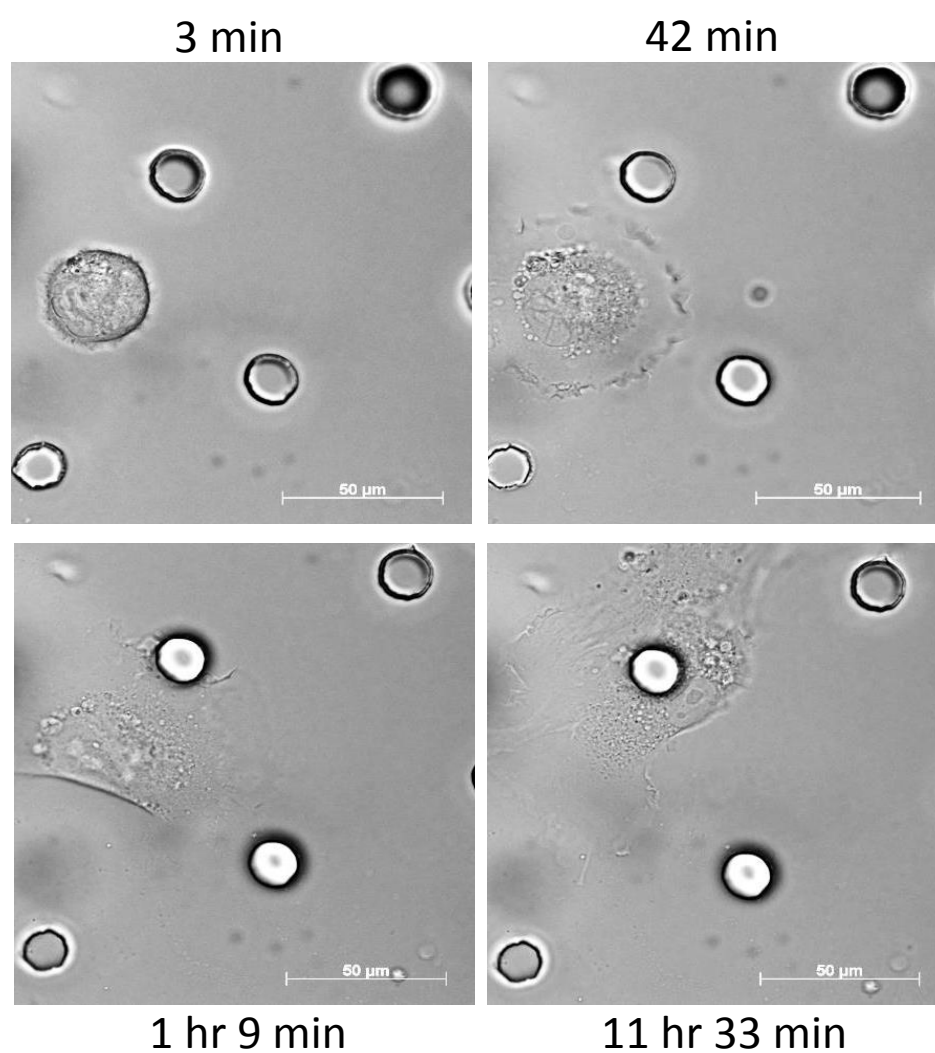


**Figure 8.** Time lapse images of interaction of hMSCs with microposts. The images show initial migration and preferential adhesion of a cell to a post during the following 12 hours, scale bar, 50 μm

**Table I**  
**PRIMERS USED FOR qPCR CONFIRMATION OF MICROARRAY RESULTS**

<b>Gene</b>	<b>Forward</b>	<b>Reverse</b>
Beta 2 Microglobulin	tttcatccatccgacattga	cctccatgatgctgcttaca
MMP13	tcccaggaattggtgataaagtaga	ctggcatgacgcgaacaata
PAXILLIN	aactggttgaagggtgttc	agggtcagtgggttcacagg
VINCULIN	cttgctgctacaggggaag	ggatatgggacgggaagttt
INTEGRIN- $\alpha$ 2	gggcattgaaaacactcgat	tcggatccaagattttctg
CALDESMON1	gcagaaaagcagtggtgtca	ccttcagcaggaacaggaag
CALPONIN3 (acidic)	atggcgagtaccaggatgac	tgagggaagaggcagaaaaa
Ki67	aagccctccagctcctagtc	tccgaagcaccacttcttct
SOX9	ttgagccttaaaacggtgct	ctggtgttctgagaggcaca

### **i. The time lapse images**

Random migration of a cell towards a post is shown at different time points (Figure 8). These images clearly show the preferential attachment of a cell to a post. At 1 hour and 33 min, the cell can even reach the adjacent post, but at 1 hour and 54 min, the cell wraps around the original post. We are aware that the microtopography was 12.5% of the flat surface, and the distance between the adjacent posts was 75  $\mu\text{m}$ , however, the images from the time lapse movie show cell to a post and even a post to post interaction, and therefore the microtopographic substrate recapitulated the cellular scale texture to the cell. Moreover, results showed that hMSCs would ignore the posts if the height of the posts was less than 15  $\mu\text{m}$  (Figure 9).

### **ii. The actin cytoskeleton**

After two days of cyclic strain, morphology of the hMSCs changed in the experimental conditions (Figure 10). Actin distribution was remodeled with respect to both strain and microtopography (Figure 11). Cells on flat surfaces contained thin layers of actin (Figure 11A); however, by straining the cells (FS), intensely-stained bundles of actin stress fibers were observed, which elongated the cell shape (Figure 11B). The cells in unstrained 3D microtopography had a high intensity of the actin wrapped closely around the post (Figure 11C). Straining hMSCs on the microtopographic substrata resulted in actin stress fibers that span the 75  $\mu\text{m}$  from post to post (Figure 11D). Actin distribution was measured morphometrically and the frequency of distribution calculated as a function of the distance from the post. The distribution was similar with or without strain

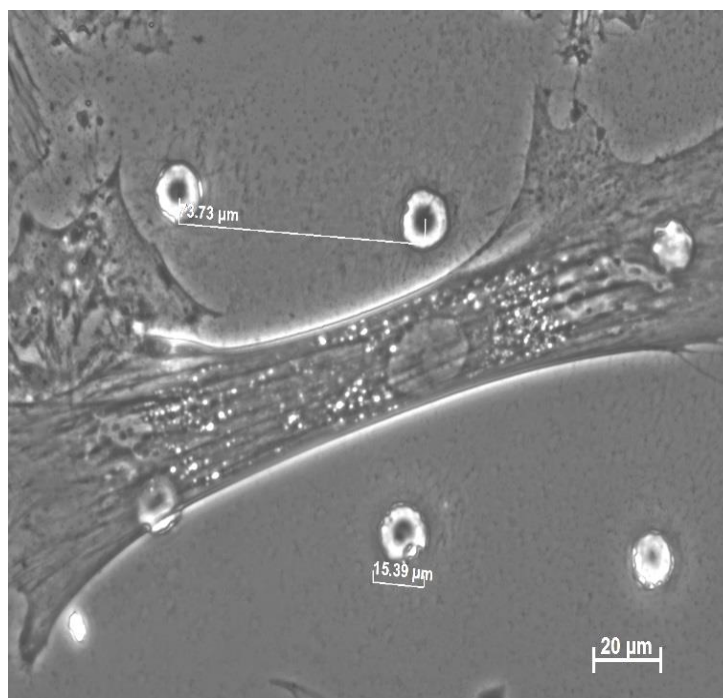


**Figure 9.** A phase image of hMSCs cultured on the microposts with less than 15 μm height. The image shows that cells ignore the posts if the height is less than 15 μm; the cells behave as they are on a flat surface, scale bar, 20 μm



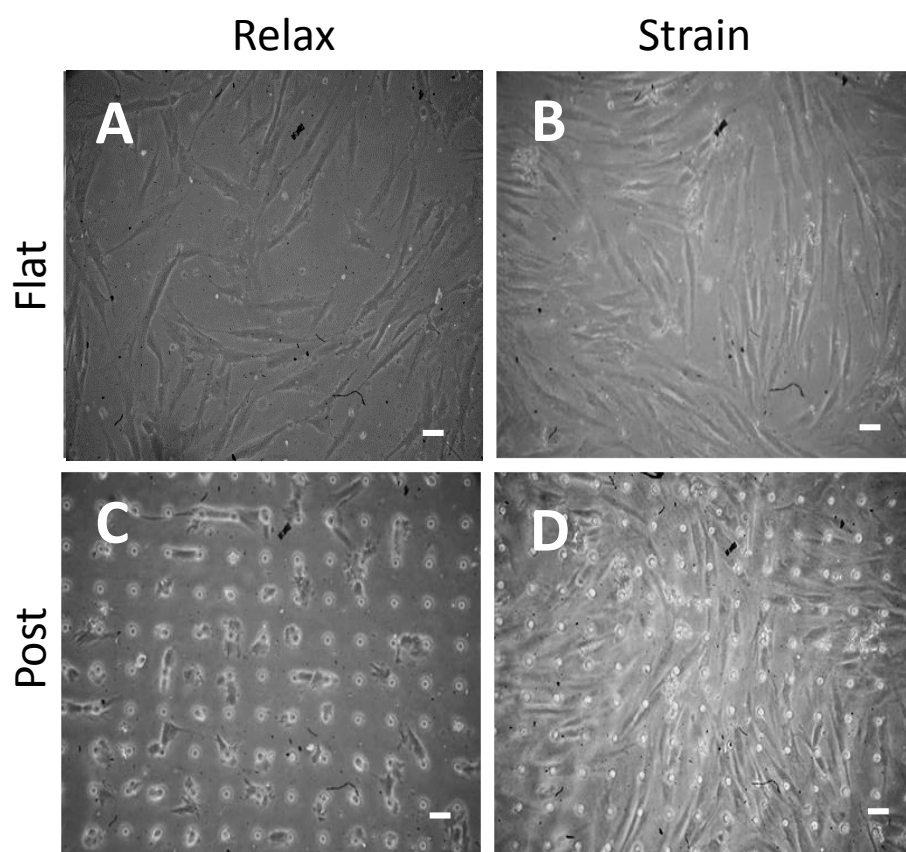


**Figure 10.** Morphology of hMSCs change with microtopography and strain. Phase images show that morphology of hMSCs vary with micropost and strain after two days of 10% cyclic strain at 1 Hz, scale bar, 50  $\mu\text{m}$

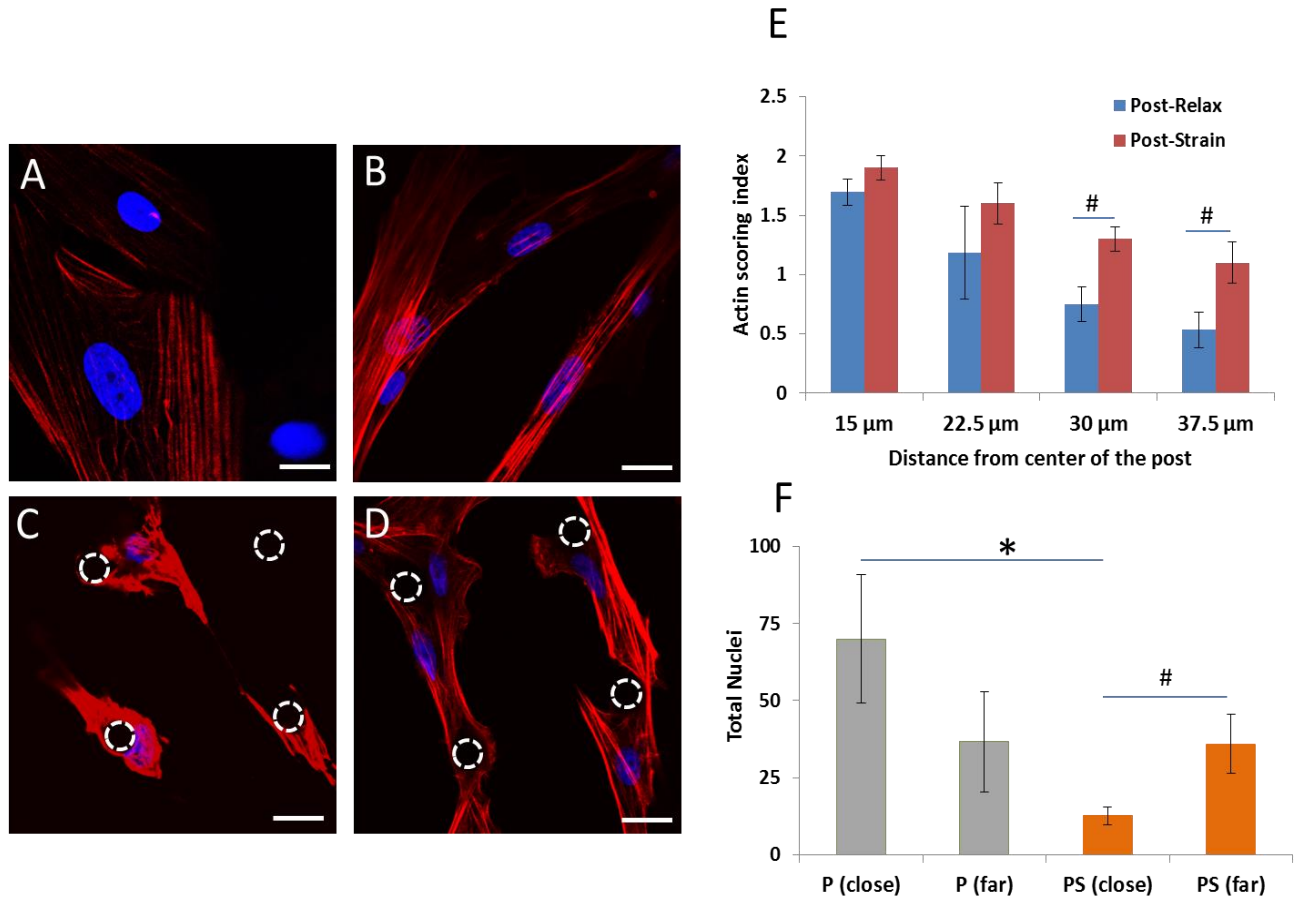


**Figure 11.** Actin remodels with microtopography and strain. Actin cytoskeleton and nuclei of hMSCs (A) Flat, (B) Flat-Strain, (C) Post, and (D) Post-Strain, seen with confocal microscopy after 2 days of strain at 1 Hz and 10%. (C) The cells containing actin fibers are wrapped around the post. (D) The actin fibers are elongated in the cells and span from post to post. (E) Frequency histogram of actin distribution at 15  $\mu\text{m}$ , 22.5  $\mu\text{m}$ , 30  $\mu\text{m}$ , and 37.5  $\mu\text{m}$  from post center. (F) Nuclear distribution shifted from close <37.5  $\mu\text{m}$  to far >37.5  $\mu\text{m}$  regions from a post with cyclic strain; The microtopographic substrata is 12.5% of the flat surface, and the result shows that in “post” and “post-strain”, 33% and 70% of the cells are on the “flat region”, respectively. The dashed circles indicate the location of post. Actin stained by rhodamine phalloidin (red); nuclei with DAPI (blue). Mean  $\pm$  SE, n=3 samples,  $p < 0.05$ . Scale bar, 20  $\mu\text{m}$

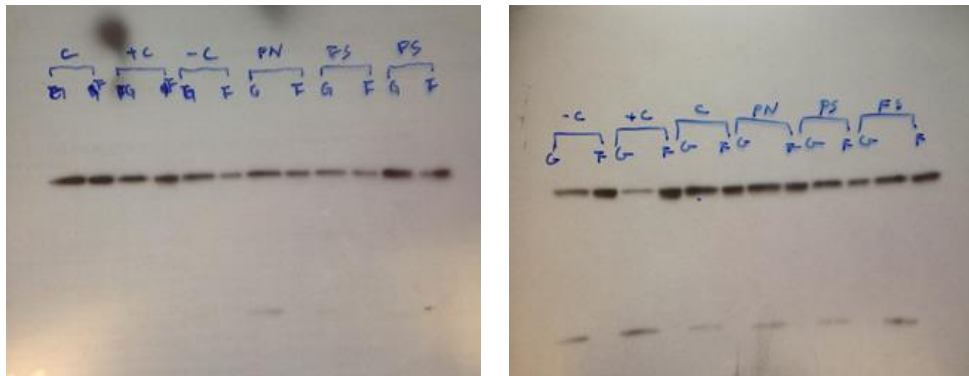
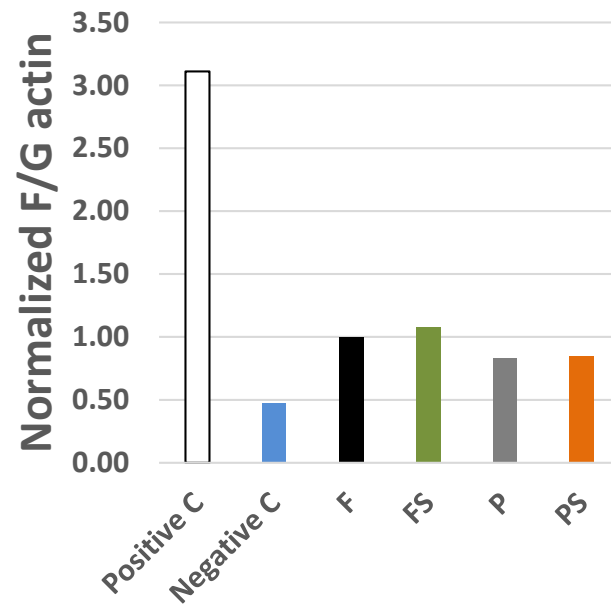


**Figure 12.** F actin to G actin ratio did not change with micropost and strain. F actin to G actin ratio was determined in order to determine the actin formation or disassembly with post and strain. The results show no significant difference between the conditions (n=2)

nearer to the post (15  $\mu\text{m}$  and 22.5  $\mu\text{m}$ ), but significant differences between the post and post-strain groups were found further away (30  $\mu\text{m}$  and 37.5  $\mu\text{m}$ ) (Figure 11E).

In addition, results showed no significant difference in F to G actin ratio between the conditions which suggests no new actin assembling occurs within this time frame with strain and posts (Figure 12).

### **iii. Nuclear shape, size and distribution**

The nuclear surface area decreased and nuclear length/width ratio increased with both strain and microtopography as seen in the images (Figure 13) and confirmed by measurements (Figure 13A and 13B). Control hMSCs have large, flat, rounded nuclei compared to the other groups where the nuclei appear smaller and more elliptical seen from above (Figure 11). In addition, the nuclei of the cells that were located close to the posts had increased height (Figure 13C). Adding strain to microtopography shifted the nuclei to the center of the cell midway between the adjacent posts (Figure 11F).

### **iv. Proliferation**

On flat surfaces, hMSCs were weakly proliferative (Figure 14A). Cells grown on the posts were also slow to divide, showing low EdU staining (Figure 14D) and a relatively smaller count (Figure 14G). Cells also showed marked differences in EdU incorporation that depended on their location on the flex dish. The BioFlex system delivers isotropic, biaxial strain to the central region but at the peripheral 5 mm annulus it is anisotropic. As expected, in the region off the base plate, when strained anisotropically the cells

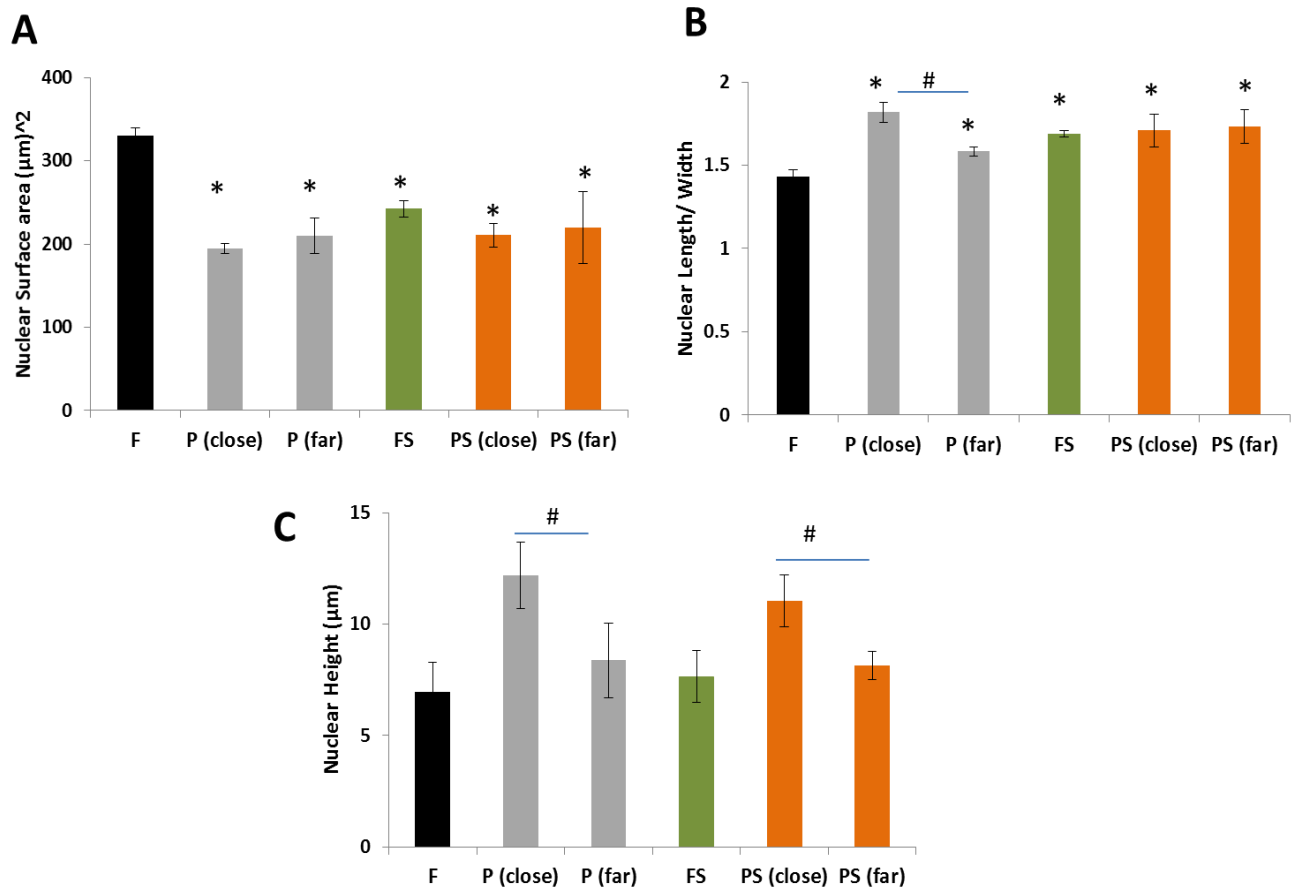


**Figure 13.** Nuclear shape and size with strain and distance from microtopography. Flat (F), Post (P), Flat-Strain (FS), and Post-Strain (PS). Close region is  $<37.5 \mu\text{m}$  and far region is  $>37.5 \mu\text{m}$  from center of a post. (A) Nuclear surface area decreased with post and strain. (B) Nuclear length/width increased with post and strain. (C) Nuclear height increased close to a post. Mean  $\pm$  SE,  $n=4$  samples. \* All vs. flat (control), # close vs. far,  $p < 0.05$

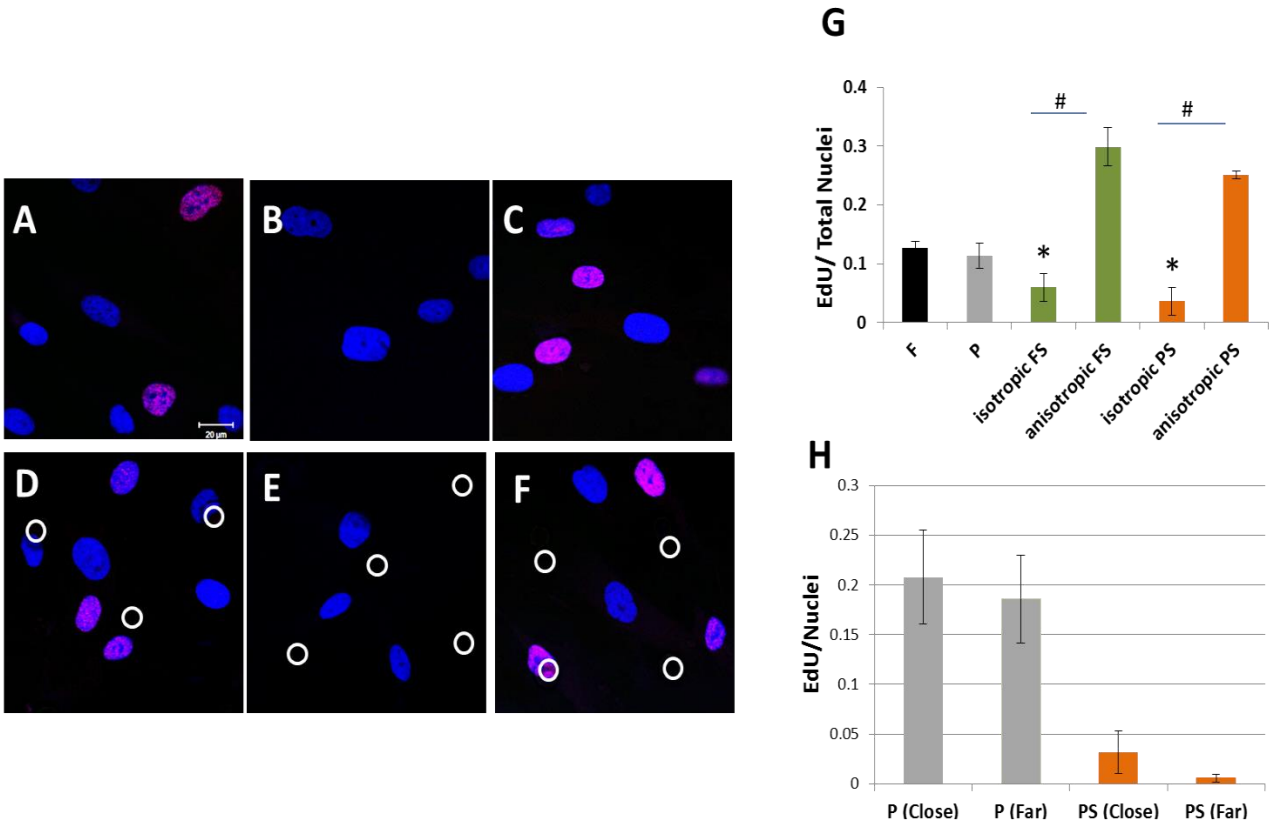


**Figure 14.** Proliferation of hMSCs is increased with strain. Confocal images show newly dividing cells (pink) vs. non-dividing cells (blue). (A) Flat (B) cells in central, flat-isotropic strained region, (C) cells in peripheral, flat-anisotropic strain region, (D) Post, (E) isotropic Post-Strain, and (F) anisotropic Post-Strain. (G) EdU/ total nuclei per condition shows that anisotropic strain increased the proliferation, and isotropic strain inhibited. (H) Proliferation did not change if a cell is close (<37  $\mu$ m) or far from the post (>37  $\mu$ m). Dividing nuclei stained with EdU (red) positive and all nuclei DAPI (blue). Mean  $\pm$  SE, n=4. \* All vs. flat, # isotropic vs. anisotropic, p < 0.05, scale bar, 20  $\mu$ m

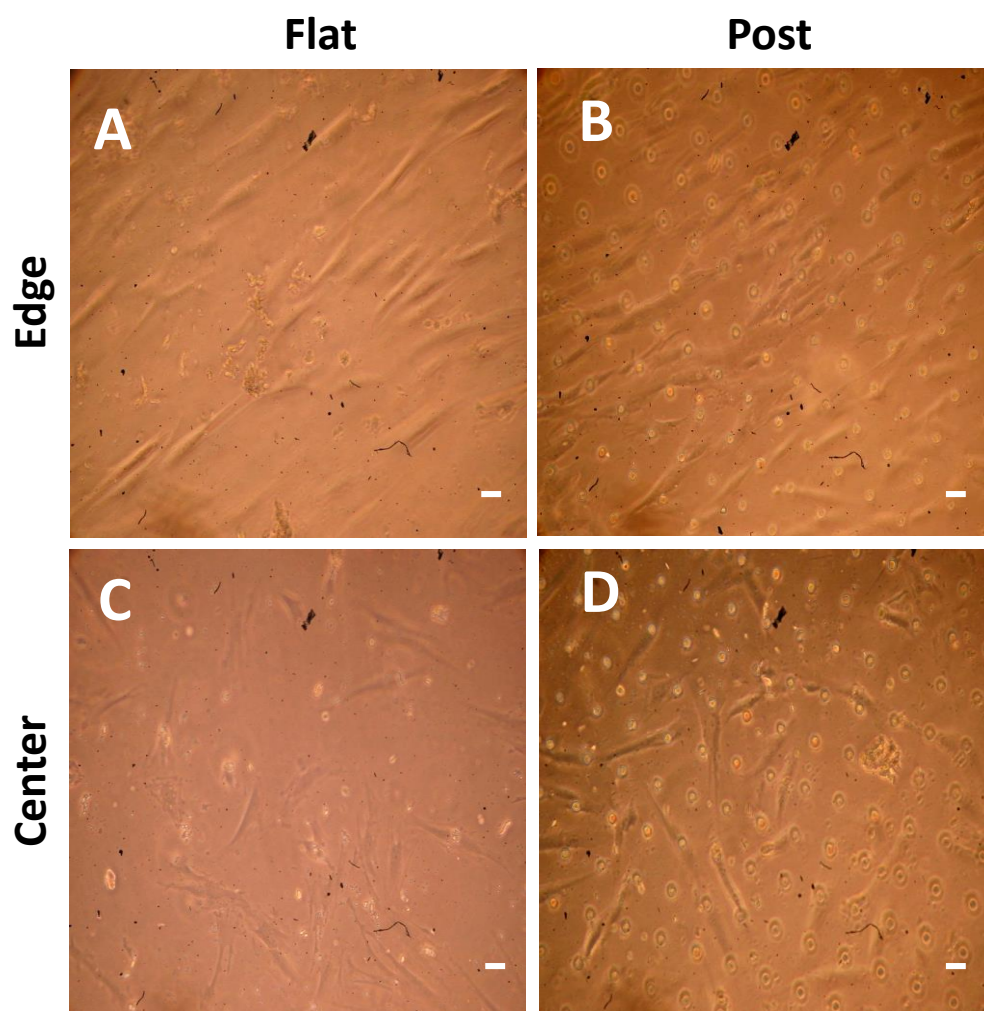


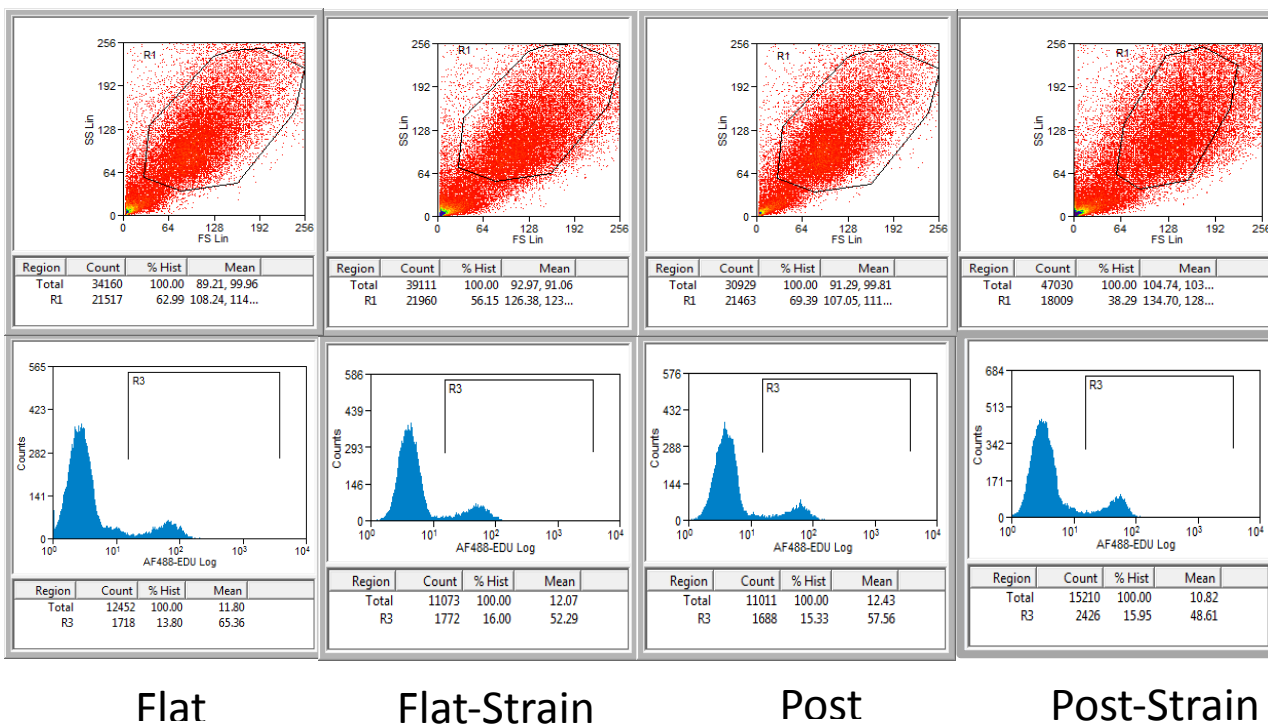
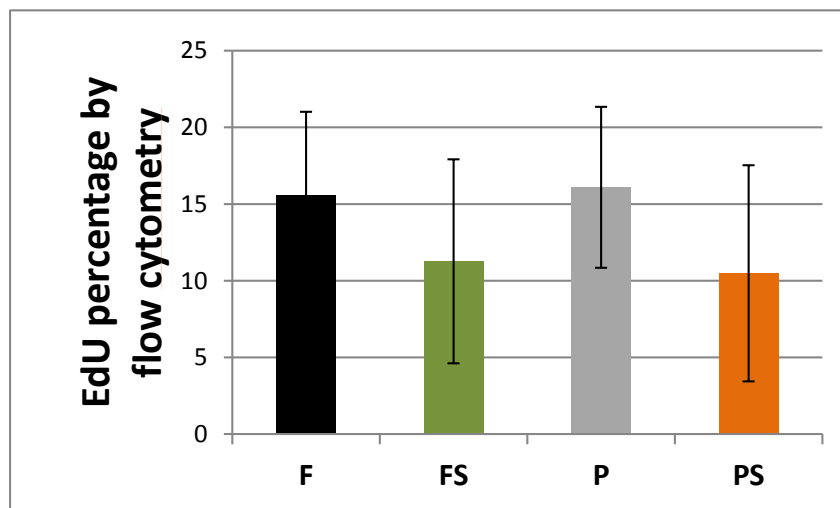
**Figure 15.** hMSC morphology with isotropic and anisotropic strain. (A) and (B) The cells on flat and post showed preferential alignment in the region off the base plate when strained anisotropically, seen with the phase images with the cell long axis being perpendicular to the strain direction. (C) and (D) The cells on flat and post were randomly oriented when strained isotropically, scale bare, 50  $\mu\text{m}$

showed preferential alignment seen with the phase images with the cell long axis being perpendicular to the strain direction (Figure 15). The cells grown on the edge of the BioFlex plates thus experienced the anisotropic strain and also showed significantly more proliferation than the cells cultured on the central regions where strain inhibited proliferation below that of unstrained cells with or without posts (Figure 14B, C, E- G). The results from the EdU flow cytometry showed no significant difference on proliferation between the conditions. This assay was not an appropriate analysis for this type of experiment. One reason was that proliferation could not be analyzed based on the cellular localization (e.g. close or far from the posts; center or edge of the membrane), and another reason was that due to the heterogeneous population of hMSCs (small vs. large cells), there were varieties in the results (Figure 16).

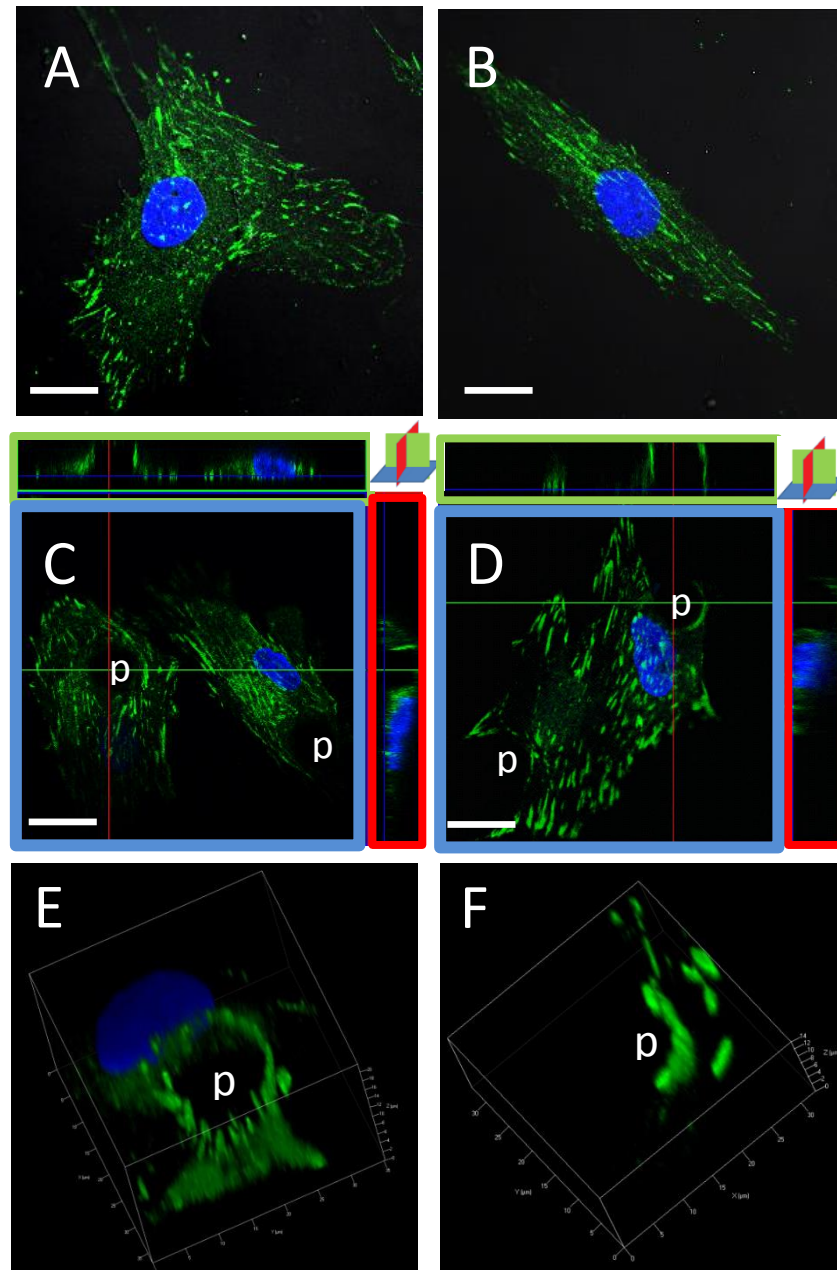
## **v. Focal adhesions**

Force-sensitive adhesion components include vinculin, talin, and paxillin. In this study, focal adhesions were identified by paxillin. Microtopography and strain both alter the distribution of paxillin. On flat, unstrained surfaces, paxillin is sparse (Figure 17A); while with strain the paxillin is aligned with the long axis of the cell (Figure 17B). The presence of the post causes a complete ring of paxillin to form, distributed evenly around the post (as seen in top view with Figure 17C); when hMSCs are strained, the paxillin adopts a semicircle appearance near the post (Figure 17D). The cross-sectional views of confocal images (X-Y, X-Z, and Y-Z planes) show paxillin along the vertical walls of the posts in conditions with or without strain (Figure 17C and 17D). Full 3D volume renders show the bright, punctuate paxillin localized on the sides and the top

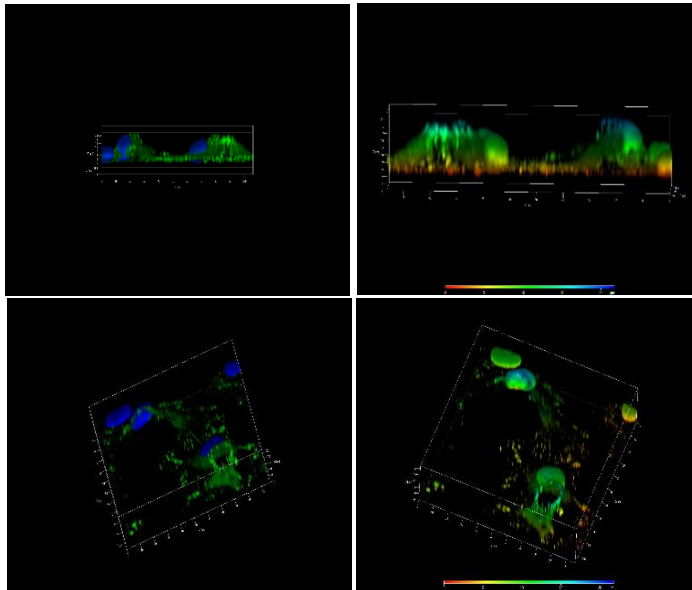
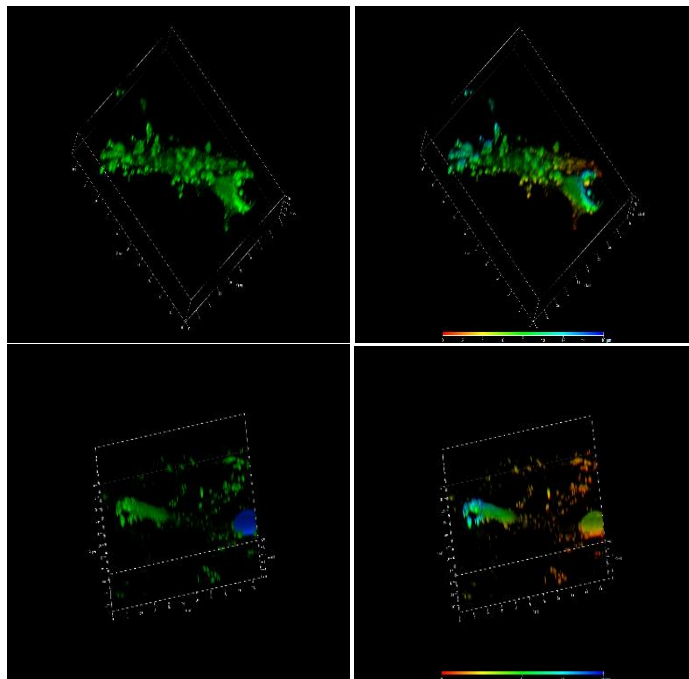


**A****B**

**Figure 16.** Flow cytometry analysis for proliferation. Flow cytometry did not show any significant changes in proliferation of hMSCs between the experimental conditions. This method measures new synthesis of DNA from the whole dish regardless of the position of the cells. Mean  $\pm$  SE,  $n=6$ ,  $p<0.2$



**Figure 17.** Focal adhesions redistributed with microtopography and strain. Paxillin staining of hMSCs after 2 days with or without straining at 1 Hz and 10% strain seen in 3D with confocal microscopy. (A) Flat, (B) Flat-Strain, (C) Post confocal orthogonal views, (D) Post-Strain orthogonal views. Volumetric renditions of 3D for (E) Post and (F) Post-Strain. (C) Paxillin surrounds the post and goes up its full height. (D) Paxillin forms a semicircular ring up the side of the post, and extends from post to post on the lower surface of the cell. (E) and (F) 3D reconstructions show punctate paxillin on the sides of the post. Paxillin (green) and DAPI (blue), scale bar, 20  $\mu\text{m}$

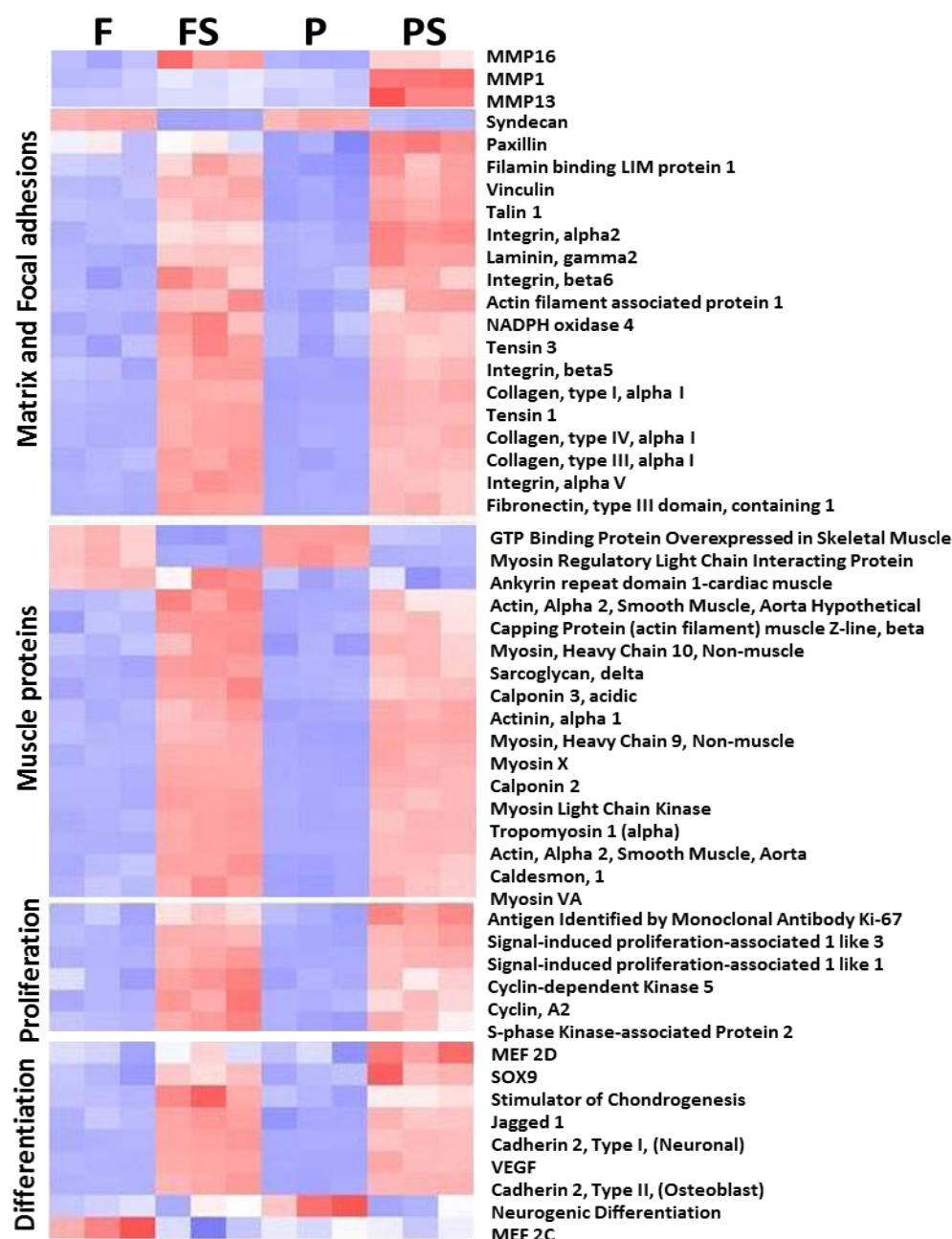
**A****B****Post-Relax****Post-Strain**

**Figure 18.** Optical profilometry of the 3D reconstructions of focal adhesion of hMSC with post-relax and post-strain. Optical profilometry of the 3D reconstructions show other views of focal adhesion distribution with a color coding vs height of a post in (A) post and (B) post-stretch conditions. (The highest point is blue), (green: paxillin, blue:DAPI in the left panels)

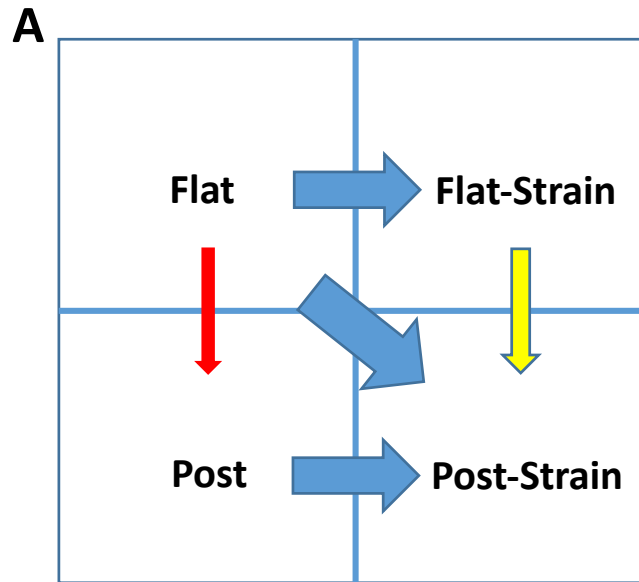
edge of the posts (Figure 17E and 17F). The full interaction of the cells in post and post-strain conditions are shown more clearly in the 3D optical profilometry images due to the color coding vs. height of a post, which blue represents the range greater than 13  $\mu\text{m}$  (Figure 18).

## **vi. Gene Expression**

Microarray results of 31,000 genes reveal many transcript-level differences between hMSCs cultured in the four conditions; namely unstrained, strained, and flat or anchored vertically to the posts. Differentially expressed transcripts were grouped as a “heat map” by hierarchical clustering into enriched functional groups including matrix and focal adhesions, differentiation, muscle proteins, and cell proliferation (Figure 19). Almost 6,000 hMSCs genes were significantly different between unstrained and strained groups, as where 1,000 genes between flat-strain, and post-strain and 500 genes between flat and post were different as filtered by raw p-values  $<0.05$  (Table 2). Number of differentiated genes in gene ontology was determined in the conditions that strain had the most significant effect (Table 3). The red columns (higher relative expression) under flat-strain, and post-strain groups from the “heat map” confirm the dominant effect of strain over microtopography. It is known that hMSCs start as a heterogeneous population of cells, and during the 4 days of the experiments more changes occur. The array data help to assess the overall population shifts under the experimental conditions.



**Figure 19.** "Heat map" with genes sorted to show matrix and focal adhesions, muscle proteins, proliferation, and differentiation. Each row represents a gene, and each column is the control and experimental groups of Flat (F), Flat-Strain (FS), Post (P), and Post-Strain (PS). The red and blue colors indicate the relative high and low expression of the genes, respectively. FS and PS have the most red boxes, and thus the most significant effect of strain.

**Table II****MICROARRAY ANALYSIS OF DIFFERENTIATED GENES****B**

Comparison	Differential expression	Up-regulated	Down-regulated
<b>F-P</b>	<b>485</b>	<b>234</b>	<b>251</b>
<b>FS-PS</b>	<b>1052</b>	<b>703</b>	<b>349</b>
<b>P-PS</b>	<b>6306</b>	<b>4141</b>	<b>2165</b>
<b>F-PS</b>	<b>5986</b>	<b>3984</b>	<b>2002</b>
<b>F-FS</b>	<b>6351</b>	<b>3876</b>	<b>2475</b>

(A) Schematic diagram with arrow width proportional to number of genes that were significantly different ( $p < 0.05$ ) between pairs of the four conditions, showing the dominant effect of strain compared to microtopography. The three blue wide arrows represent about 6,000 genes, the yellow arrow 1,000 genes, and the red arrow 500 genes. (B) Such gene lists show the differential genes between each paired group filtered by microarray data using dChip Software,  $p < 0.05$ .

**Table III**

## GLOBAL GENE EXPRESSION ONTOLOGY ANALYSIS

<b>GO TERM</b>	<b>P- PS</b>	<b>F- FS</b>	<b>F- PS</b>
Skeletal system development	123	122	117
Heart development	98	96	98
Bone development	---	53	---
Cell growth	---	30	---
Actin cytoskeletal organization	110	98	112
Cell migration	114	115	110
Response to hypoxia	58	59	60
Angiogenesis	66	68	67
Blood vessel development	115	118	116

Gene ontology sorted by affymetrix for the paired groups that were affected by strain only. This tables shows the number of differential genes that were regulated between each group.

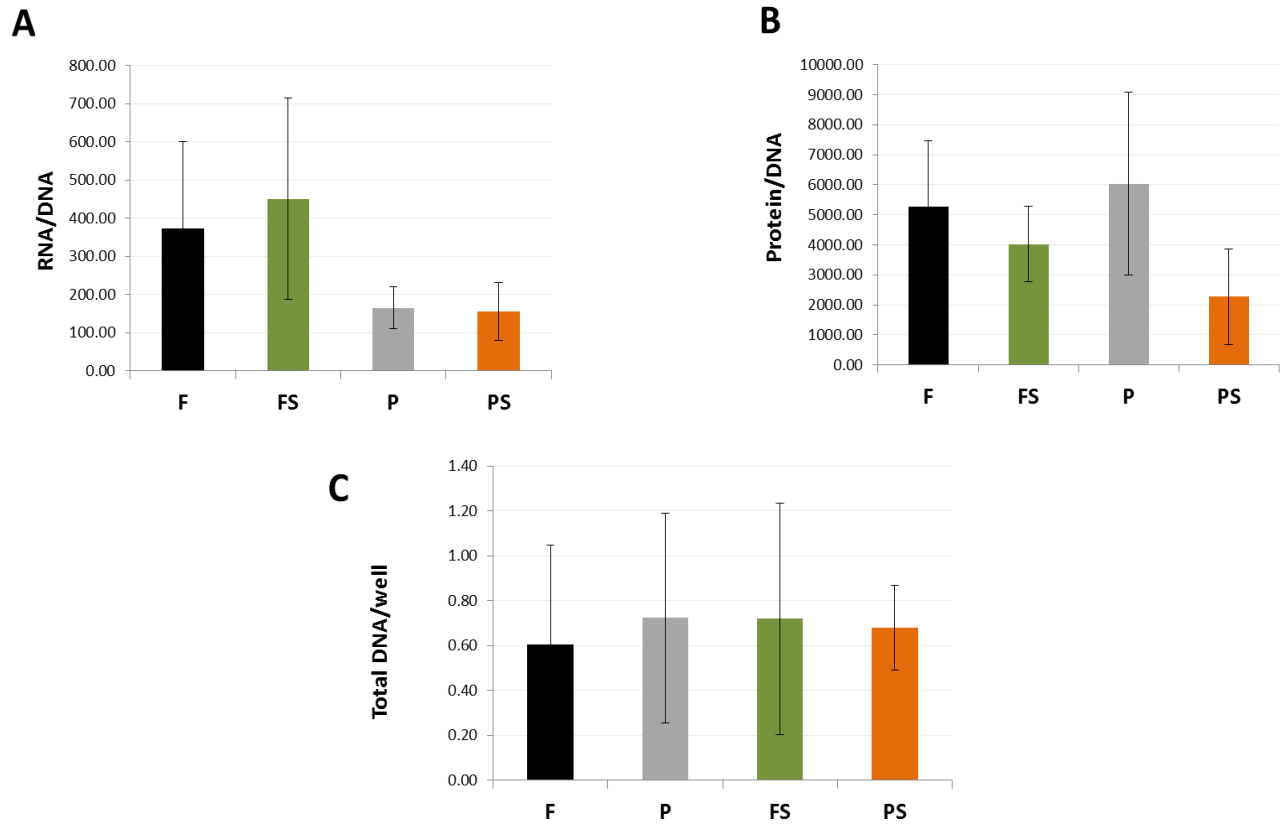


**Figure 20.** Cell density and RNA/DNA/PROTEIN of hMSCs with post and strain. Initially, at day 0, all the conditions were plated with same cell density of  $10^5$  cells/well, and at the end of the experiment: (A) The total RNA/DNA did not change between the conditions (B) The total protein/DNA did not change as well. (C) In addition, measurements of DNA amount from the whole dish showed no change between the conditions. (note: although some cells fall off the plate due to strain but there is more proliferation at the edge to compensate). Mean  $\pm$  SE,  $n=5$ ,  $p < 0.3$



Cells for all the experimental conditions were plated identically on day 0 at a density of  $10^5$  cells/well. At the end of day 4 of culture (including 2 days of stretch if used), total DNA/RNA/Protein per dish (using QIAGEN and Qbit kits), did not change between any of the conditions. DNA/well, RNA/DNA, and Protein/DNA and note that there is no significance of the paired T test, p value < 0.3 with error bars all overlap, suggesting that cells change in number but not in size or protein mass (Figure 20).

In total 8 genes were analyzed with RT-PCR (Figure 21). The genes confirmed from the functional groups were matrix metalloproteinase 13 (MMP13) from matrix; paxillin, integrin- $\alpha$ 2, and vinculin from focal adhesions; SOX9 from differentiation; caldesmon-1 and calponin-3 from muscle proteins; and ki67 from proliferation (Figure 22). Among these genes, MMP13 showed most difference between flat-strain and post-strain with an almost two fold increase. However, the most significant differences for these quantified genes came from straining the cells more than from the microtopography. Straining the cells increased proliferation of hMSCs seen by EdU staining at the edges but not the middle of the bioflex dish, and the ki67 gene transcript also increased with strain. Integrin- $\alpha$ 2 and SOX9 decreased slightly with microtopography.

#### **D. Discussion**

The major findings studying Chapter Two are that both strain and microtopography contribute to the remodeling of the actin cytoskeleton and focal adhesions in hMSCs. Focal adhesions formed on the vertical side of the post with the actin fibers wrapped the

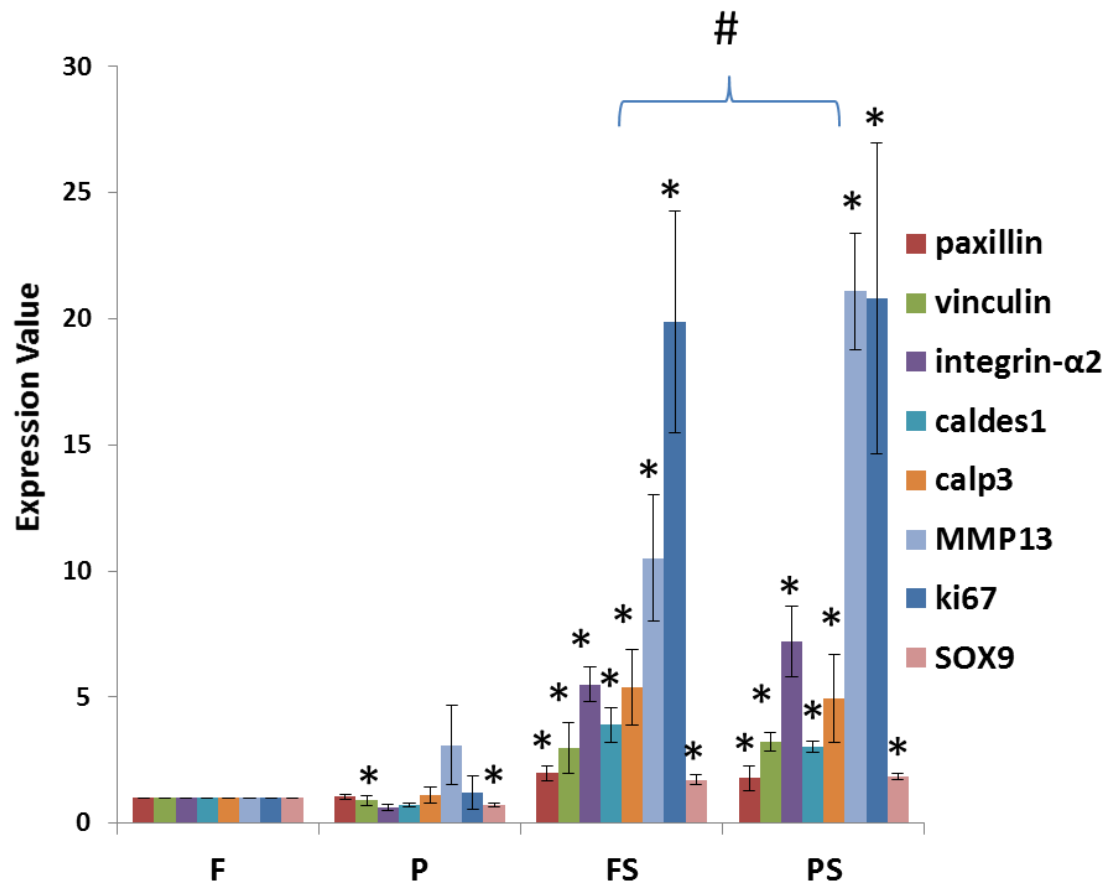


**Figure 21.** Relative gene expression of the selected genes shown all together. All the 8 genes (paxillin, vinculin, integrin- $\alpha$ 2, caldesmon1, calponin 3 acidic, MMP13, Ki67, and SOX9) confirmed by RT-PCR and compared together.

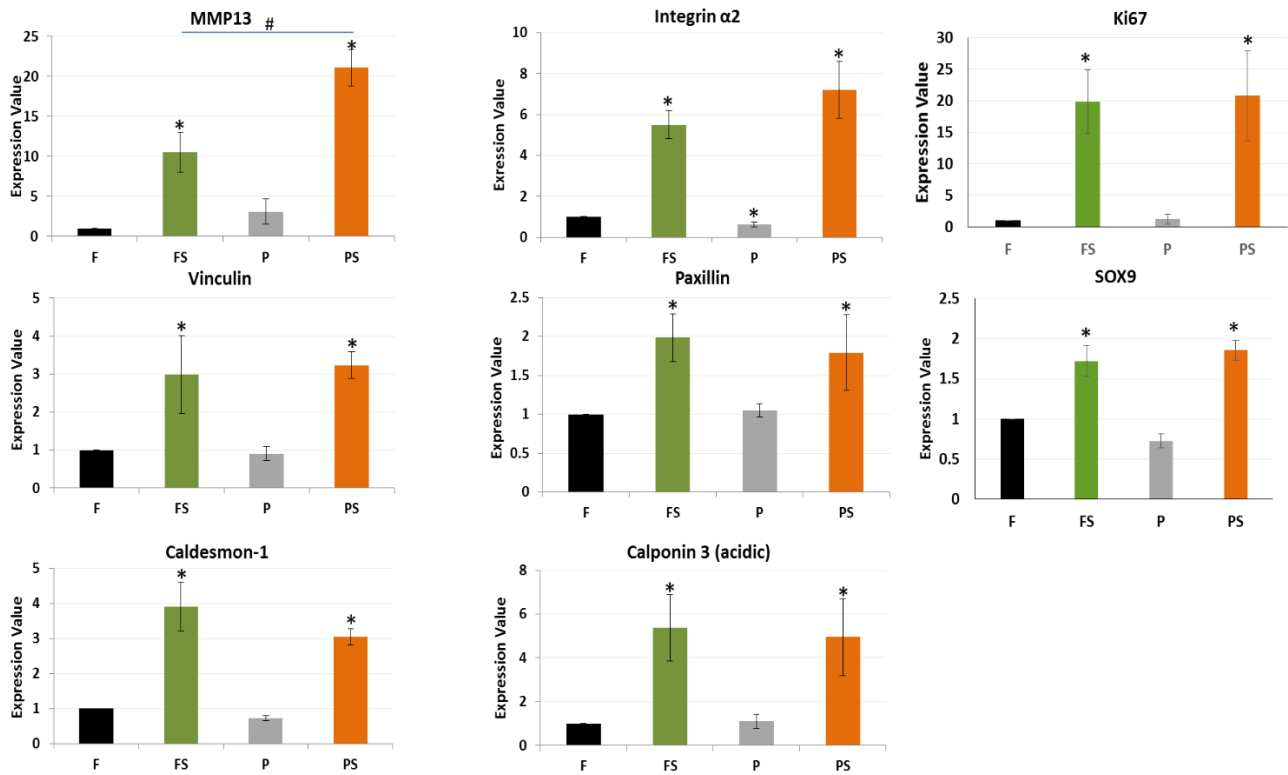


**Figure 22.** RT-PCR confirmed the dominant effect of strain over microtopography in regulating gene expression of the selected genes shown separately. RT-PCR of chosen genes from each functional group showing paxillin, vinculin, and integrin- $\alpha$ 2 from focal adhesions; caldesmon-1 and calponin3 from muscle proteins; MMP13 from matrix; ki67 from proliferation; and SOX9 from differentiation. MMP13 had the highest fold change with post-strain, but the rest of the genes, both flat-strain, and post-strain affected the genes similarly. However, SOX9 and integrin- $\alpha$ 2 were slightly decreased with microtopography. Mean  $\pm$  SE,  $n=4$ . \* All vs. flat, # FS vs. PS,  $p < 0.05$ .

cell around it. With the addition of strain, the cytoskeleton elongated and the focal adhesion attachment on the post became asymmetric. Nuclear size, shape and subcellular location also changed with both strain and microtopography, being close to the post for an unstrained cell but distant with strain. Anisotropic strain increased the proliferation of hMSCs but biaxial strain did not. Strain was dominant over microtopography in gene regulation.

A diagram shows the micromechanics of how a cell interacts with a post with or without strain (Figure 23). Tension developed in the actin stress fibers is transmitted to the extracellular substrata via the focal adhesion containing paxillin, shown in top and side views. The amount of force generated by the cell depends on the applied external force to which it is responding. Cells evaluate the level of force and make adjustments. The cytoskeleton filaments and their linkages to transmembrane proteins assemble, break down, and reassemble. Based on Newton's Third Law, internal and external reactive forces are equal and opposite under all conditions. The cell tension is greater when microtopography stabilizes anchorage to the static post (Figure 23A and 23B) and even greater when dynamic external strain is delivered via the substrata (Figure 23C and 23D). As cells probe their environment, their anchorage is determined by amount and direction of local forces, which cluster integrins stabilizing a new focal adhesion over time (Sheehy, 2011). Thus, in individual cells, the subcellular distribution of focal adhesions depends on local traction forces.

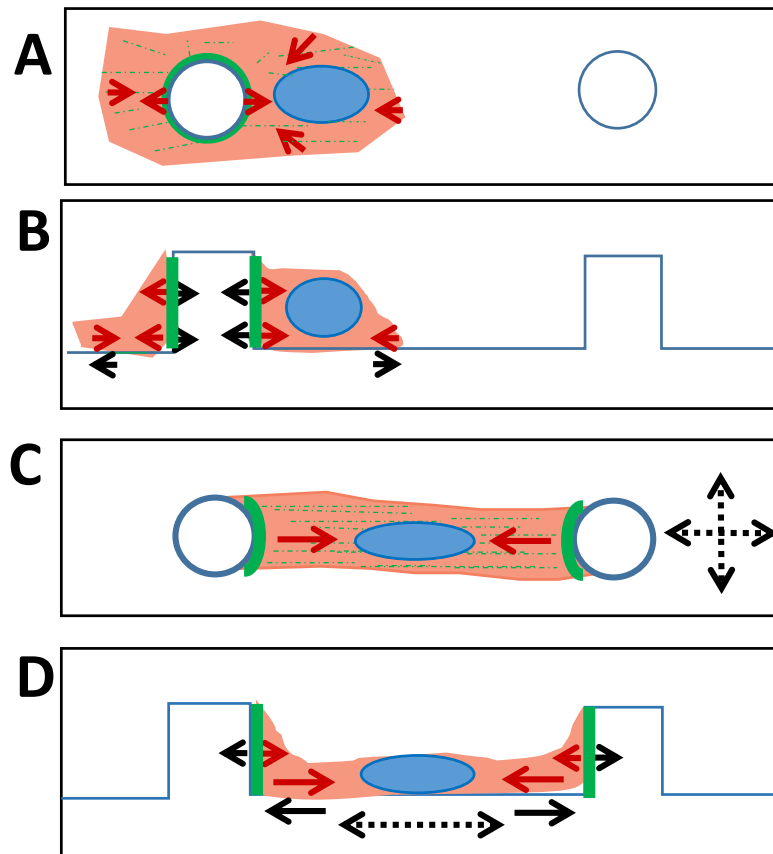


**Figure 23.** Schematic of micromechanics involved in the cell-substrata interactions for the post with or without strain. (A, B) hMSCs unstrained and (C, D) dynamically strained two days at 10% strain and 1 Hz; (A and C) top view and (B and D) side view. Solid arrows indicate force imparted by the substrata (black) or generated by the cell (red), which are equal and opposite based on the Newton's Third Law. Dashed arrows show the external force due to dynamic strain applied by flexing the substrata. Microtopography exerts static forces only. With the addition of strain, the cytoskeleton elongates and the focal adhesion attaches asymmetrically to the post. Nuclear size, shape and subcellular location also changed with both strain and microtopography, being close to the post for an unstrained cell but distant with strain. The colors represent specific cellular component: cytoskeleton (red), paxillin (green), and nucleus (blue).

### **i. Microtopography**

Early studies of cell adherence to microtopography was done by Dr Russell's group and showed focal adhesion and actin filament remodeling for myocytes (Deutsch, 2000, Motlagh, 2003a; Motlagh, 2003b) and fibroblasts (Boateng, 2003) on substrata with posts. Microtopography affects this local traction force, with a one micron-sized micropillar being sufficient to stabilize the focal adhesions visualized by vinculin staining (Riveline, 2001, Tan, 2003). The focal adhesion complex is the anchor for the cytoskeletal organization of the cells plated on posts, and depends on both focal adhesion kinase and the contractile forces generated by myosin II (Frey, 2006, Ghibaud, 2011). RhoA regulates the actin polymerization in the topography-induced focal adhesion formation (Seo, 2011). Here, hMSC encircles the post by forming actin bundles attached by focal adhesions as has been seen with other types of cells and microtopography. Myosin heavy chain of cardiomyocytes extended over the full height of the PDMS posts of 15  $\mu\text{m}$  height and 25  $\mu\text{m}$  diameter (Patel, 2011). Fibroblasts spread in between the posts with 20  $\mu\text{m}$  height, 5  $\mu\text{m}$  diameter, and spaced 4 to 12  $\mu\text{m}$  apart, where they form arc-like shapes that presented an inward curvature that increased with time, and the importance of cell tension was confirmed because the wrapping process can be reversed with a myosin II inhibitor (Ghibaud, 2011).

### **ii. Strain**

Focal adhesion formation can also be induced through application of external force by strain (Galbraith, 2002, Riveline, 2001). RhoA/ROCK and FAK regulate mechanical

strain-induced actin fiber formation and cytoskeleton reorganization of cells (Xu, 2012). 15% uniaxial strain at 1 Hz reoriented the actin fibers of MSC (Ghazanfari, 2009). Biaxial cyclic strain increased the level of insoluble vinculin and paxillin of smooth muscle cells, after a minute of strain at 10% strain by 1 Hz but  $\alpha$ -actinin was not changed (Cunningham, 2002). After 2 days of strain (20% strain at 1 Hz), more F-actin labeled fibroblasts were found in cyclic biaxial strain with random orientation compared to the statically anchored controls (Gould, 2012). Greater actin staining seen here also suggests actin polymerization increased with strain. Integrin is attached to the actin cytoskeleton through several actin-associated proteins such as paxillin, vinculin, talin, tensin, and  $\alpha$ -actinin. In this study, two-day strain of hMSCs resulted in up-regulation of isoforms of integrin, such as integrin- $\alpha$ 2, integrin- $\alpha$ 5, and integrin- $\beta$ 6 and of increased focal adhesion molecules, such as paxillin, vinculin,  $\alpha$ -actinin and talin. RT-PCR confirmed the enhanced expression of integrin- $\alpha$ 2, paxillin and vinculin with strain.

### **iii. Combination of microtopography and strain**

Adding mechanical strain to the microtopographical substrata caused the redistribution of focal adhesions for anchorage so that the hMSCs were still elongated but also preferentially anchored to the posts rather than the intervening flat spaces. Thus, strain caused the actin stress fibers to elongate and span from post to post. The dynamic flexing of the substrata increases the internal tension as for strain alone, but the focal adhesion stabilized in a semi-circle on the sides of the post because of the local increase in traction force there as compared to the flat region.

#### **iv. Matrix remodeling**

hMSCs not only remodel their interior architecture in response to 3D microtopography and strain, but they also remodel the extracellular matrix in which they reside. This was achieved by regulating transcription of collagen, laminin, fibronectin, and metalloproteinases (MMPs). Mechanical strain of fibroblasts grown in microgrooves increased the collagen I, and fibronectin expression at 1 Hz with 8% strain (Loesberg, 2005), similar to findings here with hMSCs for collagen type I and fibronectin type III, which were up-regulated with strain. Strikingly, MMP13 was affected by the combination of microtopography and strain with two fold changes more than the strain alone. MMP13 (collagenase 3) has been shown to degrade the native interstitial collagens in several tissues and to participate in situations where rapid and effective remodeling of collagenous extracellular matrix (ECM) is required. Biaxial strain increased ECM degradation of osteoblastic cells by MMP13 (Yang, 2004). ECM remodeling by up-regulation of MMP13 may correlate with increased differentiation of fibroblasts on topography (Dalby, 2002).

#### **v. Nuclear shape and location**

The cytoskeleton forms a network, connecting the extracellular matrix with the nucleus (Sims, 1992). The change in the cytoskeletal organization of the cells alters the nuclear shape and position so that the large flattened nucleus is deformed by the thin, spread layer of actin in the control cells, as seen in Figure 11. Nuclear deformation is seen in many cell types, such as cardiomyocytes grown on grooves or posts (Heidkamp, 2001), and with fibroblasts on posts (Ghibaudo, 2011, Patel, 2011). Geometric cues provided



by the ECM caused the aspect ratio of the nucleus of neonatal cardiomyocytes to increase as the aspect ratio of the cardiomyocytes increased (Heidkamp, 2001). In this study, the nuclei of hMSCs reach full height close to the post with an increased length/width ratio. However, the volume of the nucleus may have not changed due to increased nuclear height and decreased nuclear area with posts. A popular hypothesis is that changing the nuclear shape directly affects transcription via sub-nuclear forces. Indeed, nuclear components are mechanically coupled to the cytoskeleton, providing a more complete understanding of the role of nuclear positioning (Burke, 2009). However, an exception is seen that uncouples nuclear shape from gene expression, which is dominated by strain. The microtopography also changes nuclear shape but does not affect gene expression to the same extent as with strain.

## **vi. Proliferation**

Another important cellular activity is proliferation. Proliferation varies with cell type, cell culture and topography. Proliferation of fibroblasts was inhibited by surface microtopography (Boateng, 2003). hMSCs proliferation increased in culture when microstructures were added to 3D gel (Collins, 2009) whereas division was inhibited in mouse embryonic stem cells near to a post (Biehl, 2009). Mechanical strain also affects cell division and depends on the duration, frequency, amplitude and direction of strain. MSC proliferation increased with 10% uniaxial strain at either 1 Hz after 4 hours or 0.26 Hz after 3 days (Ghazanfari, 2009, Jang, 2011). Bone marrow stromal cells proliferate significantly more at 5%, 10%, and 15% strain compared to control group without strain or at very low frequency (Koike, 2005). Uniaxial strain increased MSC proliferation with

cell alignment parallel to the strain axis by using microgrooves. However, when micropatterning was used to align cells perpendicularly to the axis of mechanical strain, MSC proliferation was not affected (Kurpinski, 2006). Fibroblast proliferation is also greater in anisotropic than for isotropic strain (Gould, 2012). Cell division of strained hMSCs cultured on flat or post substrata, was also higher in the anisotropic regions at the edge of the bioflex plates, but proliferation was actually decreased in the middle isotropically strained region, again demonstrating the importance of the direction of strain not only its frequency or amplitude.

## **vii. Differentiation**

The 3D niche and micromechanics affect differentiation in the embryo and in adult cell plasticity to altered microenvironmental cues. Since the microenvironmental niche is thought to affect cell lineage, microtopography and strain were used to determine whether there was any regulation of differentiation genes. Strained hMSCs gene expression confirmed by RT-PCR showed significant difference for two muscle proteins (calponin-3, acidic, and caldesmon-1). A differentiation gene, SOX9, involved in chondrogenesis was up-regulated here as has been found in mesenchymal cells with mechanical strain (Xiong, 2005). However, SOX9 slightly decreased with microtopography in this experiment. The acidic calponin 3 (CNN3) is an actin filament-associated regulatory protein, which has been found in smooth muscle and non-muscle cells (Applegate, 1994). CNN3 has been shown to up-regulate with combination of transforming growth factor beta and cyclic mechanical straining of cultured hMSC with microgrooves (Kurpinski, 2009). Caldesmon-1 is a calmodulin binding protein that plays

an essential role in the regulation of smooth muscle and non-muscle contraction. 10% cyclic strain increased caldesmon-1 (Cevallos, 2006, Jang, 2011). Thus, despite the predictions that the combination of mechanical cues from physical deformation by externally applied force and also from microtopography might both be necessary for differentiation, the addition of microtopography to strain did not yield any notable regulation in lineage specification.

### **E. Conclusion and summary**

The mechanical cues of microtopography and strain altered local forces, which in turn affected focal adhesion formation and cytoskeletal reorganization. Gene expression in hMSCs was induced more readily in conditions of strain than microtopography alone, which reinforces the expected dominance of external strain stimuli over static influence of microtopography. However, with the combination of strain and microtopography, local remodeling of the focal adhesion on the vertical post stabilizes the cytoskeleton over time so that there is preferential elongation from post to post.

Clearly more work is needed to understand how a cell type with potential clinical use responds to mechanical strain in the presence of tightly controlled 3D geometry. Exactly how the mechanical forces link to the cellular activities remains elusive but actin fiber reorganization and focal adhesion redistribution are essential for regulation of specific cellular functions.

### **III. SUSTAINED DELIVERY OF MGF PEPTIDE FROM MICRORODS ATTRACTS STEM CELLS AND REDUCES APOPTOSIS OF MYOCYTES**

#### **A. Introduction**

Cells are regulated by both mechanical and chemical stimuli arising from the surrounding extracellular matrix (ECM). They respond by subcellular reorganization, proliferation, differentiation, migration and other functions (Scadden 2006, Dicher, 2009). One goal of bioengineering is to mimic this physico-chemical microenvironment in order to control the behavior of cells for tissue regeneration. Our group has shown that microtopography affects cellular structure and function (Motlagh, 2003, Norman, 2005, 2007, Collins, 2009, Biehl, 2009, Doroudian, 2013). Furthermore, the stiffness of the surface on which stem cells are grown is sufficient to alter lineage commitment (Engler, 2006). The greatest effect on fibroblast cell function was induced by microrods with a combination of stiffness and microtopography in a 3D gel culture system (Ayala, 2010). The range of stiffness for normal cardiac ventricular tissue is 20-30 kPa (Berry, 2006) and the logical range for microstructures to be relevant for the study of cardiac cell regulation. The micron size scale of cells in cardiac tissue is also used.

Equally important to the physical parameters are the many chemical signals, which provide complex cues for the functional control of different cell types. For cardiac repair, some critical chemicals from the cellular microenvironment are those that recruit stem cells or prevent myocyte death. It is interesting that most studies now show that functional improvements associated with the direct delivery of mesenchymal stem cells (MSCs) to the heart are due to their secretion of soluble factors rather than the

engraftment of stem cells *per se* (Fazel, 2006, Paul 2009). The universal stem cell homing factor, SDF-1, is an important chemokine attracting stem cells to the heart. SDF-1 is produced by ischemic tissue and affects migration and mobilization of proangiogenic cells, however, it undergoes rapid proteolysis in blood, limiting its therapeutic potential (Hattori, 2001).

Cell homing to an injury site is also a property of insulin-like growth factor 1 (IGF-1). Local IGF-1 produced by the muscle acts to increase myocyte growth and preserve the injured myocardium (Donath, 1998, Stavropoulou, 2009). Rapid binding of IGF-1 to proteins in the circulation severely limits the bioavailability of IGF-1. An alternative splicing of IGF-1 yields a special E domain and has a distinct function from IGF-1 and does not bind to IGF-1 binding proteins. IGF-1Ec in humans (IGF-1Eb in rodents) is also known as the mechano growth factor (MGF). Additionally, native MGF blocks apoptosis of injured myocytes as well as attracting stem cells (Ates, 2007, Carpenter 2008, Musaro, 2004). The E-domain of the MGF peptide, which consists of 24 amino acids, caused increased migration of human mesenchymal stem cells (hMSCs) and human myogenic precursor cells (Collins, 2010, Mills, 2007). MGF may affect proliferation of some cell types, such as myoblast C2C12, myocardial H9C2, and osteoblasts (Yang 2002, Kandalla, 2011, Li, 2012) but not others such as MSCs and chondrocytes (Collins, 2010, Schegel, 2013).

Clinical regenerative therapy would benefit by enhancing tissue repair without the need for exogenous stem cells. Therefore, it is attractive to consider what steps are necessary to engineer the crucial features in an acellular microdevice. A rational physical design that might foster natural cardiac repair processes would be a

combination of microtopographic features, like the myocyte-shaped microrod, with stiffness in the cardiac range (30 kPa). Additionally, MGF is an attractive choice of a peptide for incorporation into microrods for cardiac regeneration and repair given its chemokine and anti-apoptotic properties. Therefore, this study takes the initial steps to manufacture an MGF-eluting microrod that can be used as an injectable microdevice for the localized delivery of bioactive MGF over sufficient time for potential regenerative therapy of the injured heart *in vivo* (Figure 24).

## **B. Materials and methods**

### **i. MGF peptide**

The native form of MGF-E domain (peptide sequence:

YQPPSTNKNTKSQRRKGSTFEERK, (Figure 25A) was custom-synthesized with a C-terminal cysteine cap at a purity of >90% and delivered in lyophilized aliquots (Genescript Corp, NJ). Peptides were dissolved in 80% acetonitrile (stock 4 mg/mL) and diluted in molecular grade water to 1000 ng/mL yielding a final concentration (30-120 ng/mL) in media. For the control without MGF (No GF), equal volumes of molecular grade water were added to media.

### **ii. Microfabrication and encapsulation of microrods with MGF**

Microrods were fabricated photolithographically using commercially available materials by processes developed by us (Ayala 2010). Briefly, the precursor solution was made by mixing poly(ethylene glycol) dimethacrylate (PEG-DMA) ( $M_N$  750, Sigma Aldrich) with

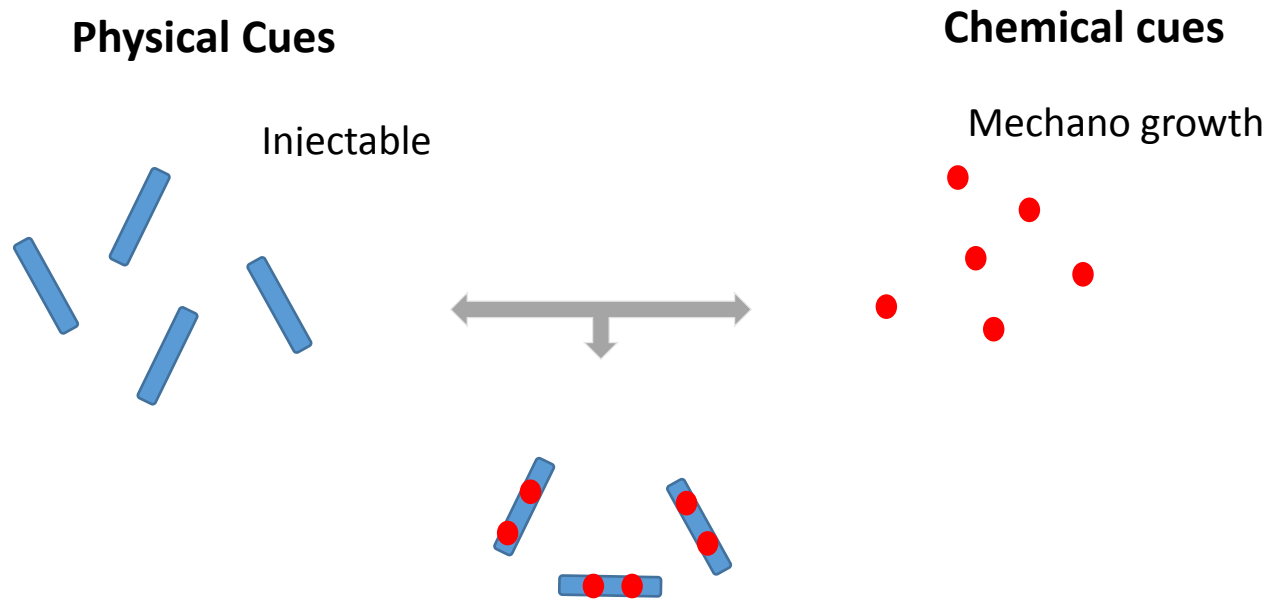
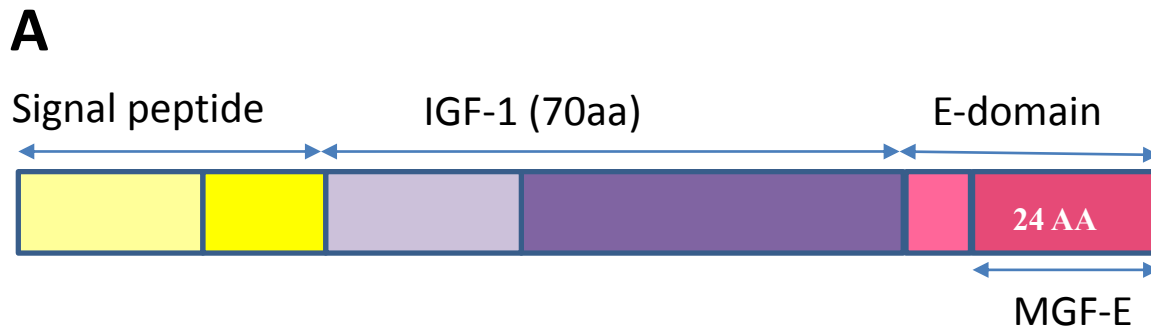
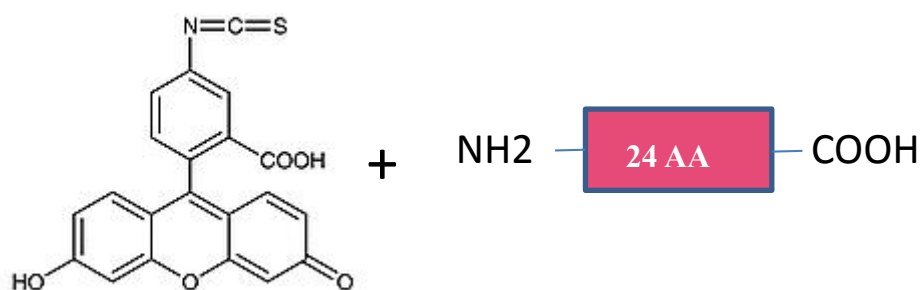


**Figure 24.** Combination of physical and chemical stimuli enhances tissue regeneration. In addition to the physical cue of microtopography, chemical cues such as growth factors play an important role in regulating the cellular function.



**B**



**C**

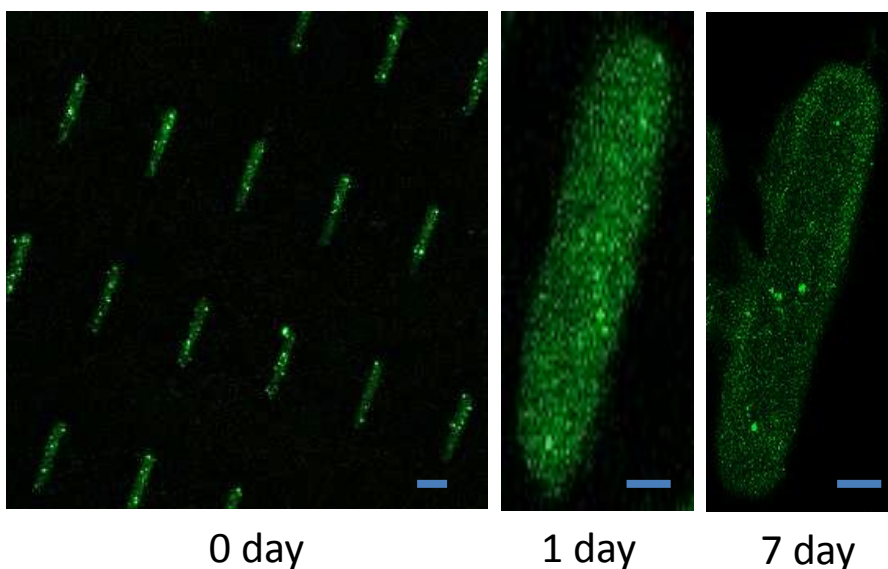


**Figure 25.** FITC-MGF encapsulation into PEG-DMA microrods. (A) MGF is an isoform of IGF-1, which includes 24 amino acids in the C terminal of the E-domain; (B) FITC is conjugated to the N terminal of the MGF peptide; (C) MGF-FITC encapsulated in the microrods still attached to the wafer (0 day), and at one day and 7 days in PBS, as seen by fluorescence microscopy (green, FITC). Scale bar, 20  $\mu$ m



1x phosphate buffered saline (PBS) and adding the photo-initiator 2, 2-dimethoxy-2-phenylacetophenone (Sigma Aldrich) solubilized in 1-vinyl-2-pyrrolidone (Sigma Aldrich) at a concentration of 150 mg/mL.

Lyophilized E-domain native Mechano Growth Factor (MGF) (Genescript Corp, NJ) was resuspended at a concentration of 4.0 mg/mL in a solution of 80% acetonitrile (HPLC Grade, Sigma Aldrich) and 20% PBS and added to the hydrogel precursor solution. Based on the desired specifications of sufficient mechanical stiffness, high hydrogel porosity for drug loading, and sufficient viscosity of precursor solution for thin layer formation, the ratio of components chosen was 4 parts PEG-DMA : 3 parts PBS :  $11/15$  parts photo-initiator solution : 1 part MGF solution. The final MGF concentration was 0.458 mg/mL. For control microrods not containing peptide, the 1 part MGF solution was replaced with a solution of 80% acetonitrile and 20% PBS with no MGF to maintain consistency between controls and peptide-loaded samples.

MGF tagged FITC was incorporated to evaluate the encapsulation and distribution of MGF in microrods. Green fluorescence of FITC shows MGF still bound to the microrods after initial washing and after one to 7 days in PBS (Figure 25B and 25C).

### **iii. Microrod size and stiffness**

The PEGDMA hydrogel microrods were designed to be the size scale and shape of cardiac myocytes, namely microrods with  $15 \times 15 \mu\text{m}^2$  cross-section and length 100  $\mu\text{m}$ . The microstructure height was accurately measured using an Ambios Technology XP-2 profilometer. Light microscopy measured length and width (Figure 26). By cross-interpolating from previous work (Ayala, 2010), the stiffness was designed to be

approximately 30 kPa chosen to mimic adult heart stiffness and based on the PEGDMA concentration and cross-linker ratio used in the precursor solution during photolithographic processing.

#### **iv. Microrod degradation**

Microrods were resuspended in sterile, warm saline and shaken in an incubator at 37°C. Microscopic images recorded over a period of 2 months were used to determine the rate of degradation by width measurement using ImageJ software. The mean width of 20 isolated microrods was measured at each time point.

#### **v. MGF elution from the microrods by ELISA**

MGF was detected by an enzyme-linked immune absorbent assay (ELISA) on Immobilized-Amino plates and directly conjugated HRP- Primary rabbit MGF antibody (After transferring cumulative MGF sample solution of about 100 µl to the microplate (Nunc) and applying TMB liquid substrate (Sigma) for color developing). Peptides were incubated for 2 hour at 37°C, and antibodies were incubated for 1 hour at 37°C. A concentration curve (0.1-120 ng MGF-E peptide range 125 ng to 0.125 ng) was generated to calibrate as standard curve to determine the unknown the amount of MGF peptide eluted over time. Varying concentrations of microrods were used so that the predicted MGF delivery would be 30, 60, 90 or 120 ng if all the loaded peptide were fully eluted. Elution of MGF peptide was compared to unloaded (empty) microrods. Elution of MGF was analyzed at 1h and daily for one week.

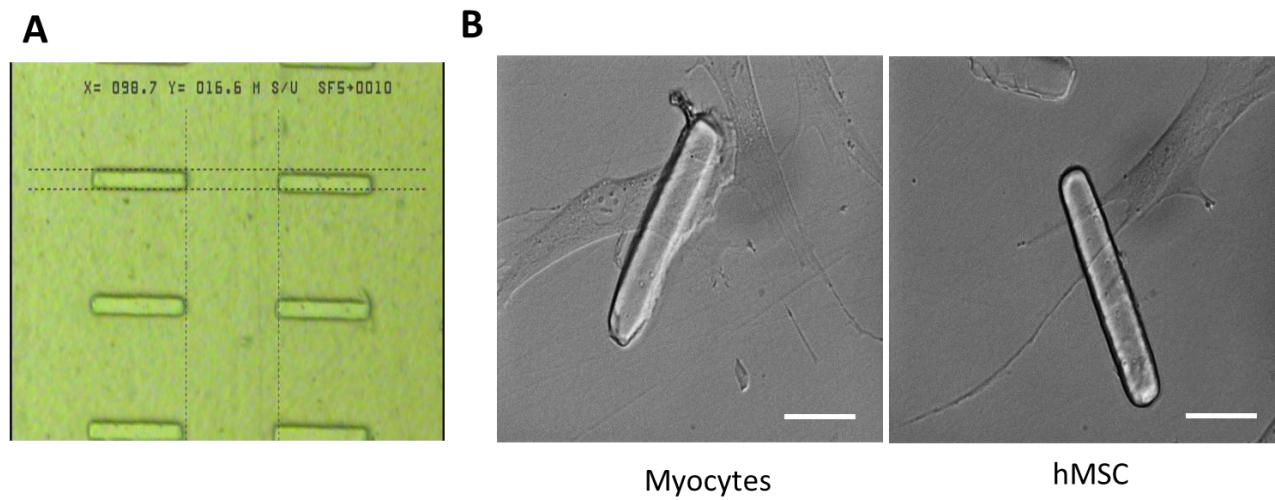


**Figure 26.** Microrod size and interaction with different cell types. (A) Length and the width of the microrods were measured with light microscopy. (B) hMSCs and NRVM interaction with the microrods, scale bar, 50  $\mu\text{m}$

#### **vi. MGF elution from the microrods by HPLC**

Elution of MGF from the hydrogel matrix of the microrods was assessed by harvesting the MGF microrods into 450,000 microrod aliquots immediately after fabrication and suspending in a small volume of PBS. The microrods were agitated gently at 37 °C. At day 1, 2, 4, 7, 14, and 21, the samples were removed from the incubator, agitated again to mix the solution thoroughly, then gently centrifuged to collect the MGF microrods at the bottom. A 110 µL sample was then drawn from the vial and replaced with fresh PBS. The collected sample was stored at -20 °C until analysis.

Prior to beginning the experiment, a standard curve for the detection of MGF was established using a 1260 Infinity HPLC system (Agilent Technologies, CA) and samples of MGF prepared in a 20% acetonitrile solution at concentrations of 0.5, 1, 5, 10, 20, and 50 µg/mL in triplicate with a PBS blank sample run between each standard curve sample. Samples were run through a Luna 5 µm C18(2) 100A, 250 x 4.6 mm column (Phenomenex, Inc, CA) equilibrated to room temperature using a process adapted from previously published protocols (Tucker, 2012). Solvents were made from HPLC grade water, acetonitrile, and trifluoroacetic acid (TFA) (VWR, PA). Solvent A was 100% water and solvent B was 100% acetonitrile. TFA was added to both solvents at a concentration of 0.1% (v/v). The mobile phase was eluted from the column at 1 mL/min beginning with 95% solvent A and 5% solvent B and increasing to 80% solvent A and 20% solvent B from 0 to 10 minutes, which was then maintained from 10 to 15 minutes. From 15 to 30 minutes, the mobile phase was transitioned to 10% solvent A and 90% solvent B. From 30 minutes to 30.5 minutes, the solvent mixture was returned to the starting mixture and the column was flushed with this solution and re-equilibrated from

30.5 to 35 minutes. Samples were analyzed by a UV detector at 205 nm. The MGF peak eluted at approximately 11.7 minutes and the area under the curve of the peak at this time was calculated to establish the linear range of the standard curve.

To ensure that small chain PEG molecules that were potentially eluted over the 14 days did not interfere with MGF detection, additional standards with 10 µg/mL MGF were doped with 0.1, 1, and 10% (v/v) un-crosslinked PEG-DMA. No interference with the MGF peak was noted at these concentrations of PEG-DMA inclusion.

Experimental samples were run with the HPLC protocol described above including a PBS blank between each sample and interpolated on the standard curve to back-calculate the mass of MGF in solution at each time point. The elution experiment was repeated with  $n = 5$  aliquots of 450,000 MGF-containing microrods and the results averaged. Control aliquots ( $n=2$ ) of empty microrods were also incubated over the 14 days, sampled at each time point for comparison, and subtracted from the readings on MGF for normalization.

**vii. Cell culture for human mesenchymal stem cells and neonatal rat ventricular myocytes (NRVM)**

Institutional approval was received to obtain and use mesenchymal stem cells (hMSCs) isolated from human bone marrow aspirates supplied by Texas A&M Health Science Center College of Medicine Temple, TX. Microarray analyses indicate that gene expression was consistent for hMSCs from different donors, isolated and expanded as described previously. Experiments were performed on passage three or lower from hMSCs obtained from 3 separate donors. hMSCs were cultured in complete culture

media (CCM) consisting of MEM- $\alpha$  supplemented with 16.5% fetal bovine serum (FBS), 2 mM L-glutamine, 100 units/mL penicillin and 100  $\mu$ g/mL streptomycin, and incubated at 37 °C as used by us (Doroudian, 2013).

Primary heart cultures were obtained from neonatal rats according to Institutional Animal Care and Use Committee and National Institutes of Health guidelines for the care and use of laboratory animals. Hearts were removed and cells were isolated from 1- to 2-day-old neonatal Sprague-Dawley rats with collagenase (Worthington), as previously described by our group (Boateng, 2003). The cells were re-suspended, filtered through a metal sieve to remove large material, and plated in PC-1 medium (Biowhittaker/Cam- brex) on fibronectin coated plates (25  $\mu$ g/ml). Cells were left undisturbed for 24 hours in a 5% CO<sub>2</sub> incubator. Unattached cells were removed by aspiration, and PC-1 media was replenished. Cells were allowed to establish beating over at least one day prior to experimental use.

#### **viii. MGF bioactivity assessed by hMSC migration**

Migration was used to test the bioactivity of MGF-microrods (MGF-rods). hMSCs were plated in the upper compartment of the porous insert in a Boyden chamber and 30ng MGF was added to the media (either directly or indirectly by 100K MGF-rods below) to assess cell migration using Calcein-AM stained cells as done by us (Collins, 2010). Cells were cultured overnight (22 hours) at 37°C, 5% CO<sub>2</sub>. Empty microrods (E-rods) were also tested as a negative control.

**ix. Microrod and MGF effects on subcellular structure**

In order to analyze subcellular features of the actin cytoskeleton, focal adhesion, and nuclei, hMSCs were cultured with the microrods still adhered to the silicon wafers with or without MGF for 48 hours. Cells were fixed with 4% paraformaldehyde in phosphate buffered saline (PBS) for 10 min at room temperature, rinsed three times with PBS and permeabilized by 0.1% Triton X-100 in PBS for 10 min, and washed 3 times with PBS. Cells were pre-incubated in blocking solution (PBS, 1% bovine serum albumin (BSA)) for 15 min and then incubated with rhodamine conjugated phalloidin (Molecular Probes) at a dilution of 1:400 to stain actin, or paxillin antibody (Abcam) at a dilution of 1:250 for 1.5 hours followed by another incubation with secondary antibody Alexa Fluor 488 (Invitrogen) at a dilution of 1:1000 for 45 min to stain the focal adhesions of the cells. DAPI (Sigma) was used for nuclear staining which artificially stained the microrods as well. Confocal images of actin and focal adhesions were obtained with Zeiss LSM 510 META and LSM 710 microscopes.

**x. Microrod and MGF effects on proliferation**

To assess cell proliferation of hMSCs after 48 hours of culture on microrods with or without MGF, cells underwent a 1-hour incorporation of 5-ethynyl-2'-deoxyuridine (EdU, 10 mM, Invitrogen Corp.). Once incorporation was complete, the wafers were cut and mounted onto glass slides with 4', 6-Diamidino-2-phenylindole (DAPI) for nuclear staining. The microrods were artificially stained with both DAPI (blue) and Alexa Fluor 594 (red) used in the EdU kit.

**xi. Chemical hypoxia**

NRVM were subjected to the chemical hypoxia induced by hydrogen 0.5 mM peroxide (H<sub>2</sub>O<sub>2</sub>) plus 0.1 mM FeSO<sub>4</sub> for 30 min.

**xii. Caspase and HIF-1 alpha staining**

In order to assess the changes mediated by the chemical hypoxia, image-iT live green caspase-3 and -7 detection kit (Molecular Probes) was used followed by the instructions, as well as HIF-1 $\alpha$  antibody (abcam). For the caspase-3 and -7 detection, Fluorescent-Labeled inhibitor of Caspases (FLICA) reagent was used, therefore, only apoptotic cells would fluoresce green, so the apoptotic cells from necrotic cells were distinguishable since the necrotic cells could be stained red with propidium iodide (PI). Late apoptotic cells fluoresce green and red, and early apoptotic cells fluoresce green only. For HIF-1 $\alpha$  staining, NRVM were fixed with 4% formaldehyde for 10 minutes at room temperature and blocked with PBS containing 10% goat serum, 0.3 M glycine, 1% BSA and 0.1% tween for 2h at room temperature. Staining of the treated cells with the primary antibody at different dilutions of 1:650 and 1:1300 was performed overnight at 4°C in PBS containing 1% BSA and 0.1% tween. Alexa Fluor 488 conjugated goat anti-mouse polyclonal antibody at 1/250 dilution was used as the secondary antibody. For both assays, nuclei were counterstained with DAPI.

**xiii. MGF bioactivity to reduce apoptosis of NRVM induced by hypoxia**

In order to induce physiological apoptosis, neonatal rat ventricular myocytes (NRVM) were cultured for four days after isolation and then placed in a humidified chamber (Sanyo, Inc) with 5% CO<sub>2</sub>, 1% O<sub>2</sub> and the remainder balanced with N<sub>2</sub> for 8 hours at 37



°C with MGF in media (free glucose and serum DMEM media), E-rods, or MGF-rods. Terminal deoxynucleotidyltransferase (TdT)-mediated dUTP nick end-labeling (TUNEL) assay was used to assess cell apoptosis. TUNEL reaction preferentially labels DNA strand breaks generated during apoptosis. The negative control was normoxia, and the positive control was induced by a DNase I recombinant (Roche Applied Science). Changes in gene expression of Bcl2 were assessed as an index of apoptosis protection from hypoxia. Total RNA was isolated from NRVMs from the experimental conditions of control, MGF in media, E-rods, and MGF-rods. The RNA Mini Kit (QIAGEN) was used to isolate RNA, which was quantified using the Qubit Quantitation Platform (Invitrogen). RNA was reverse-transcribed for 50 min at 37 °C and 15 min at 65 °C (inactivation) using M-MLV Reverse Transcriptase.

For qPCR experiments, total RNA was isolated and reverse transcribed, from independently prepared control, MGF in media, E-rods and MGF-rods. Using SYBR Green PCR Master Mix and a 7500 Fast Real-Time PCR System (Applied Biosystems, Foster City, CA). Amplification was achieved by the following protocol: 1 cycle of 50 °C for 2 min; 1 cycle of 95 °C for 10 min; 0 cycles of 95 °C for 15 s and 60 °C for 1 min. To ensure specificity of PCR, melt-curve analyses were performed at the end of all PCRs. The relative amount of target cDNA was determined from the appropriate standard curve and normalized to the amount of Histone H2B cDNA present in each sample. Each sample was analyzed in triplicate, and results were expressed relative to the control condition. The primers sequence is shown in table 4.

#### **xiv. Statistical analysis**

A statistically significant difference among groups was detected by analysis of variance (ANOVA). Sequential Holm t-tests were then performed to identify differences between specific pairs of conditions.

### **C. Results**

#### **i. Slow degradation of microrods**

Continuous shaking in saline at 37 °C did not degrade microrods over two months. At day 1 and at two months, the width of microrods was approximately 15 µm (Figure 27). There was no significant difference in the mean width value of the microrods, implying no degradation under these conditions.

#### **ii. MGF elution time course detected by ELISA**

Delivery of MGF was sustained over one week. MGF was detected as early as the first hour (Figure 28). However, due to the limitations on ELISA method, HPLC was chosen for the elution study.

**Table IV**  
PRIMERS USED FOR qPCR

<b>Gene</b>	<b>Forward</b>	<b>Reverse</b>
H2B	gatgccgcgaagagagttac	ggtcgagcgcttggtgtaat
Bcl2	cgactttgcagagatgtcca	atgccgggttcaggtactcag

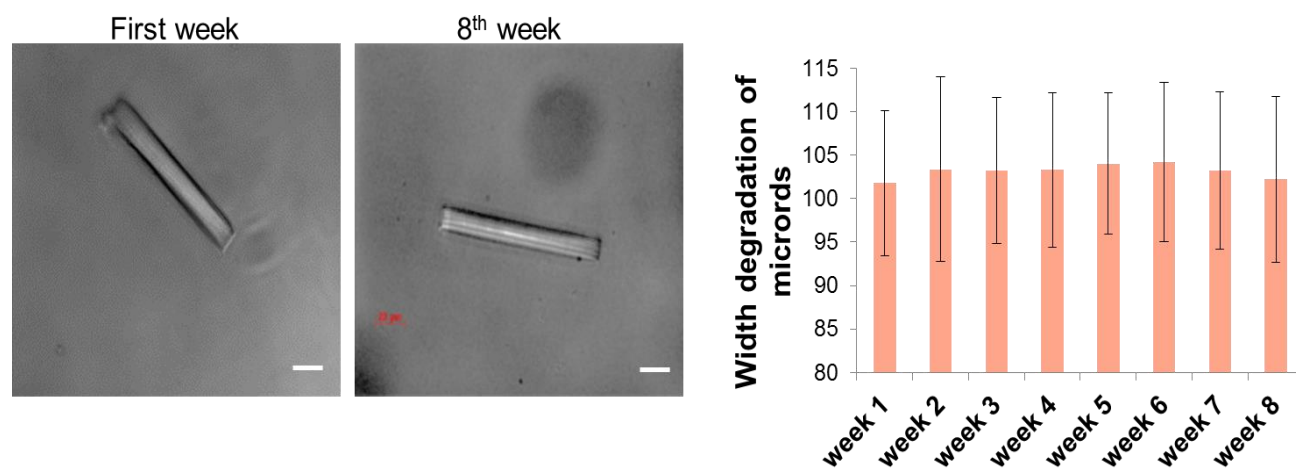


**Figure 27.** Degradation of microrods. Continuous shaking in saline at 37 °C does not degrade microrods by two months, scale care, 20  $\mu\text{m}$ .

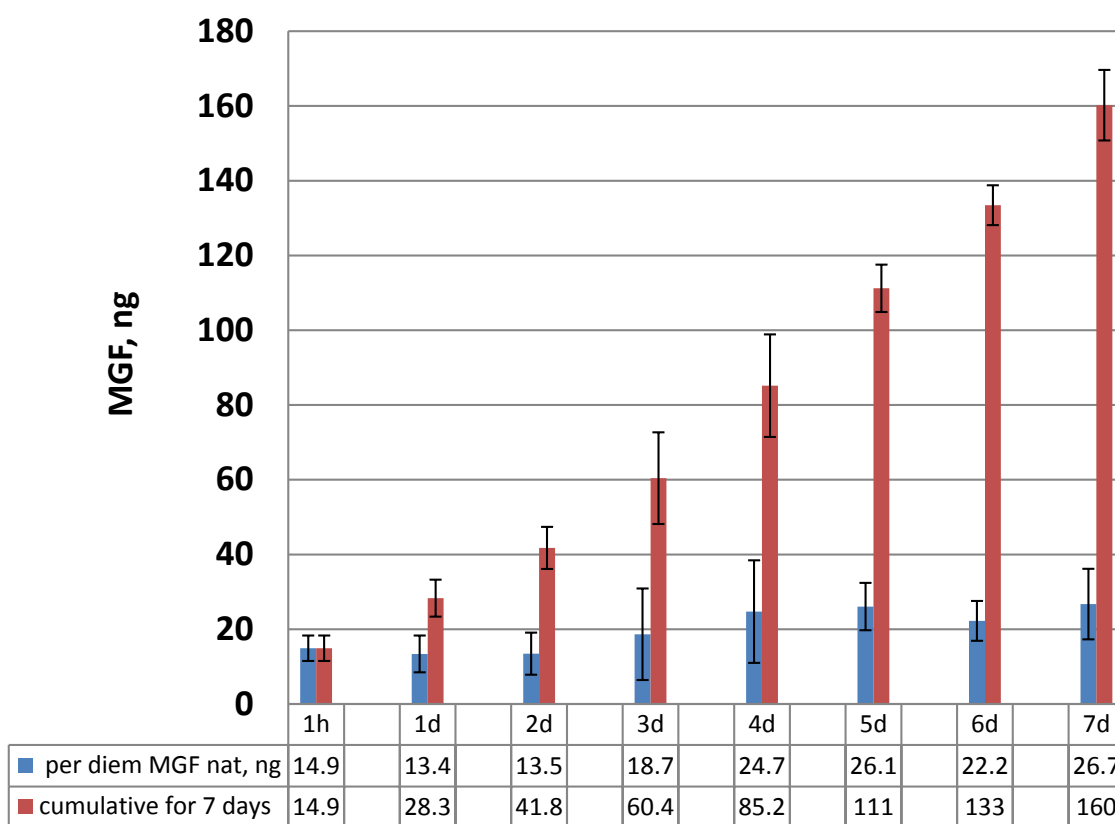


**Figure 28.** Testing MGF elution from the microrods by ELISA. Delivery of MGF from the microrods was tested through 7 days. Mean $\pm$  SE, n=4

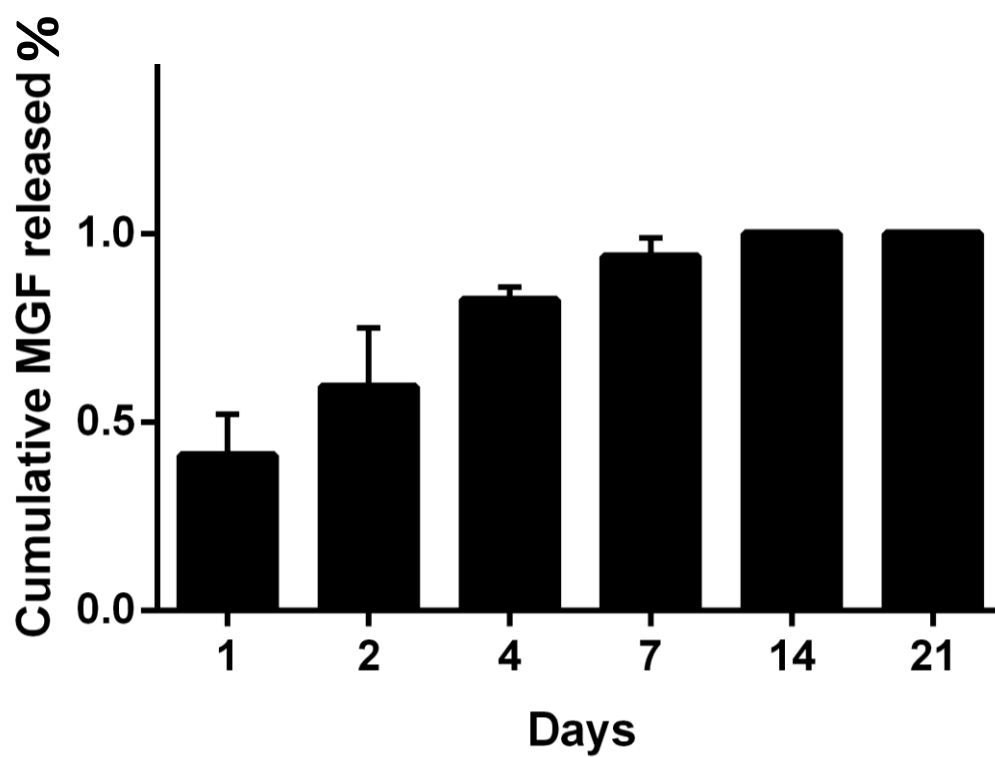


**Figure 29.** Time course of elution of MGF from the microrods detected by HPLC method. The cumulative MGF was measured at 0, 1, 2, 4, 7, 14 and 21 days. Each measurement was normalized to the 14 day MGF release. Mean $\pm$  SE, n=5

### **iii. MGF elution time course detected by HPLC**

Delivery of MGF was sustained over two weeks and no more MGF elution occurred in the third week (Figure 29). The majority of this release (~80%) occurred over the first four days before MGF release began to taper. Background detection of signal from empty microrods was small, reaching less than 20% of the total signal from the MGF-loaded rods over 14 days. The theoretical total MGF content in each aliquot of 450,000 microrods was approximately 4600 ng with an average total of approximately 570 ng released over 14 days (theoretical payload delivery efficiency ~12.4%). However, there are many factors that must be considered in order to calculate the delivery efficiency that require adjustment of the total MGF loaded in the microrods and is discussed further, below.

### **iv. Subcellular structure and proliferation**

Both the E-rods and MGF-rods remodeled morphology and adhesion of the hMSCs after 48 hours of culture (Figure 30). The hMSCs interacted with the microrods as determined by immunocytochemistry. In fact, the actin cytoskeleton of hMSCs elongated on the microrods, and focal adhesions (assessed by paxillin localization) distributed along the microrods. On the other hand, MGF in the media on flat surfaces had no effect on the cell morphology (data not shown). Microrods with or without MGF significantly blunted proliferation of hMSCs after 2 days of culture (Figure 31) ( $P < 0.05$  between microrods and flat surface), however, MGF on flat surfaces had no effects on the proliferation of hMSCs (Flat vs. MGF in media, NS). Thus, proliferation is regulated by the microrods independently of MGF.

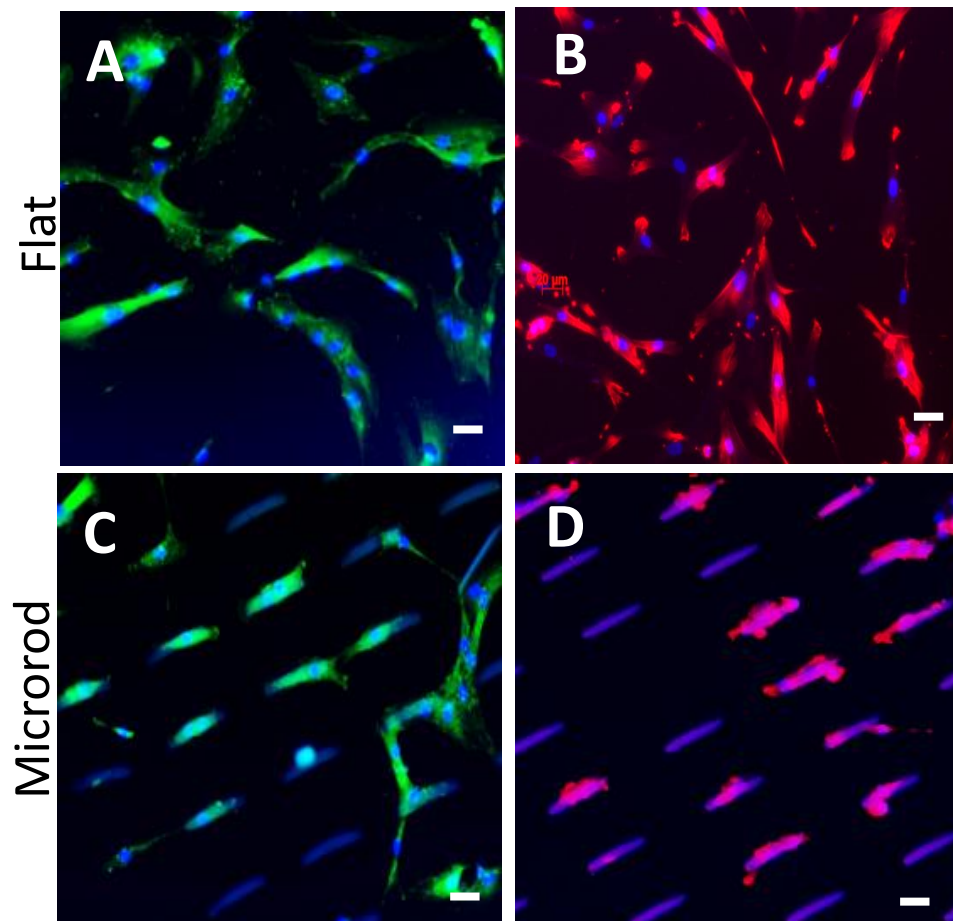


**Figure 30.** Microrods remodel hMSC morphology and adhesion. (A and B) Stem cells grown on the flat surface had the normal actin cytoskeleton and focal adhesions either with MGF (A) or without MGF (B). The microrods topography guided stem cell growth by changes to the cytoskeleton and focal adhesions either with MGF (C) or without MGF (D). Actin (red), paxillin(green), nuclei (blue) and microrods (blue), scale bar, 50  $\mu\text{m}$



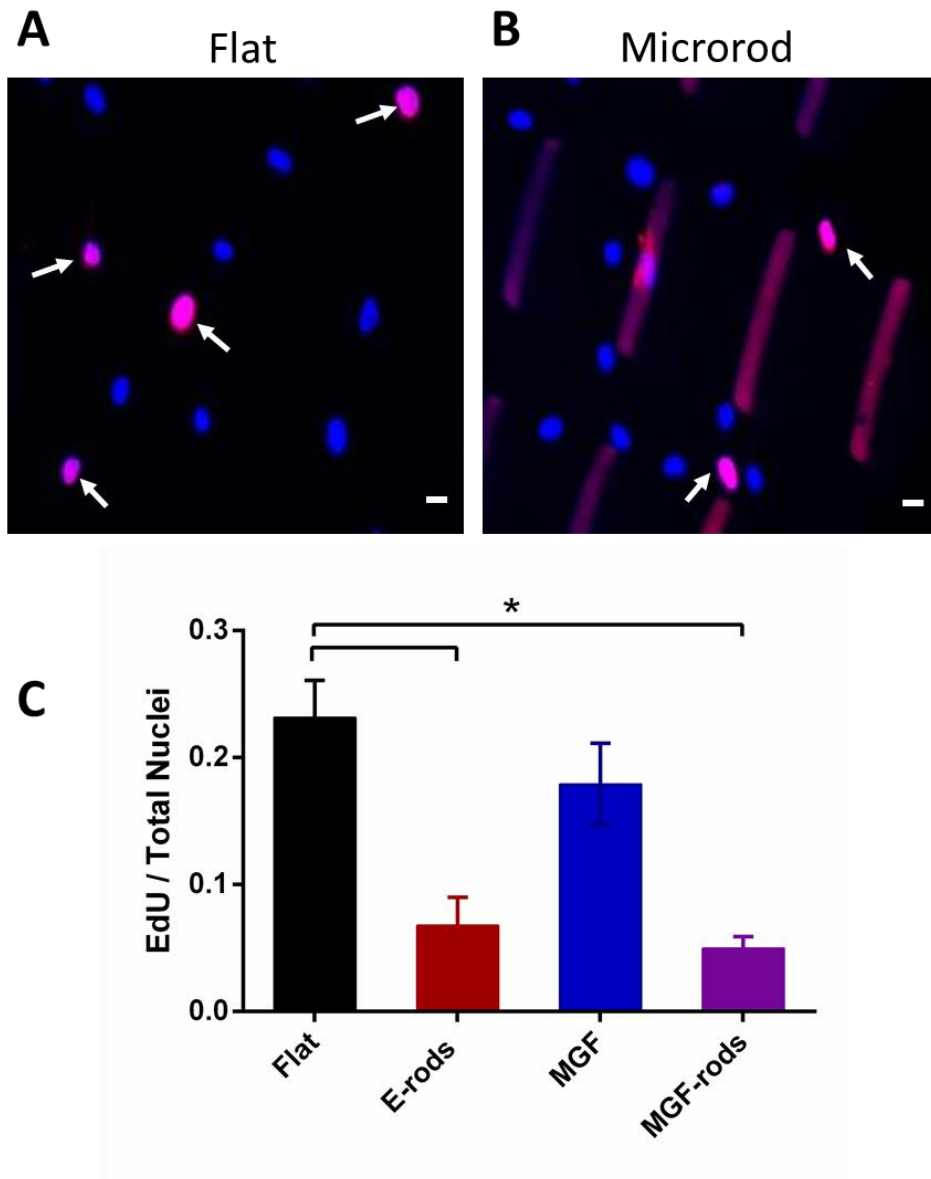


**Figure 31.** Microrods blunt proliferation of hMSCs. Newly dividing cells (pink) vs. non-dividing cells (blue) on (a) flat and (b) microrods, as seen by fluorescence microscopy. (c) EdU/total nuclei per condition shows that microrods inhibited new synthesis of DNA with or without MGF. Dividing nuclei (arrows) stained with EdU (pink), non-dividing with DAPI (blue), and microrods artificially stained with DAPI and EdU (Purple). Mean ± SE, n=4, \* p < 0.05. Scale bar, 20 μm.

#### **v. Migration**

MGF in the media and MGF eluted (30-70 ng) overnight by the microrods was bioactive and induced stem cell migration compared to the microrods without MGF ( $1.72 \pm 0.23$ ,  $p < 0.05$ ). No migration of hMSCs was seen with E-rods (Figure 32)

#### **vi. Hypoxia induction of apoptosis by chemicals**

After chemically induced apoptosis by hydrogen peroxide, cell death signaling of NRVM was determined by caspase (Figure 33) and HIF-1 $\alpha$  (Figure 34) staining. Fluorescence images show both red and green colors which represents late apoptosis of the cells. However, induction of apoptosis by the hypoxia chamber is more physiologic, therefore, we switched to severe low oxygen tension which makes NRVM apoptotic.

#### **vii. Hypoxic induction of apoptosis by hypoxia chamber**

After induction of hypoxic stress to NRVMs (Figure 35), the extent of cell death was measured by TUNEL positive nuclei (DNA fragmentation). Treatment of hypoxic heart cells with MGF showed an increase in viable cells ( $P < 0.05$  for experimental groups: MGF in media, MGF-rods vs. control groups: E-rods and Hypoxia) (Figure 36 and Figure 37A). In addition, Bcl2 gene expression (cell signaling) measured by qRT-PCR also confirmed the anti-apoptotic role of MGF peptide (Figure 37B), demonstrating that both MGF and MGF-rods increased relative expression of Bcl2. Furthermore, the eluted MGF peptide retained bioactivity after the fabrication process into the microrod.

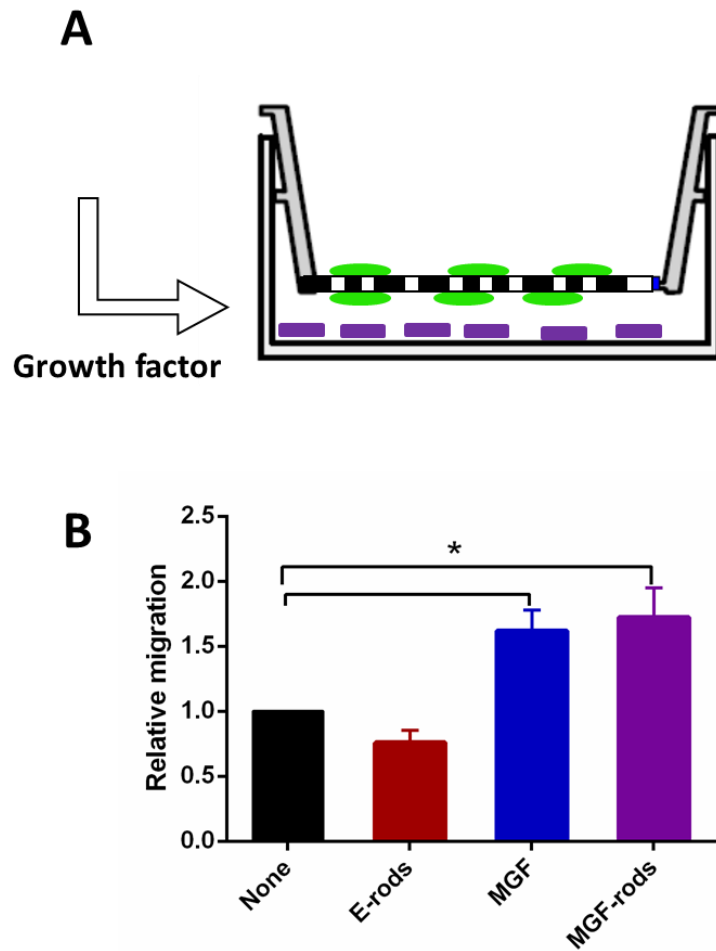


**Figure 32.** Eluted MGF is bioactive and regulates hMSCs migration. (A) Schematic diagram of Boyden chamber with cells (green) on top and the microrods (purple) eluting MGF below. (B) Migration overnight is increased both by MGF in media and MGF eluted from microrods, Mean $\pm$  SE, n=3 human samples, \* p < 0.05.

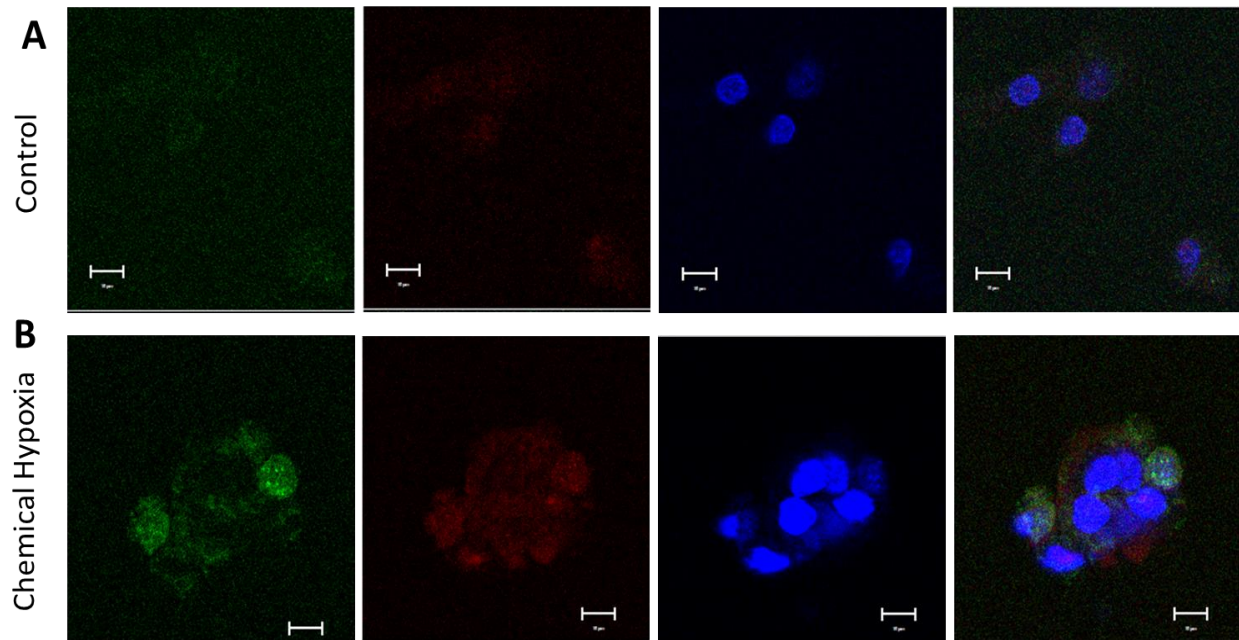


**Figure 33.** Induction of chemical hypoxia was detected by caspase 3 and 7 assay. Confocal images show NRVM cells which were stained for caspase 3 and 7 to assess cell apoptosis after 30 min exposure to hydrogen peroxide. (green: Caspase, red: PI, blue:DAPI, and the last panels on right is the merged images), scale bar 10  $\mu$ m

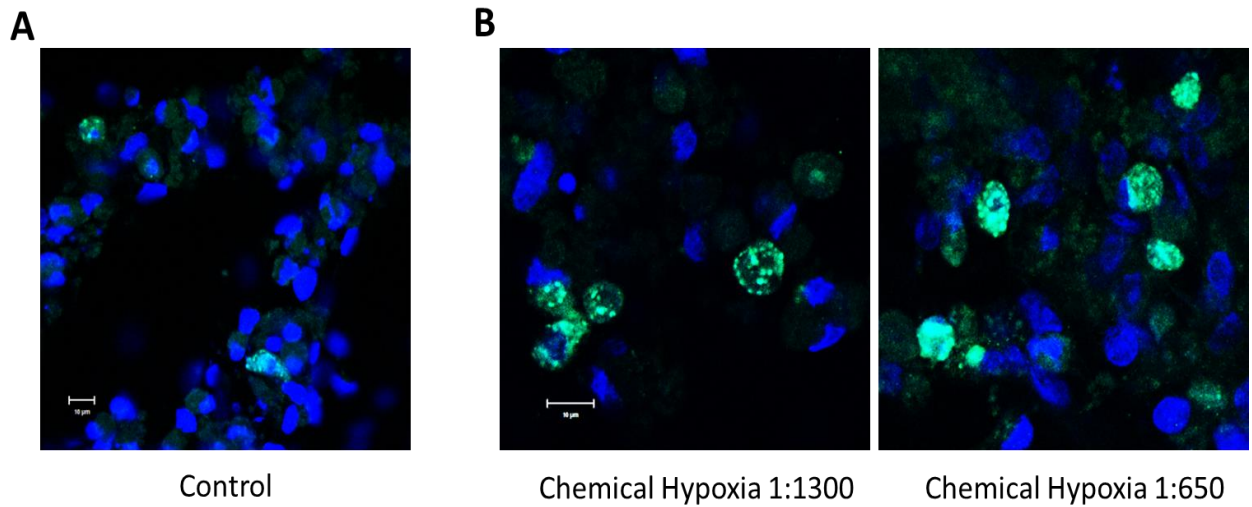


**Figure 34.** Induction of chemical hypoxia was detected by HIF-1 $\alpha$ . NRVM were stained for HIF-1 $\alpha$  (1:650 and 1:1300 ratio of the antibody) to assess cell death after 30 min chemically induced apoptosis by hydrogen peroxide seen by confocal microscopy. (Green: HIF-1 $\alpha$ , blue:DAPI), scale bar 10  $\mu$ m

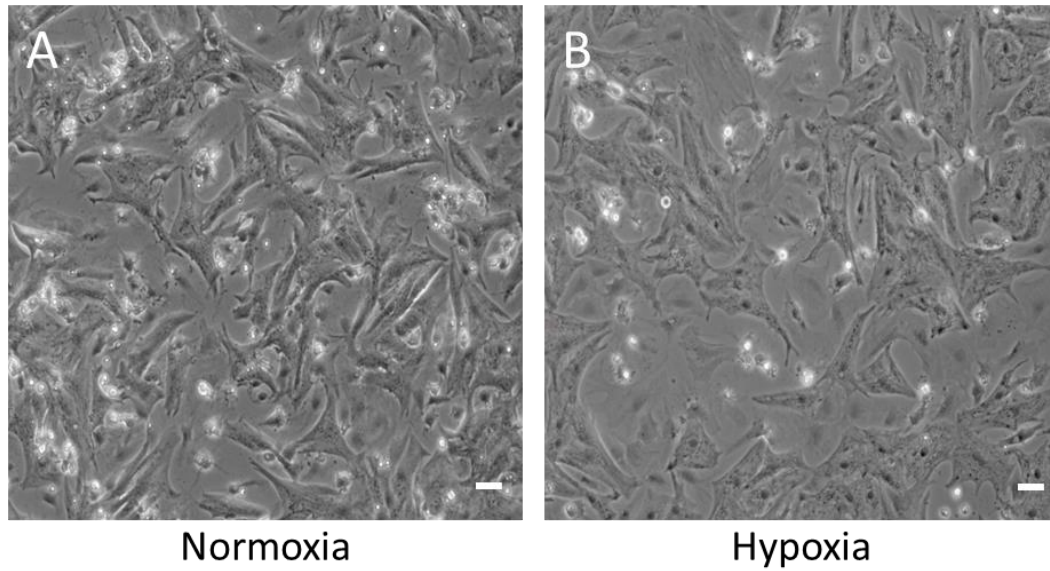


**Figure 35.** Induction of hypoxia by hypoxic chamber. NRVM in normoxia (left panel) and after 8 hours hypoxia (1% O<sub>2</sub>) (right panel)

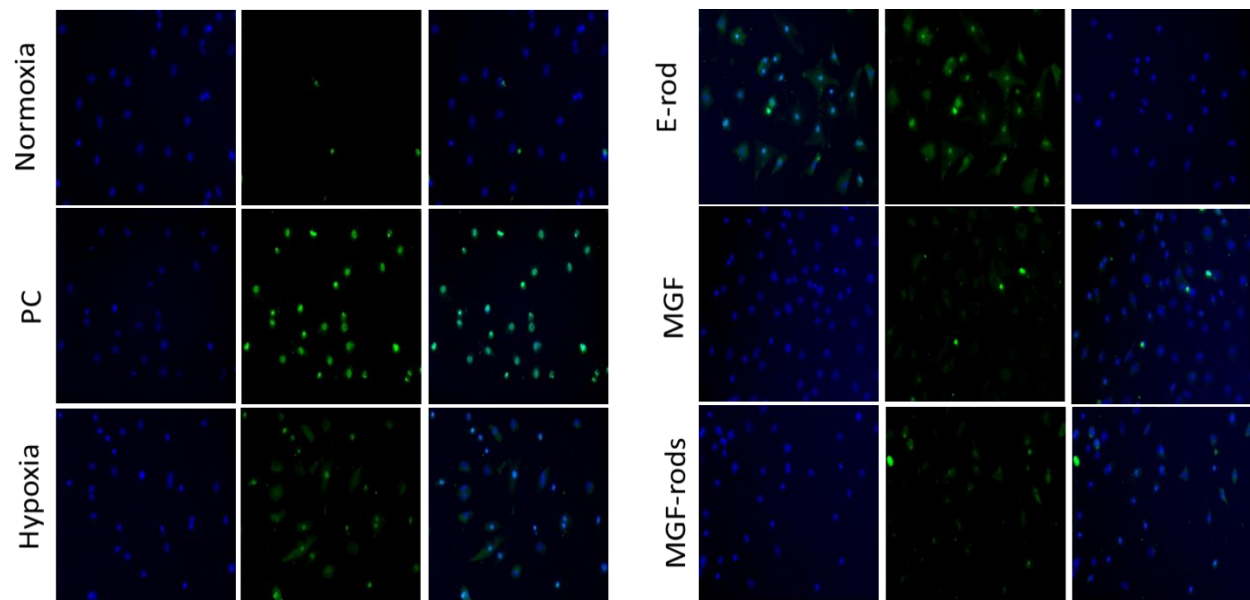


**Figure 36.** Cell death detection by TUNEL assay induced by hypoxia. TUNEL assay shows apoptotic cells after 8 hours at 1% O<sub>2</sub>, seen by fluorescence microscopy in control (normoxia), positive control (PC) induced by DNase I recombinant, hypoxia, empty rods (E-rods), MGF in media, and MGF-rods. (green: positive TUNEL nuclei, blue: DAPI) (left to the right panels are: nucleus, TUNEL, and merged images)

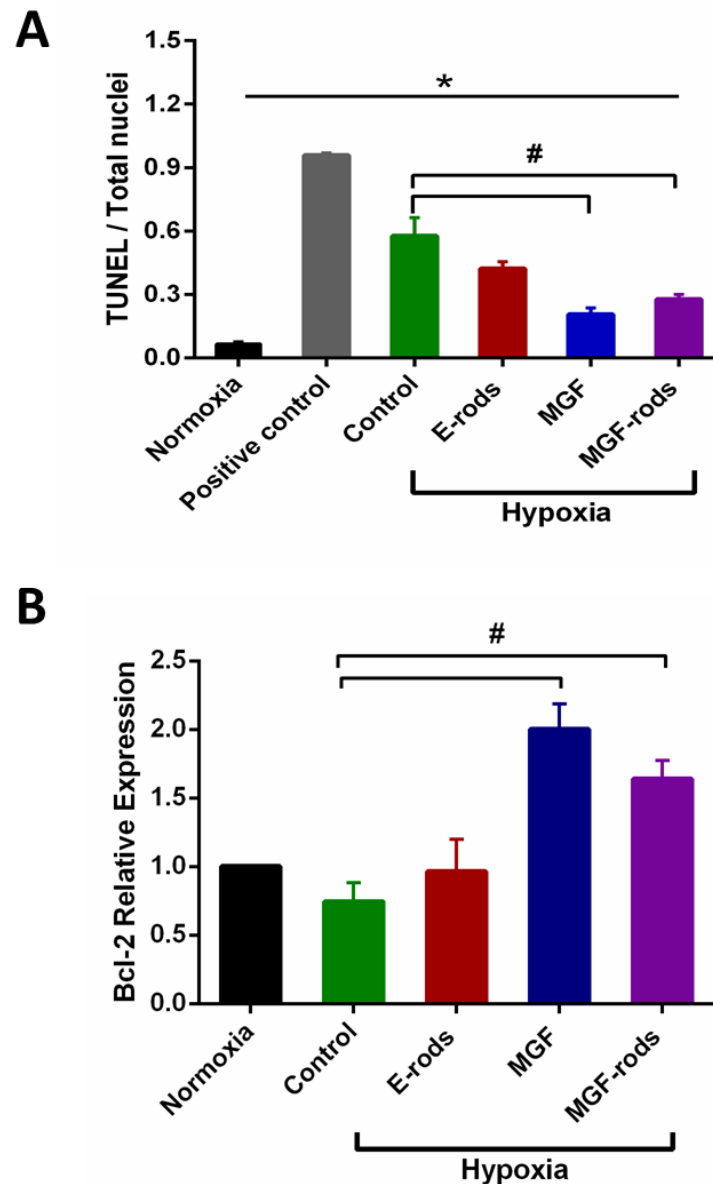


**Figure 37.** MGF protects NRVM from apoptosis induced by hypoxia. (A) NRVMs after 8 hours of hypoxia (1% O<sub>2</sub>) are apoptotic as assessed by TUNEL positive nuclei. Apoptosis is reduced by MGF added to the media (MGF) or eluted from the microrods (MGF-rods) but not by empty microrods (E-rods). Postive control is with DNase I recombinant (B) Increased relative gene expression of Bcl-2 of NRVMs after 8 hours of hypoxia treated with MGF or MGF-rods confirms that MGF improves cell survival. Mean ± SE, n = 4, \*P < 0.05



## D. Discussion

The major findings of this study were the successful encapsulation of native MGF peptide within microrods that sustained delivery of MGF up to two weeks. The native MGF eluted from the microrods retained bioactivity as assessed by induction of hMSC migration and, moreover, the inhibition of the apoptotic pathway in NRVMs subjected to hypoxia. Microrods alone without MGF regulated the cytoskeleton, adhesion, and proliferation of hMSCs. Therefore, the combination microdevice provides the mechanical cues and MGF bioactivity after fabrication, which may provide for potential therapeutic delivery and cardiac repair and regeneration *in vivo*.

### i. PEGDMA microrods in drug elution applications

For effective application in the heart, a hydrogel material was chosen for the microrods that was biocompatible, able to be modulated in terms of stiffness for cell anchorage, compatible with high-throughput photolithographic processing, exhibits harmless long-term degradation byproducts and, finally, capable of drug elution over a biologically relevant time period of several days in the wake of acute cardiac injury. Many studies model the mechanical microenvironment using polyacrylamide substrates with tunable mechanical properties. However, due to cytotoxicity, polyacrylamide substrates are unsuitable for long-term *in vitro* studies or eventual *in vivo* applications. PEGDMA, on the other hand, is used extensively for tissue engineering and drug delivery applications and displays excellent biocompatibility (Bryant 2003, Diramio 2005). It is photopolymerizable, allowing us to precisely control the microrod geometry. In fact, this shape feature of the microrods is chosen to provide a high aspect ratio

microstructure to affect higher mechanical influence on cells interacting with the microrod, and the size of the feature is chosen to mimic the scale of normal cell size found physiologically to provide biologically relevant mechanical cues to cells that interact with the microstructure. In addition, we have previously shown that the stiffness of PEGDMA can be tuned by changing the concentration and ultimately the cross-linking density, which are important factors in degradation rate (Ayala, 2010).

## **ii. Microrods degradation**

Due to the nature of the polymeric cross-linking in PEGDMA hydrogel constructs, microrods fabricated from this material will undergo hydrolysis over time, leaving behind small, inert PEG chains. This process appears to be slow, and previous work has shown minimal degradation over three weeks (Tucker, 2012). Although our experience with these types of constructs has further shown relative morphological stability of microrods in non-physiological conditions for months, a thorough analysis of the long-term degradation of microrods under physiologic conditions *in vivo* would be valuable. Degradation rate is sensitive to the size scale, polymeric composition, and particular polymerization process of the construct, and understanding how each of these components affects PEGDMA microstructure stability will enable precision temporal tuning of incorporated drug release and microstructure deterioration for various applications. Conceivably, the incorporation of more rapidly hydrolysable cross-linking agents could also accelerate the drug release or microstructure degradation process as may be required in certain physiologic settings.

### iii. Physiological effect of the microrods alone

Microrods in a 3D system inhibited fibroblast proliferation and down-regulated expression of key extracellular matrix proteins involved in scar tissue formation (Norman, 2007, Ayala, 2010). hMSCs attached to 30 kPa microrods displayed elongated morphology as compared to cells not exposed to discrete micromechanical cues. The local stresses induced by microrods were recognized by the cells, which consequently altered the cytoskeletal architecture adjacent to the microrod (Norman, 2007, Collins, 2009, Ayala, 2010). This remodeling of cells by the external topography of microrods is due to the interactions that link the transmembrane integrin receptors to the actin cytoskeleton via adaptor proteins such as vinculin, paxillin, and  $\alpha$ -actinin (Samarel 2005). This similar behavior by hMSCs was also observed in this study. In addition, a previously developed in vitro model system has shown that the inclusion of SU-8 microrods in three dimensions (3D) can alter long-term growth responses of neonatal ventricular myocytes (Curtis 2010a, 2013b), the mechanism of which depends on aspects of RhoA/ROCK and PKC signaling. The use of geometric boundaries that force neonatal rat ventricular myocytes to spread into an elongated shape, similar to that of cardiomyocytes *in vivo*, leads to more myofibril alignment and clear axes of contraction (Motlagh 2003, Bray, 2008). As expected, however, (Collins 2010) MGF did not affect hMSC proliferation or the subcellular architecture.

### iv. Microrods retain bioactivity of MGF

Encapsulation of native MGF in the microrods is one way to protect it from rapid degradation *in vivo*. Early work on MGF in muscle tissue described this form of the *IGF-*

1 gene as being unglycosylated and probably having a shorter half-life time in the serum or tissue due to proteolytic cleavage (Yang and Goldspink, 2001). Therefore, native MGF was protected from degradation by chemically modifying the E-domain to stabilize the peptide by pegylation and replacement of an L-arginine with a D-arginine to withstand the interstitial cleavage enzymes (Dluzniewska, 2005). Unfortunately, there are concerns regarding side effects with systemic delivery of the stable form due to stimulation of the IGF pathway systemically: an issue especially in women with certain types of breast cancer (Nahta, 2005). The incorporation and protection of MGF within microrod hydrogel constructs was achieved in this study, which allowed us to further study the potential for local delivery and bioactivity of MGF.

#### **v. Sustained delivery of MGF for two weeks**

Using E-peptide specific probes, the mRNA of MGF was found to be markedly increased during the acute stress (24 hours) but then declined in skeletal muscle or cardiac cells following injury (Hill 2003, Mavrommatis, 2013, Stavropoulou, 2009). Two days of cyclic stretch at high strain (20%) at 1 Hz caused increased MGF gene expression in NRVMs, again suggesting MGF is related to stress or injury and showing that myocytes produce MGF (Collins, 2010). Thus, the native MGF delivery window of one day to at least 2 weeks may be effective for cardiac repair *in vivo*.

We were able to attain this objective with a delivery profile of MGF from the PEGDMA microrods from one day up to at least 14 days. However, it is important to note that the actual delivery efficiency of the MGF-containing microrod system is likely considerably higher than the calculated theoretical efficiency. The theoretical MGF

content potentially overestimates the available drug to be delivered in the microrods in several ways. Firstly, it requires an assumption that the microrods are solid objects with a material volume equal to the spatial volume of the structure itself. However, the highly porous nature of the microstructures can significantly decrease the volume of material available to hold and deliver the peptide. In addition, a considerable portion of the MGF may be damaged or eluted prior to the start of the measured elution during UV exposure, cold storage, or water and alcohol rinses after fabrication of the microstructures. MGF may be further destroyed throughout the course of the experiment by general hydrolytic processes, obscuring our ability to detect the cumulative eluted peptide at later time points by HPLC. Lastly, inhomogeneities in the microrod population may lead to different loading capacities of each microrod, so the presumed total MGF content is taken as an average potential drug capacity. These factors were mitigated to an extent by isolating only microrods of the proper size and shape and minimizing time spent in water or ethanol solutions to reduce the amount of drug released prior to the start of the experiment. Further experiments to understand the nature and stability with which MGF is incorporated into the matrix would be valuable as a tool to understand extended clinical applications of this technology.

#### **vi. Migration of hMSCs as a bioactivity assay**

Elution of MGF from the microrods established a growth factor gradient and induced migration of hMSCs. There is still controversy whether the migration mechanism of stem cells via these growth factors is dependent or independent of IGF-1 receptor (Yang, 2002, Mills, 2007). However, previous work has suggested that the

migration effect of MGF peptide on MSCs depends on IGF-1 receptor via Erk1/2 signal pathway (Cui, 2014, Wu, 2013). MGF promotes rat tenocyte migration by lessening cell stiffness and increasing pseudopodia formation via the FAK-ERK1/2 signaling pathway (Zhang, 2014), while the peptide intervention caused MSCs to stiffen (Wu, 2013). Our results suggest that the injectable MGF-microrods may foster stem cell homing *in vivo*, by generating a chemotactic gradient that is translated into a mechanotactic response through the IGF-1 receptor mediated pathways.

#### **vii. Prevention of NRVM apoptosis as a bioactivity assay**

In addition to increasing cell migration, eluted MGF retained bioactivity to prevent apoptosis in cardiac muscle cells. The E-domain of MGF appears to have beneficiary effects in injured tissue either distinctly or synergistically to the mature peptide of IGF-1 (Carpenter, 2008, Dluzniewska 2005). Here, we altered the oxygenation conditions *in vitro* to establish changes in gene expression and cell survival of NRVMs under hypoxic conditions that mimic the ischemic heart. Results of the TUNEL assay and Bcl-2 expression confirm MGF protection for myocytes from apoptosis that should, confer longevity to progenitor and effector cells in tissues (Hockenberry, 1990, Korsmeyer, 1992, Grünenfelder, 2001). By improving cell survival, the likelihood of regeneration will be improved and cell death of the pre-existing myocardium attenuated, which could translate into an improvement in function. Thus, the effective delivery of MGF from the microrods may permit myocytes to thrive *in vivo* even under hypoxic conditions.

## **E. Conclusion and summary**

Bioengineering approaches were able to achieve a therapeutically relevant two-week time course of MGF delivery and to protect native MGF peptide in a bioactive state. Stem cell migration was preserved and myocyte apoptosis under hypoxic stress was reduced. The ability to incorporate and protect a peptide therapeutic in a monolithic hydrogel device to extend its half-life *in vivo* has great potential for countless translational applications. Thus, outcomes in a therapeutic setting of injection of this MGF loaded microdevice into injured regions of the heart might be beneficial in reducing myocyte loss in ischemia and boosting repair by the chemo-attraction of stem cells to the damaged area.

By adapting a stable and well-understood polymer system to serve as both a mechanical stimulus as well as provide highly-localized, long-term delivery of bioactive peptides, we may be able to expand the therapeutic profile of many existing biomolecules.

#### IV. MAJOR CONCLUSIONS

This thesis uses engineering and biological techniques to assess basic cellular function with the goal of applying the results to cardiac regeneration therapy. The approach is to understand both physical and chemical cues of the microenvironment that control structure and function of human mesenchymal stem cells and neonatal rat ventricular myocytes (hMSCs and NRVM, respectively). The major conclusions of this research are divided into two parts: A) the effects of physical cues, and B) the effects of chemical cues. It is the combination of these cues that will be necessary for the optional control of cells *in vivo*.

##### **Part A: Physical cues of the microenvironment affect cell function.**

*A1: Microfabrication is a useful method to fabricate substrates for cell growth.*

- A. PDMS microposts and PEGDMA microrods are biocompatible with both hMSCs and NRVMs
- B. hMSCs ignore the posts with less than 15 $\mu$ m height and behave like cells on a flat surface.
- C. The structural organization of the cytoskeleton and focal adhesions of hMSCs are remodeled by the microrods as assessed by actin and paxillin immunostaining.
- D. Focal adhesions form on the vertical side of the post with the actin fibers wrapped the cell around it as determined by paxillin staining.
- E. Nuclear size, shape, and height change with micropost topography, and the cells are mostly in close contact with the posts.



- F. hMSC proliferation is inhibited by the microrods as determined by the EdU assay for DNA replication.

*A2: Cyclic strain is a useful method to apply external forces to cells.*

- G. The cytoskeleton elongates and the focal adhesion attachment on the post become asymmetric with cyclic strain of hMSCs.
- H. Nuclear size, shape and subcellular location also change with strain where the cells are more distant from the posts.
- I. Anisotropic strain increase the proliferation of hMSCs but biaxial strain does not as determined by an EdU assay.

*A3: The combination of strain and topography provides the complex physical cues as seen in living tissue.*

- J. Biaxial or uniaxial strain was applied to hMSCs via substrates with micropost topography.
- K. Both strain and microtopography contribute to the remodeling of the cytoskeleton and focal adhesions in hMSCs as determined by actin and paxillin staining.
- L. Microarray analysis demonstrates significant difference of transcript levels between hMSCs in strain conditions (strain and post-strain) and non-strained conditions (flat and post) after two days of culture.
- M. Quantitative PCR confirms microarray data indicating that gene expression corresponding to the functional ontology group “Matrix and Focal adhesions”, “Muscle proteins”, “Proliferation” and “Differentiation” is enhanced more significantly with cyclic strain than without.

- N. RNA/DNA/Protein do not change between the control (flat) and experimental groups (post, strain, and post-strain).

**Part B: Chemical cues affect stem cell and cardiac cell function.**

- A. Mechano growth factor delivery from the microrods is sustained for two weeks.
- B. Migration of hMSCs overnight increase when exposed to MGF in the media or MGF released from microrods as determined by Boyden chamber.
- C. Proliferation of hMSCS is not regulated by native MGF as determined by EdU.
- D. Hypoxia (1% O<sub>2</sub>) induces apoptosis in NRVM as measured by the TUNEL assay.
- E. MGF in media or MGF released from the microrods protect NVRM from severe hypoxia as shown by reduced cell death.
- F. Bcl-2 gene expression by quantitative PCR shows improved NRVM survival with MGF in media or MGF from the microrods.

Stem cells delivery and tissue engineering of cardiac patches are being investigated in regenerative medicine because of the need to replace heart muscle lost after myocardial infarction. The enhancement of regeneration is being actively studies by research on scaffolds, stem cells, gene therapy, and chemical and mechanical signals. The infracted myocardium is not an environment conducive to stem cell survival and differentiation into myocytes is not yet well controlled. Even though a small percentage of implanted cells do survive and differentiate into cardiomyocytes in the injured myocardium, these are not sufficient to improve cardiac function. Engineered

constructs made in vitro have problems with function when implanted in vivo because of the lack of oxygen and adequate nutrients prevent cell death. Nonetheless, cardiac tissue engineering has been proposed as an appropriate method to repair myocardial infarction (Eschenhagen, 2012, Tulloch and Murry, 2013).

To further understand the role of stem cells in regeneration, it is essential to develop instrumentation and technologies to track the process of the development by regulating their migration, differentiation, proliferation, and apoptosis. We must begin to identify the environmental cues that are needed for stem cell trafficking and we must define the genetic and cellular mechanisms underlying their function in order to realize the full potential of stem cells in regenerative medicine.

The objectives in this dissertation is on the importance of the stem cell response to physical cues, which are manipulated in a quantitative manner by the microstructures and mechanical load. Furthermore, the combination of biomimetic materials and chemical factors are explored to stimulate, enhance, or control cardiac's innate regenerative capacity.

Of note in findings in this thesis are the complexities with which different mechanical stimuli regulate cells. For example, “self-renewal” of hMSCs is regulated by anisotropic strain but not by equibiaxial strain and also by the 30 kPa PEGDMA microrods and not the 1.7 MPa PDMS posts. Proliferation of embryonic stem cells was inhibited by the PDMS microposts while hMSC proliferation was increased with the Su-8 microrods incorporated in a 3D soft gel (Collins, 2009, Biehl, 2009). Cell type and 2D vs. 3D environment are all other important factors, which could impact the stem cell function.

Taken together, the results suggest that the mechanotransduction processes differ with specific physical cues (e.g. material, stiffness, geometry and dimension).

For the second part of the thesis, the main challenge is to optimize the microdevice for the regeneration therapy. Local chemical cues will also be necessary to optimize tissue regeneration. MGF was chosen as a chemical cue to be incorporated into microstructures. In addition to the homing effect of MGF, it is anti-apoptotic agent that improves cell survival after cardiac injury. Therefore, MGF elution from microrods may enhance regeneration by recruiting the number of stem cells in the heart and also preventing cell death after infarct or injury. Additionally, this platform could be modified to deliver different stiffness and topography, and other chemical factors such as SDF-1 or estrogen can be used for recruiting more stem cells to the injured heart. The properties of the PEGDMA microrods could be modified to attain that goal.

This thesis has yielded new information about how cells respond to local physical and chemical cues. These novel polymeric microstructures were designed with mechanical stiffness and size optimal application in cardiac tissue, as well as to release highly localized, bioactive peptides over a two-week period. Therefore, injection of this MGF microrod device *in vivo* should be beneficial in cardiac repair and regeneration.

Additionally, specific stiffness, microtopography, strain profiles and a variety of drugs and growth peptides could permit us to expand the therapeutic profile of many existing biomolecules into many different tissue applications.

## V. FUTURE WORK

Further work is needed in order to understand the mechanisms underlying the changes observed. For the first part of the project, we conclude that strain is dominant over microtopography, but how exactly was not deeply explored. Previously, in our discussion, we suggested that force generation difference imposed by these mechanical cues was a main fact, which probably regulated the myosin II. However, we did not test and measure the force generated by strain and the posts, and we did not use any inhibitory drugs in order to detect cell mechanotransduction signaling pathways.

Even though hMCSc have the potential to differentiate into many cell types, the results from the microarray showed that these cells have limited potential for cardiac differentiation after two days of cyclic strain with microposts, and thus they are unlikely to regenerate the damaged heart significantly. Other cell sources such as resident progenitor cells of heart or human induced pluripotent cells are other candidates for these projects.

Even though microposts give the cells increased surface area to which the stress fibers can attach, the scaffold with the microposts is not a completely three dimensional environment. Therefore, combination of cyclic strain and microstructures in true 3D scaffolds would create a better physiological environment that might yield the cardiac differentiation of the cells. Unfortunately, we have the limitation that 3D gels cannot be strained or imaged.

In order to enhance the mechanical loads imposed by the posts on the cells, alternative topography could be made to test geometric spacing. For example, we could modify

the structure of the microposts, or the distance and area between them. Certain geometries might alter the stress fibers and influence proliferation, focal adhesion, and even differentiation

## CITED LITERATURE

- Andrews, P. W., M. M. Matin, A. R. Bahrami, I. Damjanov, P. Gokhale and J. S. Draper (2005). "Embryonic stem (ES) cells and embryonal carcinoma (EC) cells: opposite sides of the same coin." Biochem Soc Trans **33**(Pt 6): 1526-1530.
- Applegate, D., W. Feng, R. S. Green and M. B. Taubman (1994). "Cloning and expression of a novel acidic calponin isoform from rat aortic vascular smooth muscle." J Biol Chem **269**(14): 10683-10690.
- Ates, K., S. Y. Yang, R. W. Orrell, A. C. Sinanan, P. Simons, A. Solomon, S. Beech, G. Goldspink and M. P. Lewis (2007). "The IGF-I splice variant MGF increases progenitor cells in ALS, dystrophic, and normal muscle." FEBS Lett **581**(14): 2727-2732.
- Ayala, P., J. I. Lopez and T. A. Desai (2010). "Microtopographical cues in 3D attenuate fibrotic phenotype and extracellular matrix deposition: implications for tissue regeneration." Tissue Eng Part A **16**(8): 2519-2527.
- Bauwens, C., T. Yin, S. Dang, R. Peerani and P. W. Zandstra (2005). "Development of a perfusion fed bioreactor for embryonic stem cell-derived cardiomyocyte generation: oxygen-mediated enhancement of cardiomyocyte output." Biotechnol Bioeng **90**(4): 452-461.
- Beltrami, A. P., L. Barlucchi, D. Torella, M. Baker, F. Limana, S. Chimenti, H. Kasahara, M. Rota, E. Musso, K. Urbanek, A. Leri, J. Kajstura, B. Nadal-Ginard and P. Anversa (2003). "Adult cardiac stem cells are multipotent and support myocardial regeneration." Cell **114**(6): 763-776.
- Berry, M. F., A. J. Engler, Y. J. Woo, T. J. Pirolli, L. T. Bish, V. Jayasankar, K. J. Morine, T. J. Gardner, D. E. Discher and H. L. Sweeney (2006). "Mesenchymal stem cell injection after myocardial infarction improves myocardial compliance." Am J Physiol Heart Circ Physiol **290**(6): H2196-2203.
- Bettinger, C. J., B. Orrick, A. Misra, R. Langer and J. T. Borenstein (2006). "Microfabrication of poly (glycerol-sebacate) for contact guidance applications." Biomaterials **27**(12): 2558-2565.
- Bhang, S. H., S. J. Gwak, T. J. Lee, S. S. Kim, H. H. Park, M. H. Park, D. H. Lee, S. H. Lee and B. S. Kim (2010). "Cyclic mechanical strain promotes transforming-growth-factor-beta1-mediated cardiomyogenic marker expression in bone-marrow-derived mesenchymal stem cells in vitro." Biotechnol Appl Biochem **55**(4): 191-197.
- Biehl, J. K., S. Yamanaka, T. A. Desai, K. R. Boheler and B. Russell (2009). "Proliferation of mouse embryonic stem cell progeny and the spontaneous contractile activity of cardiomyocytes are affected by microtopography." Dev Dyn **238**(8): 1964-1973.

- Birukov, K. G. (2009). "Cyclic stretch, reactive oxygen species, and vascular remodeling." Antioxid Redox Signal **11**(7): 1651-1667.
- Blokhina, O., E. Virolainen and K. V. Fagerstedt (2003). "Antioxidants, oxidative damage and oxygen deprivation stress: a review." Ann Bot **91 Spec No**: 179-194.
- Boateng, S. Y., T. J. Hartman, N. Ahluwalia, H. Vidula, T. A. Desai and B. Russell (2003). "Inhibition of fibroblast proliferation in cardiac myocyte cultures by surface microtopography." Am J Physiol Cell Physiol **285**(1): C171-182.
- Boheler, K. R., R. N. Joodi, H. Qiao, O. Juhasz, A. L. Urick, S. L. Chuppa, R. L. Gundry, R. P. Wersto and R. Zhou (2011). "Embryonic stem cell-derived cardiomyocyte heterogeneity and the isolation of immature and committed cells for cardiac remodeling and regeneration." Stem Cells Int **2011**: 214203.
- Bray, M. A., S. P. Sheehy and K. K. Parker (2008). "Sarcomere alignment is regulated by myocyte shape." Cell Motil Cytoskeleton **65**(8): 641-651.
- Brown, A. F. (1982). "Neutrophil granulocytes: adhesion and locomotion on collagen substrata and in collagen matrices." J Cell Sci **58**: 455-467.
- Brunner, S., B. C. Huber, R. Fischer, M. Groebner, M. Hacker, R. David, M. M. Zaruba, M. Vallaster, C. Rischpler, A. Wilke, A. Gerbitz and W. M. Franz (2008). "G-CSF treatment after myocardial infarction: impact on bone marrow-derived vs cardiac progenitor cells." Exp Hematol **36**(6): 695-702.
- Bryant, S. J. and K. S. Anseth (2003). "Controlling the spatial distribution of ECM components in degradable PEG hydrogels for tissue engineering cartilage." J Biomed Mater Res A **64**(1): 70-79.
- Buerke, M., T. Murohara, C. Skurk, C. Nuss, K. Tomaselli and A. M. Lefer (1995). "Cardioprotective effect of insulin-like growth factor I in myocardial ischemia followed by reperfusion." Proc Natl Acad Sci U S A **92**(17): 8031-8035.
- Buggisch, M., B. Ateghang, C. Ruhe, C. Strobel, S. Lange, M. Wartenberg and H. Sauer (2007). "Stimulation of ES-cell-derived cardiomyogenesis and neonatal cardiac cell proliferation by reactive oxygen species and NADPH oxidase." J Cell Sci **120**(Pt 5): 885-894.
- Bujak, M. and N. G. Frangogiannis (2007). "The role of TGF-beta signaling in myocardial infarction and cardiac remodeling." Cardiovasc Res **74**(2): 184-195.
- Burke, B. and K. J. Roux (2009). "Nuclei take a position: managing nuclear location." Dev Cell **17**(5): 587-597.
- Carpenter, V., K. Matthews, G. Devlin, S. Stuart, J. Jensen, J. Conaglen, F. Jeanplong, P. Goldspink, S. Y. Yang, G. Goldspink, J. Bass and C. McMahon (2008).



- "Mechano-growth factor reduces loss of cardiac function in acute myocardial infarction." Heart Lung Circ **17**(1): 33-39.
- Cevallos, M., G. M. Riha, X. Wang, H. Yang, S. Yan, M. Li, H. Chai, Q. Yao and C. Chen (2006). "Cyclic strain induces expression of specific smooth muscle cell markers in human endothelial cells." Differentiation **74**(9-10): 552-561.
- Chandel, N. S. and G. R. Budinger (2007). "The cellular basis for diverse responses to oxygen." Free Radic Biol Med **42**(2): 165-174.
- Chapman, K. E., S. E. Sinclair, D. Zhuang, A. Hassid, L. P. Desai and C. M. Waters (2005). "Cyclic mechanical strain increases reactive oxygen species production in pulmonary epithelial cells." Am J Physiol Lung Cell Mol Physiol **289**(5): L834-841.
- Chen, K. D., Y. S. Li, M. Kim, S. Li, S. Yuan, S. Chien and J. Y. Shyy (1999). "Mechanotransduction in response to shear stress. Roles of receptor tyrosine kinases, integrins, and Shc." J Biol Chem **274**(26): 18393-18400.
- Cheng, C. M. and P. R. LeDuc (2006). "Micropatterning polyvinyl alcohol as a biomimetic material through soft lithography with cell culture." Mol Biosyst **2**(6-7): 299-303.
- Chew, S. L., P. Lavender, A. J. Clark and R. J. Ross (1995). "An alternatively spliced human insulin-like growth factor-I transcript with hepatic tissue expression that diverts away from the mitogenic IGF1 peptide." Endocrinology **136**(5): 1939-1944.
- Christman, K. L., Q. Fang, M. S. Yee, K. R. Johnson, R. E. Sievers and R. J. Lee (2005). "Enhanced neovasculature formation in ischemic myocardium following delivery of pleiotrophin plasmid in a biopolymer." Biomaterials **26**(10): 1139-1144.
- Christman, K. L., H. H. Fok, R. E. Sievers, Q. Fang and R. J. Lee (2004). "Fibrin glue alone and skeletal myoblasts in a fibrin scaffold preserve cardiac function after myocardial infarction." Tissue Eng **10**(3-4): 403-409.
- Collins, J. M., P. Ayala, T. A. Desai and B. Russell (2010). "Three-dimensional culture with stiff microstructures increases proliferation and slows osteogenic differentiation of human mesenchymal stem cells." Small **6**(3): 355-360.
- Collins, J. M., P. H. Goldspink and B. Russell (2010). "Migration and proliferation of human mesenchymal stem cells is stimulated by different regions of the mechano-growth factor prohormone." J Mol Cell Cardiol **49**(6): 1042-1045.
- Collins, J. M. and B. Russell (2009). "Stem cell therapy for cardiac repair." J Cardiovasc Nurs **24**(2): 93-97.

- Cuevas, P., F. Carceller, V. Martinez-Coso, E. Asin-Cardiel and G. Gimenez-Gallego (2000). "Fibroblast growth factor cardioprotection against ischemia-reperfusion injury may involve K<sup>+</sup> ATP channels." Eur J Med Res **5**(4): 145-149.
- Cui, H., Q. Yi, J. Feng, L. Yang and L. Tang (2014). "Mechano growth factor E peptide regulates migration and differentiation of bone marrow mesenchymal stem cells." J Mol Endocrinol **52**(2): 111-120.
- Cunningham, J. J., J. J. Linderman and D. J. Mooney (2002). "Externally applied cyclic strain regulates localization of focal contact components in cultured smooth muscle cells." Ann Biomed Eng **30**(7): 927-935.
- Curtis, M. W., E. Budyn, T. A. Desai, A. M. Samarel and B. Russell (2013). "Microdomain heterogeneity in 3D affects the mechanics of neonatal cardiac myocyte contraction." Biomech Model Mechanobiol **12**(1): 95-109.
- Curtis, M. W., S. Sharma, T. A. Desai and B. Russell (2010). "Hypertrophy, gene expression, and beating of neonatal cardiac myocytes are affected by microdomain heterogeneity in 3D." Biomed Microdevices **12**(6): 1073-1085.
- Czyz, J., C. Wiese, A. Rolletschek, P. Blyszczuk, M. Cross and A. M. Wobus (2003). "Potential of embryonic and adult stem cells in vitro." Biol Chem **384**(10-11): 1391-1409.
- Dadsetan, M., T. E. Hefferan, J. P. Szatkowski, P. K. Mishra, S. I. Macura, L. Lu and M. J. Yaszemski (2008). "Effect of hydrogel porosity on marrow stromal cell phenotypic expression." Biomaterials **29**(14): 2193-2202.
- Dai, W., G. L. Kay and R. A. Kloner (2014). "The Therapeutic Effect of Cell Transplantation Versus Noncellular Biomaterial Implantation on Cardiac Structure and Function Following Myocardial Infarction." J Cardiovasc Pharmacol Ther.
- Dai, Z., F. Wu, E. W. Yeung and Y. Li (2010). "IGF-IEc expression, regulation and biological function in different tissues." Growth Horm IGF Res **20**(4): 275-281.
- Dalby, M. J., S. J. Yarwood, H. J. Johnstone, S. Affrossman and M. O. Riehle (2002). "Fibroblast signaling events in response to nanotopography: a gene array study." IEEE Trans Nanobioscience **1**(1): 12-17.
- Davis, M. E., P. C. Hsieh, T. Takahashi, Q. Song, S. Zhang, R. D. Kamm, A. J. Grodzinsky, P. Anversa and R. T. Lee (2006). "Local myocardial insulin-like growth factor 1 (IGF-1) delivery with biotinylated peptide nanofibers improves cell therapy for myocardial infarction." Proc Natl Acad Sci U S A **103**(21): 8155-8160.
- Deutsch, J., D. Motlagh, B. Russell and T. A. Desai (2000). "Fabrication of microtextured membranes for cardiac myocyte attachment and orientation." J Biomed Mater Res **53**(3): 267-275.

- Dimmeler, S., A. M. Zeiher and M. D. Schneider (2005). "Unchain my heart: the scientific foundations of cardiac repair." J Clin Invest **115**(3): 572-583.
- Diramio, J. A., W. S. Kisaalita, G. F. Majetich and J. M. Shimkus (2005). "Poly(ethylene glycol) methacrylate/dimethacrylate hydrogels for controlled release of hydrophobic drugs." Biotechnol Prog **21**(4): 1281-1288.
- Discher, D. E., D. J. Mooney and P. W. Zandstra (2009). "Growth factors, matrices, and forces combine and control stem cells." Science **324**(5935): 1673-1677.
- Dluzniewska, J., A. Sarnowska, M. Beresewicz, I. Johnson, S. K. Srai, B. Ramesh, G. Goldspink, D. C. Gorecki and B. Zablocka (2005). "A strong neuroprotective effect of the autonomous C-terminal peptide of IGF-1 Ec (MGF) in brain ischemia." FASEB J **19**(13): 1896-1898.
- Dobrowolny, G., C. Giacinti, L. Pelosi, C. Nicoletti, N. Winn, L. Barberi, M. Molinaro, N. Rosenthal and A. Musaro (2005). "Muscle expression of a local Igf-1 isoform protects motor neurons in an ALS mouse model." J Cell Biol **168**(2): 193-199.
- Donath, M. Y., W. Zierhut, M. A. Gosteli-Peter, C. Hauri, E. R. Froesch and J. Zapf (1998). "Effects of IGF-I on cardiac growth and expression of mRNAs coding for cardiac proteins after induction of heart hypertrophy in the rat." Eur J Endocrinol **139**(1): 109-117.
- Doroudian, G., M. W. Curtis, A. Gang and B. Russell (2013). "Cyclic strain dominates over microtopography in regulating cytoskeletal and focal adhesion remodeling of human mesenchymal stem cells." Biochem Biophys Res Commun **430**(3): 1040-1046.
- Drury, J. L. and D. J. Mooney (2003). "Hydrogels for tissue engineering: scaffold design variables and applications." Biomaterials **24**(24): 4337-4351.
- Dunwoodie, S. L. (2009). "The role of hypoxia in development of the Mammalian embryo." Dev Cell **17**(6): 755-773.
- E, L. L., Y. S. Zhao, X. M. Guo, C. Y. Wang, H. Jiang, J. Li, C. M. Duan and Y. Song (2006). "Enrichment of cardiomyocytes derived from mouse embryonic stem cells." J Heart Lung Transplant **25**(6): 664-674.
- Engler, A. J., S. Sen, H. L. Sweeney and D. E. Discher (2006). "Matrix elasticity directs stem cell lineage specification." Cell **126**(4): 677-689.
- Eschenhagen, T., A. Eder, I. Vollert and A. Hansen (2012). "Physiological aspects of cardiac tissue engineering." Am J Physiol Heart Circ Physiol **303**(2): H133-143.
- Evans, H. J., J. K. Sweet, R. L. Price, M. Yost and R. L. Goodwin (2003). "Novel 3D culture system for study of cardiac myocyte development." Am J Physiol Heart Circ Physiol **285**(2): H570-578.

- Ezashi, T., P. Das and R. M. Roberts (2005). "Low O<sub>2</sub> tensions and the prevention of differentiation of hES cells." Proc Natl Acad Sci U S A **102**(13): 4783-4788.
- Fazel, S., M. Cimini, L. Chen, S. Li, D. Angoulvant, P. Fedak, S. Verma, R. D. Weisel, A. Keating and R. K. Li (2006). "Cardioprotective c-kit<sup>+</sup> cells are from the bone marrow and regulate the myocardial balance of angiogenic cytokines." J Clin Invest **116**(7): 1865-1877.
- Feinberg, A. W., A. Feigel, S. S. Shevkoplyas, S. Sheehy, G. M. Whitesides and K. K. Parker (2007). "Muscular thin films for building actuators and powering devices." Science **317**(5843): 1366-1370.
- Fernandes, T. G., M. M. Diogo, A. Fernandes-Platzgummer, C. L. da Silva and J. M. Cabral (2010). "Different stages of pluripotency determine distinct patterns of proliferation, metabolism, and lineage commitment of embryonic stem cells under hypoxia." Stem Cell Res **5**(1): 76-89.
- Fink, C., S. Ergun, D. Kralisch, U. Remmers, J. Weil and T. Eschenhagen (2000). "Chronic stretch of engineered heart tissue induces hypertrophy and functional improvement." FASEB J **14**(5): 669-679.
- Fischer, B. and B. D. Bavister (1993). "Oxygen tension in the oviduct and uterus of rhesus monkeys, hamsters and rabbits." J Reprod Fertil **99**(2): 673-679.
- Fisher, S. A. and W. W. Burggren (2007). "Role of hypoxia in the evolution and development of the cardiovascular system." Antioxid Redox Signal **9**(9): 1339-1352.
- Frey, M. T., I. Y. Tsai, T. P. Russell, S. K. Hanks and Y. L. Wang (2006). "Cellular responses to substrate topography: role of myosin II and focal adhesion kinase." Biophys J **90**(10): 3774-3782.
- Freyman, T., G. Polin, H. Osman, J. Crary, M. Lu, L. Cheng, M. Palasis and R. L. Wilensky (2006). "A quantitative, randomized study evaluating three methods of mesenchymal stem cell delivery following myocardial infarction." Eur Heart J **27**(9): 1114-1122.
- Galbraith, C. G., K. M. Yamada and M. P. Sheetz (2002). "The relationship between force and focal complex development." J Cell Biol **159**(4): 695-705.
- Ge, D., X. Liu, L. Li, J. Wu, Q. Tu, Y. Shi and H. Chen (2009). "Chemical and physical stimuli induce cardiomyocyte differentiation from stem cells." Biochem Biophys Res Commun **381**(3): 317-321.
- Ghazanfari, S., M. Tafazzoli-Shadpour and M. A. Shokrgozar (2009). "Effects of cyclic stretch on proliferation of mesenchymal stem cells and their differentiation to smooth muscle cells." Biochem Biophys Res Commun **388**(3): 601-605.

- Ghibaudo, M., J. M. Di Meglio, P. Hersen and B. Ladoux (2011). "Mechanics of cell spreading within 3D-micropatterned environments." Lab Chip **11**(5): 805-812.
- Glimm, H., I. H. Oh and C. J. Eaves (2000). "Human hematopoietic stem cells stimulated to proliferate in vitro lose engraftment potential during their S/G(2)/M transit and do not reenter G(0)." Blood **96**(13): 4185-4193.
- Gnecchi, M., Z. Zhang, A. Ni and V. J. Dzau (2008). "Paracrine mechanisms in adult stem cell signaling and therapy." Circ Res **103**(11): 1204-1219.
- Goldspink, G. and S. Y. Yang (2001). "Effects of activity on growth factor expression." Int J Sport Nutr Exerc Metab **11 Suppl**: S21-27.
- Gould, R. A., K. Chin, T. P. Santisakultarm, A. Dropkin, J. M. Richards, C. B. Schaffer and J. T. Butcher (2012). "Cyclic strain anisotropy regulates valvular interstitial cell phenotype and tissue remodeling in three-dimensional culture." Acta Biomater **8**(5): 1710-1719.
- Goyal, P., N. Weissmann, F. Grimminger, C. Hegel, L. Bader, F. Rose, L. Fink, H. A. Ghofrani, R. T. Schermuly, H. H. Schmidt, W. Seeger and J. Hanze (2004). "Upregulation of NAD(P)H oxidase 1 in hypoxia activates hypoxia-inducible factor 1 via increase in reactive oxygen species." Free Radic Biol Med **36**(10): 1279-1288.
- Gronthos, S., A. C. Zannettino, S. J. Hay, S. Shi, S. E. Graves, A. Kortessidis and P. J. Simmons (2003). "Molecular and cellular characterisation of highly purified stromal stem cells derived from human bone marrow." J Cell Sci **116**(Pt 9): 1827-1835.
- Grunenfelder, J., D. N. Miniati, S. Murata, V. Falk, E. G. Hoyt, M. Kown, M. L. Koransky and R. C. Robbins (2001). "Upregulation of Bcl-2 through caspase-3 inhibition ameliorates ischemia/reperfusion injury in rat cardiac allografts." Circulation **104**(12 Suppl 1): I202-206.
- Guan, J., F. Wang, Z. Li, J. Chen, X. Guo, J. Liao and N. I. Moldovan (2011). "The stimulation of the cardiac differentiation of mesenchymal stem cells in tissue constructs that mimic myocardium structure and biomechanics." Biomaterials **32**(24): 5568-5580.
- Guo, X. M., Y. S. Zhao, H. X. Chang, C. Y. Wang, L. L. E, X. A. Zhang, C. M. Duan, L. Z. Dong, H. Jiang, J. Li, Y. Song and X. J. Yang (2006). "Creation of engineered cardiac tissue in vitro from mouse embryonic stem cells." Circulation **113**(18): 2229-2237.
- Guzy, R. D. and P. T. Schumacker (2006). "Oxygen sensing by mitochondria at complex III: the paradox of increased reactive oxygen species during hypoxia." Exp Physiol **91**(5): 807-819.

- Gwak, S. J., S. H. Bhang, I. K. Kim, S. S. Kim, S. W. Cho, O. Jeon, K. J. Yoo, A. J. Putnam and B. S. Kim (2008). "The effect of cyclic strain on embryonic stem cell-derived cardiomyocytes." Biomaterials **29**(7): 844-856.
- Harun, R., L. Ruban, M. Matin, J. Draper, N. M. Jenkins, G. C. Liew, P. W. Andrews, T. C. Li, S. M. Laird and H. D. Moore (2006). "Cytotrophoblast stem cell lines derived from human embryonic stem cells and their capacity to mimic invasive implantation events." Hum Reprod **21**(6): 1349-1358.
- Harvey, A. J., K. L. Kind, M. Pantaleon, D. T. Armstrong and J. G. Thompson (2004). "Oxygen-regulated gene expression in bovine blastocysts." Biol Reprod **71**(4): 1108-1119.
- Hattori, F. and K. Fukuda (2010). "Strategies for ensuring that regenerative cardiomyocytes function properly and in cooperation with the host myocardium." Exp Mol Med **42**(3): 155-165.
- Hattori, K., B. Heissig, K. Tashiro, T. Honjo, M. Tateno, J. H. Shieh, N. R. Hackett, M. S. Quitarano, R. G. Crystal, S. Rafii and M. A. Moore (2001). "Plasma elevation of stromal cell-derived factor-1 induces mobilization of mature and immature hematopoietic progenitor and stem cells." Blood **97**(11): 3354-3360.
- Hausenloy, D. J. and D. M. Yellon (2009). "Cardioprotective growth factors." Cardiovasc Res **83**(2): 179-194.
- Heidkamp, M. C. and B. Russell (2001). "Calcium not strain regulates localization of alpha-myosin heavy chain mRNA in oriented cardiac myocytes." Cell Tissue Res **305**(1): 121-127.
- Heinzel, F. R., Y. Luo, G. Dodoni, K. Boengler, F. Petrat, F. Di Lisa, H. de Groot, R. Schulz and G. Heusch (2006). "Formation of reactive oxygen species at increased contraction frequency in rat cardiomyocytes." Cardiovasc Res **71**(2): 374-382.
- Heo, J. S. and J. C. Lee (2011). "beta-Catenin mediates cyclic strain-stimulated cardiomyogenesis in mouse embryonic stem cells through ROS-dependent and integrin-mediated PI3K/Akt pathways." J Cell Biochem **112**(7): 1880-1889.
- Hermes-Lima, M. and T. Zenteno-Savin (2002). "Animal response to drastic changes in oxygen availability and physiological oxidative stress." Comp Biochem Physiol C Toxicol Pharmacol **133**(4): 537-556.
- Herrmann, J. L., Y. Wang, A. M. Abarbanell, B. R. Weil, J. Tan and D. R. Meldrum (2010). "Preconditioning mesenchymal stem cells with transforming growth factor-alpha improves mesenchymal stem cell-mediated cardioprotection." Shock **33**(1): 24-30.

- Heydarkhan-Hagvall, S., J. M. Gluck, C. Delman, M. Jung, N. Ehsani, S. Full and R. J. Shemin (2012). "The effect of vitronectin on the differentiation of embryonic stem cells in a 3D culture system." Biomaterials **33**(7): 2032-2040.
- Hill, M. and G. Goldspink (2003). "Expression and splicing of the insulin-like growth factor gene in rodent muscle is associated with muscle satellite (stem) cell activation following local tissue damage." J Physiol **549**(Pt 2): 409-418.
- Hockenbery, D., G. Nunez, C. Milliman, R. D. Schreiber and S. J. Korsmeyer (1990). "Bcl-2 is an inner mitochondrial membrane protein that blocks programmed cell death." Nature **348**(6299): 334-336.
- Hoffman, A. S. (2002). "Hydrogels for biomedical applications." Adv Drug Deliv Rev **54**(1): 3-12.
- Hofmann, M., K. C. Wollert, G. P. Meyer, A. Menke, L. Arseniev, B. Hertenstein, A. Ganser, W. H. Knapp and H. Drexler (2005). "Monitoring of bone marrow cell homing into the infarcted human myocardium." Circulation **111**(17): 2198-2202.
- Holle, A. W. and A. J. Engler (2011). "More than a feeling: discovering, understanding, and influencing mechanosensing pathways." Curr Opin Biotechnol **22**(5): 648-654.
- Hosseinkhani, M., K. Hasegawa, K. Ono, T. Kawamura, T. Takaya, T. Morimoto, H. Wada, A. Shimatsu, S. G. Prat, H. Suemori, N. Nakatsuji and T. Kita (2007). "Trichostatin A induces myocardial differentiation of monkey ES cells." Biochem Biophys Res Commun **356**(2): 386-391.
- Hosseinkhani, M., H. Hosseinkhani, A. Khademhosseini, F. Bolland, H. Kobayashi and S. P. Gonzalez (2007). "Bone morphogenetic protein-4 enhances cardiomyocyte differentiation of cynomolgus monkey ESCs in knockout serum replacement medium." Stem Cells **25**(3): 571-580.
- Hsieh, P. C., C. MacGillivray, J. Gannon, F. U. Cruz and R. T. Lee (2006). "Local controlled intramyocardial delivery of platelet-derived growth factor improves postinfarction ventricular function without pulmonary toxicity." Circulation **114**(7): 637-644.
- Huang, L., H. Li and Z. Xie (1997). "Ouabain-induced hypertrophy in cultured cardiac myocytes is accompanied by changes in expression of several late response genes." J Mol Cell Cardiol **29**(2): 429-437.
- Ingber, D. E. (1997). "Tensegrity: the architectural basis of cellular mechanotransduction." Annu Rev Physiol **59**: 575-599.
- Ingber, D. E. (2003). "Tensegrity I. Cell structure and hierarchical systems biology." J Cell Sci **116**(Pt 7): 1157-1173.

- Iwakura, A., M. Fujita, K. Kataoka, K. Tambara, Y. Sakakibara, M. Komeda and Y. Tabata (2003). "Intramyocardial sustained delivery of basic fibroblast growth factor improves angiogenesis and ventricular function in a rat infarct model." Heart Vessels **18**(2): 93-99.
- Jacot, J. G., J. C. Martin and D. L. Hunt (2010). "Mechanobiology of cardiomyocyte development." J Biomech **43**(1): 93-98.
- Jang, J. Y., S. W. Lee, S. H. Park, J. W. Shin, C. Mun, S. H. Kim, D. H. Kim and J. W. Shin (2011). "Combined effects of surface morphology and mechanical straining magnitudes on the differentiation of mesenchymal stem cells without using biochemical reagents." J Biomed Biotechnol **2011**: 860652.
- Jauniaux, E., B. Gulbis and G. J. Burton (2003). "Physiological implications of the materno-fetal oxygen gradient in human early pregnancy." Reprod Biomed Online **7**(2): 250-253.
- Jiang, B. H., G. L. Semenza, C. Bauer and H. H. Marti (1996). "Hypoxia-inducible factor 1 levels vary exponentially over a physiologically relevant range of O<sub>2</sub> tension." Am J Physiol **271**(4 Pt 1): C1172-1180.
- Kandalla, P. K., G. Goldspink, G. Butler-Browne and V. Mouly (2011). "Mechano Growth Factor E peptide (MGF-E), derived from an isoform of IGF-1, activates human muscle progenitor cells and induces an increase in their fusion potential at different ages." Mech Ageing Dev **132**(4): 154-162.
- Kanno, S., P. K. Kim, K. Sallam, J. Lei, T. R. Billiar and L. L. Shears, 2nd (2004). "Nitric oxide facilitates cardiomyogenesis in mouse embryonic stem cells." Proc Natl Acad Sci U S A **101**(33): 12277-12281.
- Kawamoto, A., H. Iwasaki, K. Kusano, T. Murayama, A. Oyamada, M. Silver, C. Hulbert, M. Gavin, A. Hanley, H. Ma, M. Kearney, V. Zak, T. Asahara and D. W. Losordo (2006). "CD34-positive cells exhibit increased potency and safety for therapeutic neovascularization after myocardial infarction compared with total mononuclear cells." Circulation **114**(20): 2163-2169.
- Kearney, E. M., P. J. Prendergast and V. A. Campbell (2008). "Mechanisms of strain-mediated mesenchymal stem cell apoptosis." J Biomech Eng **130**(6): 061004.
- Kehat, I. and L. Gepstein (2003). "Human embryonic stem cells for myocardial regeneration." Heart Fail Rev **8**(3): 229-236.
- Keskar, V., N. W. Marion, J. J. Mao and R. A. Gemeinhart (2009). "In vitro evaluation of macroporous hydrogels to facilitate stem cell infiltration, growth, and mineralization." Tissue Eng Part A **15**(7): 1695-1707.
- Kofidis, T., K. Muller-Stahl and A. Haverich (2007). "Myocardial restoration and tissue engineering of heart structures." Methods Mol Med **140**: 273-290.



- Koike, M., H. Shimokawa, Z. Kanno, K. Ohya and K. Soma (2005). "Effects of mechanical strain on proliferation and differentiation of bone marrow stromal cell line ST2." J Bone Miner Metab **23**(3): 219-225.
- Korsmeyer, S. J. (1992). "Bcl-2: a repressor of lymphocyte death." Immunol Today **13**(8): 285-288.
- Kucia, M., B. Dawn, G. Hunt, Y. Guo, M. Wysoczynski, M. Majka, J. Ratajczak, F. Rezzoug, S. T. Ildstad, R. Bolli and M. Z. Ratajczak (2004). "Cells expressing early cardiac markers reside in the bone marrow and are mobilized into the peripheral blood after myocardial infarction." Circ Res **95**(12): 1191-1199.
- Kurosawa, H., M. Kimura, T. Noda and Y. Amano (2006). "Effect of oxygen on in vitro differentiation of mouse embryonic stem cells." J Biosci Bioeng **101**(1): 26-30.
- Kurpinski, K., J. Chu, C. Hashi and S. Li (2006). "Anisotropic mechanosensing by mesenchymal stem cells." Proc Natl Acad Sci U S A **103**(44): 16095-16100.
- Kurpinski, K., J. Chu, D. Wang and S. Li (2009). "Proteomic Profiling of Mesenchymal Stem Cell Responses to Mechanical Strain and TGF-beta1." Cell Mol Bioeng **2**(4): 606-614.
- Laflamme, M. A., K. Y. Chen, A. V. Naumova, V. Muskheli, J. A. Fugate, S. K. Dupras, H. Reinecke, C. Xu, M. Hassanipour, S. Police, C. O'Sullivan, L. Collins, Y. Chen, E. Minami, E. A. Gill, S. Ueno, C. Yuan, J. Gold and C. E. Murry (2007). "Cardiomyocytes derived from human embryonic stem cells in pro-survival factors enhance function of infarcted rat hearts." Nat Biotechnol **25**(9): 1015-1024.
- Langer, R. and J. P. Vacanti (1993). "Tissue engineering." Science **260**(5110): 920-926.
- Lee, W. C., T. M. Maul, D. A. Vorp, J. P. Rubin and K. G. Marra (2007). "Effects of uniaxial cyclic strain on adipose-derived stem cell morphology, proliferation, and differentiation." Biomech Model Mechanobiol **6**(4): 265-273.
- Lee, Y. M., C. H. Jeong, S. Y. Koo, M. J. Son, H. S. Song, S. K. Bae, J. A. Raleigh, H. Y. Chung, M. A. Yoo and K. W. Kim (2001). "Determination of hypoxic region by hypoxia marker in developing mouse embryos in vivo: a possible signal for vessel development." Dev Dyn **220**(2): 175-186.
- Lehoux, S. (2006). "Redox signalling in vascular responses to shear and stretch." Cardiovasc Res **71**(2): 269-279.
- Lele, T. P., C. K. Thodeti and D. E. Ingber (2006). "Force meets chemistry: analysis of mechanochemical conversion in focal adhesions using fluorescence recovery after photobleaching." J Cell Biochem **97**(6): 1175-1183.

- Leor, J., S. Gerecht, S. Cohen, L. Miller, R. Holbova, A. Ziskind, M. Shachar, M. S. Feinberg, E. Guetta and J. Itskovitz-Eldor (2007). "Human embryonic stem cell transplantation to repair the infarcted myocardium." Heart **93**(10): 1278-1284.
- Leri, A., T. Hosoda, J. Kajstura and P. Anversa (2006). "Heart failure and regenerative cardiology." Regen Med **1**(2): 153-159.
- Li, C. and W. H. Wong (2001). "Model-based analysis of oligonucleotide arrays: expression index computation and outlier detection." Proc Natl Acad Sci U S A **98**(1): 31-36.
- Li, J., M. Stouffs, L. Serrander, B. Banfi, E. Bettiol, Y. Charnay, K. Steger, K. H. Krause and M. E. Jaconí (2006). "The NADPH oxidase NOX4 drives cardiac differentiation: Role in regulating cardiac transcription factors and MAP kinase activation." Mol Biol Cell **17**(9): 3978-3988.
- Li, Q., B. Li, X. Wang, A. Leri, K. P. Jana, Y. Liu, J. Kajstura, R. Baserga and P. Anversa (1997). "Overexpression of insulin-like growth factor-1 in mice protects from myocyte death after infarction, attenuating ventricular dilation, wall stress, and cardiac hypertrophy." J Clin Invest **100**(8): 1991-1999.
- Li, Y., Y. Wang, P. Wang, B. Zhang, W. Yan, J. Sun and J. Pan (2013). "In vitro cytocompatibility evaluation of MGF-Ct24E chemically grafted and physically blended with maleic anhydride modified poly(D, L-lactic acid)." J Biomater Sci Polym Ed **24**(7): 849-864.
- Loesberg, W. A., X. F. Walboomers, J. J. van Loon and J. A. Jansen (2005). "The effect of combined cyclic mechanical stretching and microgrooved surface topography on the behavior of fibroblasts." J Biomed Mater Res A **75**(3): 723-732.
- Lowe, W. L., Jr., S. R. Lasky, D. LeRoith and C. T. Roberts, Jr. (1988). "Distribution and regulation of rat insulin-like growth factor I messenger ribonucleic acids encoding alternative carboxyterminal E-peptides: evidence for differential processing and regulation in liver." Mol Endocrinol **2**(6): 528-535.
- Martin, C. M., A. P. Meeson, S. M. Robertson, T. J. Hawke, J. A. Richardson, S. Bates, S. C. Goetsch, T. D. Gallardo and D. J. Garry (2004). "Persistent expression of the ATP-binding cassette transporter, Abcg2, identifies cardiac SP cells in the developing and adult heart." Dev Biol **265**(1): 262-275.
- Martinez-Sanchez, G. and A. Giuliani (2007). "Cellular redox status regulates hypoxia inducible factor-1 activity. Role in tumour development." J Exp Clin Cancer Res **26**(1): 39-50.
- Mavrommatis, E., K. M. Shioura, T. Los and P. H. Goldspink (2013). "The E-domain region of mechano-growth factor inhibits cellular apoptosis and preserves cardiac function during myocardial infarction." Mol Cell Biochem **381**(1-2): 69-83.

- McKoy, G., W. Ashley, J. Mander, S. Y. Yang, N. Williams, B. Russell and G. Goldspink (1999). "Expression of insulin growth factor-1 splice variants and structural genes in rabbit skeletal muscle induced by stretch and stimulation." J Physiol **516** ( Pt 2): 583-592.
- Mills, P., J. F. Lafreniere, B. F. Benabdallah, M. El Fahime el and J. P. Tremblay (2007). "A new pro-migratory activity on human myogenic precursor cells for a synthetic peptide within the E domain of the mechano growth factor." Exp Cell Res **313**(3): 527-537.
- Motlagh, D., T. J. Hartman, T. A. Desai and B. Russell (2003). "Microfabricated grooves recapitulate neonatal myocyte connexin43 and N-cadherin expression and localization." J Biomed Mater Res A **67**(1): 148-157.
- Motlagh, D., S. E. Senyo, T. A. Desai and B. Russell (2003). "Microtextured substrata alter gene expression, protein localization and the shape of cardiac myocytes." Biomaterials **24**(14): 2463-2476.
- Musaro, A., C. Giacinti, G. Borsellino, G. Dobrowolny, L. Pelosi, L. Cairns, S. Ottolenghi, G. Cossu, G. Bernardi, L. Battistini, M. Molinaro and N. Rosenthal (2004). "Stem cell-mediated muscle regeneration is enhanced by local isoform of insulin-like growth factor 1." Proc Natl Acad Sci U S A **101**(5): 1206-1210.
- Muta, K. and S. B. Krantz (1993). "Apoptosis of human erythroid colony-forming cells is decreased by stem cell factor and insulin-like growth factor I as well as erythropoietin." J Cell Physiol **156**(2): 264-271.
- Naderi, H., M. M. Matin and A. R. Bahrami (2011). "Review paper: critical issues in tissue engineering: biomaterials, cell sources, angiogenesis, and drug delivery systems." J Biomater Appl **26**(4): 383-417.
- Nahta, R., L. X. Yuan, B. Zhang, R. Kobayashi and F. J. Esteva (2005). "Insulin-like growth factor-I receptor/human epidermal growth factor receptor 2 heterodimerization contributes to trastuzumab resistance of breast cancer cells." Cancer Res **65**(23): 11118-11128.
- Nanduri, J. and R. P. Nanduri (2007). "Cellular mechanisms associated with intermittent hypoxia." Essays Biochem **43**: 91-104.
- Ng, K. M., Y. K. Lee, Y. C. Chan, W. H. Lai, M. L. Fung, R. A. Li, C. W. Siu and H. F. Tse (2010). "Exogenous expression of HIF-1 alpha promotes cardiac differentiation of embryonic stem cells." J Mol Cell Cardiol **48**(6): 1129-1137.
- Niebruegge, S., C. L. Bauwens, R. Peerani, N. Thavandiran, S. Masse, E. Sevaptisidis, K. Nanthakumar, K. Woodhouse, M. Husain, E. Kumacheva and P. W. Zandstra (2009). "Generation of human embryonic stem cell-derived mesoderm and cardiac cells using size-specified aggregates in an oxygen-controlled bioreactor." Biotechnol Bioeng **102**(2): 493-507.

- Nieponice, A., T. M. Maul, J. M. Cumer, L. Soletti and D. A. Vorp (2007). "Mechanical stimulation induces morphological and phenotypic changes in bone marrow-derived progenitor cells within a three-dimensional fibrin matrix." J Biomed Mater Res A **81**(3): 523-530.
- Nombela-Arrieta, C., J. Ritz and L. E. Silberstein (2011). "The elusive nature and function of mesenchymal stem cells." Nat Rev Mol Cell Biol **12**(2): 126-131.
- Norman, J. J., J. M. Collins, S. Sharma, B. Russell and T. A. Desai (2008). "Microstructures in 3D biological gels affect cell proliferation." Tissue Eng Part A **14**(3): 379-390.
- Norman, J. J. and T. A. Desai (2005). "Control of cellular organization in three dimensions using a microfabricated polydimethylsiloxane-collagen composite tissue scaffold." Tissue Eng **11**(3-4): 378-386.
- Oh, H., S. B. Bradfute, T. D. Gallardo, T. Nakamura, V. Gaussin, Y. Mishina, J. Pocius, L. H. Michael, R. R. Behringer, D. J. Garry, M. L. Entman and M. D. Schneider (2003). "Cardiac progenitor cells from adult myocardium: homing, differentiation, and fusion after infarction." Proc Natl Acad Sci U S A **100**(21): 12313-12318.
- Orlic, D., J. Kajstura, S. Chimenti, F. Limana, I. Jakoniuk, F. Quaini, B. Nadal-Ginard, D. M. Bodine, A. Leri and P. Anversa (2001). "Mobilized bone marrow cells repair the infarcted heart, improving function and survival." Proc Natl Acad Sci U S A **98**(18): 10344-10349.
- Pandur, P., M. Lasche, L. M. Eisenberg and M. Kuhl (2002). "Wnt-11 activation of a non-canonical Wnt signalling pathway is required for cardiogenesis." Nature **418**(6898): 636-641.
- Paquin, J., B. A. Danalache, M. Jankowski, S. M. McCann and J. Gutkowska (2002). "Oxytocin induces differentiation of P19 embryonic stem cells to cardiomyocytes." Proc Natl Acad Sci U S A **99**(14): 9550-9555.
- Park, J. S., J. S. Chu, C. Cheng, F. Chen, D. Chen and S. Li (2004). "Differential effects of equiaxial and uniaxial strain on mesenchymal stem cells." Biotechnol Bioeng **88**(3): 359-368.
- Parker, K. K., J. Tan, C. S. Chen and L. Tung (2008). "Myofibrillar architecture in engineered cardiac myocytes." Circ Res **103**(4): 340-342.
- Passier, R., D. W. Oostwaard, J. Snapper, J. Kloots, R. J. Hassink, E. Kuijk, B. Roelen, A. B. de la Riviere and C. Mummery (2005). "Increased cardiomyocyte differentiation from human embryonic stem cells in serum-free cultures." Stem Cells **23**(6): 772-780.
- Patel, A. A., T. A. Desai and S. Kumar (2011). "Microtopographical assembly of cardiomyocytes." Integr Biol (Camb) **3**(10): 1011-1019.

- Paul, D., S. M. Samuel and N. Maulik (2009). "Mesenchymal stem cell: present challenges and prospective cellular cardiomyoplasty approaches for myocardial regeneration." Antioxid Redox Signal **11**(8): 1841-1855.
- Pedersen, J. A. and M. A. Swartz (2005). "Mechanobiology in the third dimension." Ann Biomed Eng **33**(11): 1469-1490.
- Pelham, R. J., Jr. and Y. Wang (1997). "Cell locomotion and focal adhesions are regulated by substrate flexibility." Proc Natl Acad Sci U S A **94**(25): 13661-13665.
- Pelham, R. J., Jr. and Y. L. Wang (1998). "Cell locomotion and focal adhesions are regulated by the mechanical properties of the substrate." Biol Bull **194**(3): 348-349; discussion 349-350.
- Polak, J. M. and A. E. Bishop (2006). "Stem cells and tissue engineering: past, present, and future." Ann N Y Acad Sci **1068**: 352-366.
- Poobalarahi, F., C. F. Baicu and A. D. Bradshaw (2006). "Cardiac myofibroblasts differentiated in 3D culture exhibit distinct changes in collagen I production, processing, and matrix deposition." Am J Physiol Heart Circ Physiol **291**(6): H2924-2932.
- Quesada, A., P. Micevych and A. Handforth (2009). "C-terminal mechano growth factor protects dopamine neurons: a novel peptide that induces heme oxygenase-1." Exp Neurol **220**(2): 255-266.
- Ramirez-Bergeron, D. L., A. Runge, K. D. Dahl, H. J. Fehling, G. Keller and M. C. Simon (2004). "Hypoxia affects mesoderm and enhances hemangioblast specification during early development." Development **131**(18): 4623-4634.
- Ramirez-Bergeron, D. L. and M. C. Simon (2001). "Hypoxia-inducible factor and the development of stem cells of the cardiovascular system." Stem Cells **19**(4): 279-286.
- Reddi, A. H. (2000). "Morphogenesis and tissue engineering of bone and cartilage: inductive signals, stem cells, and biomimetic biomaterials." Tissue Eng **6**(4): 351-359.
- Reinecke, H., M. Zhang, T. Bartosek and C. E. Murry (1999). "Survival, integration, and differentiation of cardiomyocyte grafts: a study in normal and injured rat hearts." Circulation **100**(2): 193-202.
- Reiss, K., W. Cheng, A. Ferber, J. Kajstura, P. Li, B. Li, G. Olivetti, C. J. Homcy, R. Baserga and P. Anversa (1996). "Overexpression of insulin-like growth factor-1 in the heart is coupled with myocyte proliferation in transgenic mice." Proc Natl Acad Sci U S A **93**(16): 8630-8635.

- Rezai, N., T. J. Podor and B. M. McManus (2004). "Bone marrow cells in the repair and modulation of heart and blood vessels: emerging opportunities in native and engineered tissue and biomechanical materials." Artif Organs **28**(2): 142-151.
- Riveline, D., E. Zamir, N. Q. Balaban, U. S. Schwarz, T. Ishizaki, S. Narumiya, Z. Kam, B. Geiger and A. D. Bershadsky (2001). "Focal contacts as mechanosensors: externally applied local mechanical force induces growth of focal contacts by an mDia1-dependent and ROCK-independent mechanism." J Cell Biol **153**(6): 1175-1186.
- Rodriguez-Tarduchy, G., M. K. Collins, I. Garcia and A. Lopez-Rivas (1992). "Insulin-like growth factor-I inhibits apoptosis in IL-3-dependent hemopoietic cells." J Immunol **149**(2): 535-540.
- Roger, V. L., A. S. Go, D. M. Lloyd-Jones, E. J. Benjamin, J. D. Berry, W. B. Borden, D. M. Bravata, S. Dai, E. S. Ford, C. S. Fox, H. J. Fullerton, C. Gillespie, S. M. Hailpern, J. A. Heit, V. J. Howard, B. M. Kissela, S. J. Kittner, D. T. Lackland, J. H. Lichtman, L. D. Lisabeth, D. M. Makuc, G. M. Marcus, A. Marelli, D. B. Matchar, C. S. Moy, D. Mozaffarian, M. E. Mussolino, G. Nichol, N. P. Paynter, E. Z. Soliman, P. D. Sorlie, N. Sotoodehnia, T. N. Turan, S. S. Virani, N. D. Wong, D. Woo, M. B. Turner, C. American Heart Association Statistics and S. Stroke Statistics (2012). "Executive summary: heart disease and stroke statistics--2012 update: a report from the American Heart Association." Circulation **125**(1): 188-197.
- Roger, V. L., A. S. Go, D. M. Lloyd-Jones, E. J. Benjamin, J. D. Berry, W. B. Borden, D. M. Bravata, S. Dai, E. S. Ford, C. S. Fox, H. J. Fullerton, C. Gillespie, S. M. Hailpern, J. A. Heit, V. J. Howard, B. M. Kissela, S. J. Kittner, D. T. Lackland, J. H. Lichtman, L. D. Lisabeth, D. M. Makuc, G. M. Marcus, A. Marelli, D. B. Matchar, C. S. Moy, D. Mozaffarian, M. E. Mussolino, G. Nichol, N. P. Paynter, E. Z. Soliman, P. D. Sorlie, N. Sotoodehnia, T. N. Turan, S. S. Virani, N. D. Wong, D. Woo, M. B. Turner, C. American Heart Association Statistics and S. Stroke Statistics (2012). "Heart disease and stroke statistics--2012 update: a report from the American Heart Association." Circulation **125**(1): e2-e220.
- Rorth, P. (2011). "Whence directionality: guidance mechanisms in solitary and collective cell migration." Dev Cell **20**(1): 9-18.
- Russell, S. M. and E. M. Spencer (1985). "Local injections of human or rat growth hormone or of purified human somatomedin-C stimulate unilateral tibial epiphyseal growth in hypophysectomized rats." Endocrinology **116**(6): 2563-2567.
- Ryu, J. H., I. K. Kim, S. W. Cho, M. C. Cho, K. K. Hwang, H. Piao, S. Piao, S. H. Lim, Y. S. Hong, C. Y. Choi, K. J. Yoo and B. S. Kim (2005). "Implantation of bone marrow mononuclear cells using injectable fibrin matrix enhances neovascularization in infarcted myocardium." Biomaterials **26**(3): 319-326.

- Saha, S., L. Ji, J. J. de Pablo and S. P. Palecek (2006). "Inhibition of human embryonic stem cell differentiation by mechanical strain." J Cell Physiol **206**(1): 126-137.
- Sakai, T., Y. Ling, T. R. Payne and J. Huard (2002). "The use of ex vivo gene transfer based on muscle-derived stem cells for cardiovascular medicine." Trends Cardiovasc Med **12**(3): 115-120.
- Samarel, A. M. (2005). "Costameres, focal adhesions, and cardiomyocyte mechanotransduction." Am J Physiol Heart Circ Physiol **289**(6): H2291-2301.
- Sauer, H., G. Rahimi, J. Hescheler and M. Wartenberg (1999). "Effects of electrical fields on cardiomyocyte differentiation of embryonic stem cells." J Cell Biochem **75**(4): 710-723.
- Sauer, H., G. Rahimi, J. Hescheler and M. Wartenberg (2000). "Role of reactive oxygen species and phosphatidylinositol 3-kinase in cardiomyocyte differentiation of embryonic stem cells." FEBS Lett **476**(3): 218-223.
- Scadden, D. T. (2006). "The stem-cell niche as an entity of action." Nature **441**(7097): 1075-1079.
- Schlegel, W., A. Raimann, D. Halbauer, D. Scharmer, S. Sagmeister, B. Wessner, M. Helmreich, G. Haeusler and M. Egerbacher (2013). "Insulin-like growth factor I (IGF-1) Ec/Mechano Growth factor--a splice variant of IGF-1 within the growth plate." PLoS One **8**(10): e76133.
- Schmelter, M., B. Ateghang, S. Helmig, M. Wartenberg and H. Sauer (2006). "Embryonic stem cells utilize reactive oxygen species as transducers of mechanical strain-induced cardiovascular differentiation." FASEB J **20**(8): 1182-1184.
- Segers, V. F. and R. T. Lee (2008). "Stem-cell therapy for cardiac disease." Nature **451**(7181): 937-942.
- Semenza, G. L. (2001). "HIF-1 and mechanisms of hypoxia sensing." Curr Opin Cell Biol **13**(2): 167-171.
- Semenza, G. L. (2006). "Regulation of physiological responses to continuous and intermittent hypoxia by hypoxia-inducible factor 1." Exp Physiol **91**(5): 803-806.
- Semenza, G. L., F. Agani, D. Feldser, N. Iyer, L. Kotch, E. Laughner and A. Yu (2000). "Hypoxia, HIF-1, and the pathophysiology of common human diseases." Adv Exp Med Biol **475**: 123-130.
- Senyo, S. E., Y. E. Koshman and B. Russell (2007). "Stimulus interval, rate and direction differentially regulate phosphorylation for mechanotransduction in neonatal cardiac myocytes." FEBS Lett **581**(22): 4241-4247.

- Seo, C. H., K. Furukawa, K. Montagne, H. Jeong and T. Ushida (2011). "The effect of substrate microtopography on focal adhesion maturation and actin organization via the RhoA/ROCK pathway." Biomaterials **32**(36): 9568-9575.
- Shimizu, N., K. Yamamoto, S. Obi, S. Kumagaya, T. Masumura, Y. Shimano, K. Naruse, J. K. Yamashita, T. Igarashi and J. Ando (2008). "Cyclic strain induces mouse embryonic stem cell differentiation into vascular smooth muscle cells by activating PDGF receptor beta." J Appl Physiol (1985) **104**(3): 766-772.
- Shimko, V. F. and W. C. Claycomb (2008). "Effect of mechanical loading on three-dimensional cultures of embryonic stem cell-derived cardiomyocytes." Tissue Eng Part A **14**(1): 49-58.
- Simon, M. C. and B. Keith (2008). "The role of oxygen availability in embryonic development and stem cell function." Nat Rev Mol Cell Biol **9**(4): 285-296.
- Simpson, D., H. Liu, T. H. Fan, R. Nerem and S. C. Dudley, Jr. (2007). "A tissue engineering approach to progenitor cell delivery results in significant cell engraftment and improved myocardial remodeling." Stem Cells **25**(9): 2350-2357.
- Sims, J. R., S. Karp and D. E. Ingber (1992). "Altering the cellular mechanical force balance results in integrated changes in cell, cytoskeletal and nuclear shape." J Cell Sci **103** ( Pt 4): 1215-1222.
- Spradling, A., D. Drummond-Barbosa and T. Kai (2001). "Stem cells find their niche." Nature **414**(6859): 98-104.
- Stamm, C., Y. H. Choi, B. Nasser and R. Hetzer (2009). "A heart full of stem cells: the spectrum of myocardial progenitor cells in the postnatal heart." Ther Adv Cardiovasc Dis **3**(3): 215-229.
- Stavropoulou, A., A. Halapas, A. Sourla, A. Philippou, E. Papageorgiou, A. Papalois and M. Koutsilieris (2009). "IGF-1 expression in infarcted myocardium and MGF E peptide actions in rat cardiomyocytes in vitro." Mol Med **15**(5-6): 127-135.
- Steinhauser, M. L. and R. T. Lee (2009). "Cardiovascular regeneration: pushing and pulling on progenitors." Cell Stem Cell **4**(4): 277-278.
- Stephanou, A., B. Brar, R. Heads, R. D. Knight, M. S. Marber, D. Pennica and D. S. Latchman (1998). "Cardiotrophin-1 induces heat shock protein accumulation in cultured cardiac cells and protects them from stressful stimuli." J Mol Cell Cardiol **30**(4): 849-855.
- Szafranski, J. D., A. J. Grodzinsky, E. Burger, V. Gaschen, H. H. Hung and E. B. Hunziker (2004). "Chondrocyte mechanotransduction: effects of compression on deformation of intracellular organelles and relevance to cellular biosynthesis." Osteoarthritis Cartilage **12**(12): 937-946.



- Takahashi, K., K. Tanabe, M. Ohnuki, M. Narita, T. Ichisaka, K. Tomoda and S. Yamanaka (2007). "Induction of pluripotent stem cells from adult human fibroblasts by defined factors." Cell **131**(5): 861-872.
- Takahashi, K. and S. Yamanaka (2006). "Induction of pluripotent stem cells from mouse embryonic and adult fibroblast cultures by defined factors." Cell **126**(4): 663-676.
- Tan, J. L., J. Tien, D. M. Pirone, D. S. Gray, K. Bhadriraju and C. S. Chen (2003). "Cells lying on a bed of microneedles: an approach to isolate mechanical force." Proc Natl Acad Sci U S A **100**(4): 1484-1489.
- Thakar, R. G., M. G. Chown, A. Patel, L. Peng, S. Kumar and T. A. Desai (2008). "Contractility-dependent modulation of cell proliferation and adhesion by microscale topographical cues." Small **4**(9): 1416-1424.
- Tidball, J. G. (2005). "Inflammatory processes in muscle injury and repair." Am J Physiol Regul Integr Comp Physiol **288**(2): R345-353.
- Tsutsumi, S., A. Shimazu, K. Miyazaki, H. Pan, C. Koike, E. Yoshida, K. Takagishi and Y. Kato (2001). "Retention of multilineage differentiation potential of mesenchymal cells during proliferation in response to FGF." Biochem Biophys Res Commun **288**(2): 413-419.
- Tucker, R. M., B. W. Parcher, E. F. Jones and T. A. Desai (2012). "Single-injection HPLC method for rapid analysis of a combination drug delivery system." AAPS PharmSciTech **13**(2): 605-610.
- Tulloch, N. L. and C. E. Murry (2013). "Trends in cardiovascular engineering: organizing the human heart." Trends Cardiovasc Med **23**(8): 282-286.
- Uemura, R., M. Xu, N. Ahmad and M. Ashraf (2006). "Bone marrow stem cells prevent left ventricular remodeling of ischemic heart through paracrine signaling." Circ Res **98**(11): 1414-1421.
- Urbanek, K., F. Quaini, G. Tasca, D. Torella, C. Castaldo, B. Nadal-Ginard, A. Leri, J. Kajstura, E. Quaini and P. Anversa (2003). "Intense myocyte formation from cardiac stem cells in human cardiac hypertrophy." Proc Natl Acad Sci U S A **100**(18): 10440-10445.
- Vande Geest, J. P., E. S. Di Martino and D. A. Vorp (2004). "An analysis of the complete strain field within Flexercell membranes." J Biomech **37**(12): 1923-1928.
- Vandervelde, S., M. J. van Luyn, R. A. Tio and M. C. Harmsen (2005). "Signaling factors in stem cell-mediated repair of infarcted myocardium." J Mol Cell Cardiol **39**(2): 363-376.

- Varner, V. D., D. A. Voronov and L. A. Taber (2010). "Mechanics of head fold formation: investigating tissue-level forces during early development." Development **137**(22): 3801-3811.
- Vetter, U., J. Zapf, W. Heit, G. Helbing, E. Heinze, E. R. Froesch and W. M. Teller (1986). "Human fetal and adult chondrocytes. Effect of insulinlike growth factors I and II, insulin, and growth hormone on clonal growth." J Clin Invest **77**(6): 1903-1908.
- Wakitani, S., K. Takaoka, T. Hattori, N. Miyazawa, T. Iwanaga, S. Takeda, T. K. Watanabe and A. Tanigami (2003). "Embryonic stem cells injected into the mouse knee joint form teratomas and subsequently destroy the joint." Rheumatology (Oxford) **42**(1): 162-165.
- Wan, C. R., S. Chung and R. D. Kamm (2011). "Differentiation of embryonic stem cells into cardiomyocytes in a compliant microfluidic system." Ann Biomed Eng **39**(6): 1840-1847.
- Wang, N. and D. E. Ingber (1994). "Control of cytoskeletal mechanics by extracellular matrix, cell shape, and mechanical tension." Biophys J **66**(6): 2181-2189.
- Welch, S., D. Plank, S. Witt, B. Glascock, E. Schaefer, S. Chimenti, A. M. Andreoli, F. Limana, A. Leri, J. Kajstura, P. Anversa and M. A. Sussman (2002). "Cardiac-specific IGF-1 expression attenuates dilated cardiomyopathy in tropomodulin-overexpressing transgenic mice." Circ Res **90**(6): 641-648.
- Weyts, F. A., B. Bosmans, R. Niesing, J. P. van Leeuwen and H. Weinans (2003). "Mechanical control of human osteoblast apoptosis and proliferation in relation to differentiation." Calcif Tissue Int **72**(4): 505-512.
- Wobus, A. M., G. Kaomei, J. Shan, M. C. Wellner, J. Rohwedel, G. Ji, B. Fleischmann, H. A. Katus, J. Hescheler and W. M. Franz (1997). "Retinoic acid accelerates embryonic stem cell-derived cardiac differentiation and enhances development of ventricular cardiomyocytes." J Mol Cell Cardiol **29**(6): 1525-1539.
- Wozniak, M. A. and C. S. Chen (2009). "Mechanotransduction in development: a growing role for contractility." Nat Rev Mol Cell Biol **10**(1): 34-43.
- Wu, J., K. Wu, F. Lin, Q. Luo, L. Yang, Y. Shi, G. Song and K. L. Sung (2013). "Mechano-growth factor induces migration of rat mesenchymal stem cells by altering its mechanical properties and activating ERK pathway." Biochem Biophys Res Commun **441**(1): 202-207.
- Xiao, Y. and G. A. Truskey (1996). "Effect of receptor-ligand affinity on the strength of endothelial cell adhesion." Biophys J **71**(5): 2869-2884.
- Xiong, H., A. B. Rabie and U. Hagg (2005). "Mechanical strain leads to condylar growth in adult rats." Front Biosci **10**: 67-73.

- Xu, B., G. Song, Y. Ju, X. Li, Y. Song and S. Watanabe (2012). "RhoA/ROCK, cytoskeletal dynamics, and focal adhesion kinase are required for mechanical stretch-induced tenogenic differentiation of human mesenchymal stem cells." J Cell Physiol **227**(6): 2722-2729.
- Yamanaka, S., I. Zahanich, R. P. Wersto and K. R. Boheler (2008). "Enhanced proliferation of monolayer cultures of embryonic stem (ES) cell-derived cardiomyocytes following acute loss of retinoblastoma." PLoS One **3**(12): e3896.
- Yang, C. M., C. S. Chien, C. C. Yao, L. D. Hsiao, Y. C. Huang and C. B. Wu (2004). "Mechanical strain induces collagenase-3 (MMP-13) expression in MC3T3-E1 osteoblastic cells." J Biol Chem **279**(21): 22158-22165.
- Yang, F., C. G. Williams, D. A. Wang, H. Lee, P. N. Manson and J. Elisseeff (2005). "The effect of incorporating RGD adhesive peptide in polyethylene glycol diacrylate hydrogel on osteogenesis of bone marrow stromal cells." Biomaterials **26**(30): 5991-5998.
- Yang, S. Y. and G. Goldspink (2002). "Different roles of the IGF-I Ec peptide (MGF) and mature IGF-I in myoblast proliferation and differentiation." FEBS Lett **522**(1-3): 156-160.
- Yue, X. and R. J. Tomanek (1999). "Stimulation of coronary vasculogenesis/angiogenesis by hypoxia in cultured embryonic hearts." Dev Dyn **216**(1): 28-36.
- Zhang, B., Q. Luo, X. Mao, B. Xu, L. Yang, Y. Ju and G. Song (2014). "A synthetic mechano-growth factor E peptide promotes rat tenocyte migration by lessening cell stiffness and increasing F-actin formation via the FAK-ERK1/2 signaling pathway." Exp Cell Res **322**(1): 208-216.
- Zimmermann, W. H., M. Didie, S. Doker, I. Melnychenko, H. Naito, C. Rogge, M. Tiburcy and T. Eschenhagen (2006). "Heart muscle engineering: an update on cardiac muscle replacement therapy." Cardiovasc Res **71**(3): 419-429.
- Zimmermann, W. H., K. Schneiderbanger, P. Schubert, M. Didie, F. Munzel, J. F. Heubach, S. Kostin, W. L. Neuhuber and T. Eschenhagen (2002). "Tissue engineering of a differentiated cardiac muscle construct." Circ Res **90**(2): 223-230.
- Zwaginga, J. J. and P. Doevendans (2003). "Stem cell-derived angiogenic/vasculogenic cells: possible therapies for tissue repair and tissue engineering." Clin Exp Pharmacol Physiol **30**(11): 900-908.

## APPENMDIX – animal approval form



September 18, 2013

Brenda Russell  
Physiology & Biophysics  
M/C 901

Office of Animal Care and  
Institutional Biosafety Committees (MC 672)  
Office of the Vice Chancellor for Research  
206 Administrative Office Building  
1737 West Polk Street  
Chicago, Illinois 60612-7227

Dear Dr. Russell:

The protocol indicated below was reviewed at a convened ACC meeting in accordance with the Animal Care Policies of the University of Illinois at Chicago on 9/17/2013. *The protocol is approved for a period of 3 years with annual continuation.*

**Title of Application:** Isolation of Heart Cells from Neonatal Rats**ACC Number:** 13-146**Initial Approval Period:** 9/17/2013 to 9/17/2014

**Current Funding:** Portions of this protocol are supported by the funding sources indicated in the table below.

**Number of funding sources:** 2

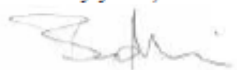
Funding Agency	Funding Title			Portion of Proposal Matched
NIH	Integrated Mechanisms Of Cardiac Maladaptation			Protocol is linked to form G (13-055)
Funding Number	Current Status	UIC PAF NO.	Performance Site	Funding PI
PO1HL62426 (Years 11-15)	Funded	2009-06478	UIC	John Solaro (Brenda Russell, PI of project 2)
Funding Agency	Funding Title			Portion of Proposal Matched
AHA- American Heart Association	Regulation of Actin Assembly in Cardiomyocytes with Mechanical Stimulation			All matched
Funding Number	Current Status	UIC PAF NO.	Performance Site	Funding PI
12PRE12050371	Funded	2012-03610	UIC	Ying-His Lin

This institution has Animal Welfare Assurance Number A3460.01 on file with the Office of Laboratory Animal Welfare (OLAW), NIH. This letter may only be provided as proof of IACUC approval for those specific funding sources listed above in which all portions of the funding proposal are matched to this ACC protocol.

In addition, all investigators are responsible for ensuring compliance with all federal and institutional policies and regulations related to use of animals under this protocol and the funding

sources listed on this protocol. Please use OLAW's "*What Investigators Need to Know about the Use of Animals*" (<http://grants.nih.gov/grants/olaw/InvestigatorsNeed2Know.pdf>) as a reference guide. Thank you for complying with the Animal Care Policies and Procedures of UIC.

Sincerely yours,



Bradley Merrill, PhD  
Chair, Animal Care Committee

BM/ss

cc: BRL, ACC File, Ying Hsi Lin, PAF # 2012-03610

## APPENDIX – copy right clearance

3/14/2014

RightsLink Printable License

### ELSEVIER LICENSE TERMS AND CONDITIONS

Mar 14, 2014

---

This is a License Agreement between Golnar Doroudian ("You") and Elsevier ("Elsevier") provided by Copyright Clearance Center ("CCC"). The license consists of your order details, the terms and conditions provided by Elsevier, and the payment terms and conditions.

**All payments must be made in full to CCC. For payment instructions, please see information listed at the bottom of this form.**

Supplier	Elsevier Limited The Boulevard, Langford Lane Kidlington, Oxford, OX5 1GB, UK
Registered Company Number	1982084
Customer name	Golnar Doroudian
Customer address	1620 S. Michigan ave, apt 510 CHICAGO, IL 60616
License number	3347820528859
License date	Mar 14, 2014
Licensed content publisher	Elsevier
Licensed content publication	Biochemical and Biophysical Research Communications
Licensed content title	Cyclic strain dominates over microtopography in regulating cytoskeletal and focal adhesion remodeling of human mesenchymal stem cells
Licensed content author	Golnar Doroudian, Matthew W. Curtis, Anjulie Gang, Brenda Russell
Licensed content date	18 January 2013
Licensed content volume number	430
Licensed content issue number	3
Number of pages	7
Start Page	1040
End Page	1046
Type of Use	reuse in a thesis/dissertation
Portion	full article
Format	both print and electronic
Are you the author of this Elsevier article?	Yes
Will you be translating?	No

<https://s100.copyright.com/AppDispatchServlet>

3/14/2014

Rightslink Printable License

Title of your thesis/dissertation	Delivery of mechanical and chemical stimuli to advance regeneration
Expected completion date	Mar 2014
Estimated size (number of pages)	137
Elsevier VAT number	GB 494 6272 12
Permissions price	0.00 USD
VAT/Local Sales Tax	0.00 USD / 0.00 GBP
Total	0.00 USD
Terms and Conditions	

## INTRODUCTION

1. The publisher for this copyrighted material is Elsevier. By clicking "accept" in connection with completing this licensing transaction, you agree that the following terms and conditions apply to this transaction (along with the Billing and Payment terms and conditions established by Copyright Clearance Center, Inc. ("CCC"), at the time that you opened your Rightslink account and that are available at any time at <http://myaccount.copyright.com>).

## GENERAL TERMS

2. Elsevier hereby grants you permission to reproduce the aforementioned material subject to the terms and conditions indicated.

3. Acknowledgement: If any part of the material to be used (for example, figures) has appeared in our publication with credit or acknowledgement to another source, permission must also be sought from that source. If such permission is not obtained then that material may not be included in your publication/copies. Suitable acknowledgement to the source must be made, either as a footnote or in a reference list at the end of your publication, as follows:

"Reprinted from Publication title, Vol/edition number, Author(s), Title of article / title of chapter, Pages No., Copyright (Year), with permission from Elsevier [OR APPLICABLE SOCIETY COPYRIGHT OWNER]." Also Lancet special credit - "Reprinted from The Lancet, Vol number, Author(s), Title of article, Pages No., Copyright (Year), with permission from Elsevier."

4. Reproduction of this material is confined to the purpose and/or media for which permission is hereby given.

5. Altering/Modifying Material: Not Permitted. However figures and illustrations may be altered/adapted minimally to serve your work. Any other abbreviations, additions, deletions and/or any other alterations shall be made only with prior written authorization of Elsevier Ltd. (Please contact Elsevier at [permissions@elsevier.com](mailto:permissions@elsevier.com))

6. If the permission fee for the requested use of our material is waived in this instance, please be advised that your future requests for Elsevier materials may attract a fee.

7. Reservation of Rights: Publisher reserves all rights not specifically granted in the combination of (i) the license details provided by you and accepted in the course of this licensing transaction, (ii) these

<https://is100.copyright.com/AppDispatchServlet>



terms and conditions and (iii) CCC's Billing and Payment terms and conditions.

8. License Contingent Upon Payment: While you may exercise the rights licensed immediately upon issuance of the license at the end of the licensing process for the transaction, provided that you have disclosed complete and accurate details of your proposed use, no license is finally effective unless and until full payment is received from you (either by publisher or by CCC) as provided in CCC's Billing and Payment terms and conditions. If full payment is not received on a timely basis, then any license preliminarily granted shall be deemed automatically revoked and shall be void as if never granted. Further, in the event that you breach any of these terms and conditions or any of CCC's Billing and Payment terms and conditions, the license is automatically revoked and shall be void as if never granted. Use of materials as described in a revoked license, as well as any use of the materials beyond the scope of an unrevoked license, may constitute copyright infringement and publisher reserves the right to take any and all action to protect its copyright in the materials.

9. Warranties: Publisher makes no representations or warranties with respect to the licensed material.

10. Indemnity: You hereby indemnify and agree to hold harmless publisher and CCC, and their respective officers, directors, employees and agents, from and against any and all claims arising out of your use of the licensed material other than as specifically authorized pursuant to this license.

11. No Transfer of License: This license is personal to you and may not be sublicensed, assigned, or transferred by you to any other person without publisher's written permission.

12. No Amendment Except in Writing: This license may not be amended except in a writing signed by both parties (or, in the case of publisher, by CCC on publisher's behalf).

13. Objection to Contrary Terms: Publisher hereby objects to any terms contained in any purchase order, acknowledgment, check endorsement or other writing prepared by you, which terms are inconsistent with these terms and conditions or CCC's Billing and Payment terms and conditions. These terms and conditions, together with CCC's Billing and Payment terms and conditions (which are incorporated herein), comprise the entire agreement between you and publisher (and CCC) concerning this licensing transaction. In the event of any conflict between your obligations established by these terms and conditions and those established by CCC's Billing and Payment terms and conditions, these terms and conditions shall control.

14. Revocation: Elsevier or Copyright Clearance Center may deny the permissions described in this License at their sole discretion, for any reason or no reason, with a full refund payable to you. Notice of such denial will be made using the contact information provided by you. Failure to receive such notice will not alter or invalidate the denial. In no event will Elsevier or Copyright Clearance Center be responsible or liable for any costs, expenses or damage incurred by you as a result of a denial of your permission request, other than a refund of the amount(s) paid by you to Elsevier and/or Copyright Clearance Center for denied permissions.

### LIMITED LICENSE

The following terms and conditions apply only to specific license types:



**15. Translation:** This permission is granted for non-exclusive world **English** rights only unless your license was granted for translation rights. If you licensed translation rights you may only translate this content into the languages you requested. A professional translator must perform all translations and reproduce the content word for word preserving the integrity of the article. If this license is for use 1 or 2 figures then permission is granted for non-exclusive world rights in all languages.

**16. Posting licensed content on any Website:** The following terms and conditions apply as follows: **Licensing material from an Elsevier journal:** All content posted to the web site must maintain the copyright information line on the bottom of each image; A hyper-text must be included to the Homepage of the journal from which you are licensing at <http://www.sciencedirect.com/science/journal/xxxxx> or the Elsevier homepage for books at <http://www.elsevier.com>; **CentralStorage:** This license does not include permission for a scanned version of the material to be stored in a central repository such as that provided by Heron/XanEdu.

**Licensing material from an Elsevier book:** A hyper-text link must be included to the Elsevier homepage at <http://www.elsevier.com>. All content posted to the web site must maintain the copyright information line on the bottom of each image.

**Posting licensed content on Electronic reserve:** In addition to the above the following clauses are applicable: The web site must be password-protected and made available only to bona fide students registered on a relevant course. This permission is granted for 1 year only. You may obtain a new license for future website posting.

**For journal authors:** the following clauses are applicable in addition to the above: Permission granted is limited to the author accepted manuscript version\* of your paper.

**\*Accepted Author Manuscript (AAM) Definition:** An accepted author manuscript (AAM) is the author's version of the manuscript of an article that has been accepted for publication and which may include any author-incorporated changes suggested through the processes of submission processing, peer review, and editor-author communications. AAMs do not include other publisher value-added contributions such as copy-editing, formatting, technical enhancements and (if relevant) pagination.

You are not allowed to download and post the published journal article (whether PDF or HTML, proof or final version), nor may you scan the printed edition to create an electronic version. A hyper-text must be included to the Homepage of the journal from which you are licensing at <http://www.sciencedirect.com/science/journal/xxxxx>. As part of our normal production process, you will receive an e-mail notice when your article appears on Elsevier's online service ScienceDirect ([www.sciencedirect.com](http://www.sciencedirect.com)). That e-mail will include the article's Digital Object Identifier (DOI). This number provides the electronic link to the published article and should be included in the posting of your personal version. We ask that you wait until you receive this e-mail and have the DOI to do any posting.

**Posting to a repository:** Authors may post their AAM immediately to their employer's institutional repository for internal use only and may make their manuscript publicly available after the journal-specific embargo period has ended.

Please also refer to Elsevier's Article Posting Policy for further information.

18. For book authors the following clauses are applicable in addition to the above: Authors are permitted to place a brief summary of their work online only. You are not allowed to download and post the published electronic version of your chapter, nor may you scan the printed edition to create an electronic version. Posting to a repository: Authors are permitted to post a summary of their chapter only in their institution's repository.

20. Thesis/Dissertation: If your license is for use in a thesis/dissertation your thesis may be submitted to your institution in either print or electronic form. Should your thesis be published commercially, please reapply for permission. These requirements include permission for the Library and Archives of Canada to supply single copies, on demand, of the complete thesis and include permission for UMI to supply single copies, on demand, of the complete thesis. Should your thesis be published commercially, please reapply for permission.

### **Elsevier Open Access Terms and Conditions**

Elsevier publishes Open Access articles in both its Open Access journals and via its Open Access articles option in subscription journals.

Authors publishing in an Open Access journal or who choose to make their article Open Access in an Elsevier subscription journal select one of the following Creative Commons user licenses, which define how a reader may reuse their work: Creative Commons Attribution License (CC BY), Creative Commons Attribution – Non Commercial – Share Alike (CC BY NC SA) and Creative Commons Attribution – Non Commercial – No Derivatives (CC BY NC ND)

### **Terms & Conditions applicable to all Elsevier Open Access articles:**

Any reuse of the article must not represent the author as endorsing the adaptation of the article nor should the article be modified in such a way as to damage the author's honour or reputation.

The author(s) must be appropriately credited.

If any part of the material to be used (for example, figures) has appeared in our publication with credit or acknowledgement to another source it is the responsibility of the user to ensure their reuse complies with the terms and conditions determined by the rights holder.

### **Additional Terms & Conditions applicable to each Creative Commons user license:**

**CC BY:** You may distribute and copy the article, create extracts, abstracts, and other revised versions, adaptations or derivative works of or from an article (such as a translation), to include in a collective work (such as an anthology), to text or data mine the article, including for commercial purposes without permission from Elsevier

**CC BY NC SA:** For non-commercial purposes you may distribute and copy the article, create extracts, abstracts and other revised versions, adaptations or derivative works of or from an article

3/14/2014

RightsLink Printable License

(such as a translation), to include in a collective work (such as an anthology), to text and data mine the article and license new adaptations or creations under identical terms without permission from Elsevier

**CC BY-NC-ND:** For non-commercial purposes you may distribute and copy the article and include it in a collective work (such as an anthology), provided you do not alter or modify the article, without permission from Elsevier

Any commercial reuse of Open Access articles published with a CC BY-NC-SA or CC BY-NC-ND license requires permission from Elsevier and will be subject to a fee.

Commercial reuse includes:

- Promotional purposes (advertising or marketing)
- Commercial exploitation (e.g. a product for sale or loan)
- Systematic distribution (for a fee or free of charge)

Please refer to Elsevier's Open Access Policy for further information.

## 21. Other Conditions:

v1.7

If you would like to pay for this license now, please remit this license along with your payment made payable to "COPYRIGHT CLEARANCE CENTER" otherwise you will be invoiced within 48 hours of the license date. Payment should be in the form of a check or money order referencing your account number and this invoice number RLNK501251550. Once you receive your invoice for this order, you may pay your invoice by credit card. Please follow instructions provided at that time.

**Make Payment To:**  
Copyright Clearance Center  
Dept 001  
P.O. Box 843006  
Boston, MA 02284-3006

For suggestions or comments regarding this order, contact RightsLink Customer Support: [customer-care@copyright.com](mailto:customer-care@copyright.com) or +1-877-622-5543 (toll free in the US) or +1-978-646-2777.

Gratis licenses (referencing \$0 in the Total field) are free. Please retain this printable license for your reference. No payment is required.

## VITA

### Golnar Doroudian

#### Education

##### **University of Illinois at Chicago, Chicago (UIC), IL**

Ph.D., Bioengineering, August 2009-Present

##### **University of New Mexico, Albuquerque (UNM), NM**

B.S., Chemical Engineering, Biomedical Engineering Concentration, 2006-2009

##### **Iran University of Science and Technology, Tehran**

(First year of B.S.), Chemical Engineering, 2004-2005

#### Research Experience

##### **The effect of physical stimuli and growth factor delivery from encapsulated microstructures on stem cells**

Determined differentiation, proliferation, adhesion, and migration of human bone marrow stem cells

*Graduate Research Assistant*, Advisor: Dr. Brenda Russell (UIC), 2009-Present

##### **The effect of encapsulation on enzyme structure stability**

Determined protein secondary structure by Circular Dichroism

*Undergraduate Research Assistant*, Advisor: Dr. Eva Chi (UNM), 2008-2009

##### **The effect of copolymer architectures on glass transition temperature in confined geometries and on critical micelle concentration (cmc)**

Determined glass transition temperature and critical micelle conc. by ellipsometry and fluorescence spectroscopy

*Undergraduate Research Assistant*, Advisor: Dr. John Torkelson (Northwestern University), 2008

#### Journal Publication

**Doroudian, G**, Curtis MW, Gang A, Russell B. Cyclic strain dominates over microtopography in regulating cytoskeletal and focal adhesion remodeling of human mesenchymal stem cells. *Biochem Biophys Res Commun*. 2013 Jan 18; 430(3): 1040-6

#### Book Publication

Pinney JR, **Doroudian G**, Chew P, Desai TA, Russell B. "Cells, Forces and the Microenvironment" Chapter Title: Micromechanical cues converging on fibroblasts, cardiac myocytes and stem cells. (in Press)  
Pan Stanford Publishing Pte. Ltd., Singapore. Editors: Prof. Andrew E., Canada Research Chair, University of Ottawa Pelling Dr. Charles M. Guerrier, Fonds de la Recherche en Santé du Québec Fellow, University of Ottawa

### **Presentation and Abstracts**

**Doroudian, G.**, James Pinney, Tamara Los, Tejal Desai, and Brenda Russell. "Local delivery of mechano growth factor from microrods attracts mesenchymal stem cells" Stem Cell Regenerative Medicine, 20 September, 2013, Chicago, IL

**Doroudian, G.**, James Pinney, Tamara Los, Tejal Desai, and Brenda Russell. "Local delivery of mechano growth factor from microrods attracts mesenchymal stem cells" CCVR Research, 17 September, 2013, Chicago, IL

**Doroudian, G.**, Gang, A., Curtis, M.W., and B. Russell. "Simulation of Physiologic Strain to Aligned Cells Anchored in 3D Affects Proliferation, Differentiation, and Organization of the Actin Cytoskeleton" Experimental Biology, 24 April, 2012, San Diego, CA

**Doroudian, G.**, Gang, A., Curtis, M.W., and B. Russell. "Simulation of Physiologic Strain to Aligned cells Anchored in 3D Affects Proliferation, Differentiation, and Organization of the Actin Cytoskeleton" Stem Cell Regenerative Medicine, 10 May, 2012

**Doroudian, G.**, Gang, A., Curtis, M.W., and B. Russell. "Simulation of Physiologic Strain to Aligned cells Anchored in 3D Affects Proliferation, Differentiation, and Organization of the Actin Cytoskeleton" UIC student research forum, 17 April, 2012

**Doroudian, G.**, Gang, A., Curtis, M.W., and B. Russell. "Cyclic Strain and microtopography differentially affect Human Mesenchymal Stem Cells" Biomedical Engineering Society, 15 Oct, 2011, cinnaticate, Hartford, CT

**Doroudian, G.**, Gang, A., Curtis, M.W., and B. Russell. "Cyclic strain and topography affect morphology and gene expression of Human Mesenchymal Stem Cells" ASME McMAT Conference: Mechanics of Biological Tissues: 31 May - 2 June 2011, Chicago, IL

**Doroudian, G.**, Gang, A., Curtis, M.W., and B. Russell. "Cyclic strain and microtopography change morphology, proliferation, and gene expression of Human Mesenchymal Stem Cells" Midwest Biomedical Engineering Career Conference (MBECC), 1 April, 2011, Chicago, IL

**Doroudian, G.**, Gang, A., Curtis, M.W., and B. Russell. "Cyclic strain and topography affect morphology and gene expression of Human Mesenchymal Stem Cells" CCVR Research, 12 Aug, 2011

**Doroudian, G.**, Gang, A., Curtis, M.W., and B. Russell. "Cyclic strain and topography affect morphology and gene expression of Human Mesenchymal Stem Cells" Stem Cell Regenerative Medicine, 20 May, 2011.

**Doroudian, G.**, Gang, A., Curtis, M.W., and B. Russell. "Cyclic strain and topography affect morphology and gene expression of Human Mesenchymal Stem Cells" UIC student research forum, 29 April, 2011.

## Technical Skills

**Computer:** Matlab, ImageJ, ASPEN, Affymetrix Data Mining Tool

**Cell Biology and Biophysics/Bioengineering Techniques:** Cell culture, RT-PCR, RNA/DNA/Protein extraction, RNA/DNA/Protein Quantification, Western Blotting, immunostaining assays, Fluorescence-activated cell sorting (FACS) analysis, Microfabrication, Immunofluorescent, Confocal, and TIRF microscopy, microarray scanning and analysis, intrinsic fluorescence technique, block, gradient, and random copolymer matrix synthesis, differential scanning calorimetry (DSC), ellipsometry, circular dichroism (CD)

## Employment History

**Laboratory assistant,** August 2007- May 2008

Stable Isotope Geochemistry Laboratory, UNM, Albuquerque, NM

Maintain and use isotope ratio mass spectroscopy equipment. Prepare and measure various samples of plants, tissues, and waters

## Scholarships and Honors

Predoctoral Trainee funded by NIH 5T32 HL07692. (Cellular Signaling in the Cardiovascular System), August 2011-Present

*PI: Dr. R.J. Solaro*

Selected as an Academic Career panelist at Midwest Biomedical Engineering Career Conference, April 2013

Graduate Student Travel Award, UIC, October 2011

NSF (Science, Engineering, Mathematics (SEM)) scholarship, August 2008

SOE, (School of Engineering) scholarship, August, 2008

New Mexico Society of Professional Engineers Albuquerque Chapter scholarship, April 2008 and April 2009

Top Rank in Chemistry Olympiad, Tehran, Iran, March 2003

## Professional Memberships

Member of Biomedical Engineering Society (BMES), 2011-Present

Member of the Engineering Honor Society of Tau Beta Pi, 2009

Member of American Institute of Chemical Engineers (AIChE), 2007-2009

Webmaster in Biomedical Engineering Society (BMES) UNM Chapter, 2008-2009

Member of the Honor Society of Phi Kappa Phi, April 2008

## Activities

Teaching Farsi at Persian School of Chicago, 2012-Present

Leader of "Shabeh Jomeh" organization, August 2013-Present

Involved in the High School Outreach Program, 2009-2009

Volunteer to Raise Funds for the Society of Women Engineers (SWE), May 2008

UNM Intramural Soccer, Fall 2005, Spring 2007, and Spring 2008

Piano Recitals, Tehran, Iran (Charitable Organization for Children with Cancer), August 2003 and August 2004